DYNAMICS AND CONTROL OF FLEXIBLE AIRCRAFT

Ilhan Tuzcu

Dissertation submitted to the Faculty of the
Virginia Polytechnic Institute and State University
in partial fulfillment of the requirements for the degree of

Doctor of Philosophy
in
Mechanical Engineering

Leonard Meirovitch, Chair
Daniel J. Inman, Co-Chair
Mehdi Ahmadian
Liviu Librescu
Alfred L. Wicks

December 19, 2001
Blacksburg, Virginia

Keywords: Flexible Aircraft Dynamics, Multidisciplinary Formulation, Perturbation Approach, Extended Aeroservoelasticity, LQG Control

DYNAMICS AND CONTROL OF FLEXIBLE AIRCRAFT

Ilhan Tuzcu

(ABSTRACT)

This dissertation integrates in a single mathematical formulation the disciplines pertinent to the flight of flexible aircraft, namely, analytical dynamics, structural dynamics, aerodynamics and controls. The unified formulation is based on fundamental principles and incorporates in a natural manner both rigid body motions of the aircraft as a whole and elastic deformations of the flexible components (fuselage, wing and empennage), as well as the aerodynamic, propulsion, gravity and control forces. The aircraft motion is described in terms of three translations (forward motion, sideslip and plunge) and three rotations (roll, pitch and yaw) of a reference frame attached to the undeformed fuselage, and acting as aircraft body axes, and elastic displacements of each of the flexible components relative to corresponding body axes. The mathematical formulation consists of six ordinary differential equations for the rigid body motions and one set of ordinary differential equations for each elastic displacement. A perturbation approach permits division of the problem into a nonlinear "zero-order problem" for the rigid body motions, corresponding to flight dynamics, and a linear "first-order problem" for the elastic deformations and perturbations in the rigid body translations and rotations, corresponding to "extended aeroelasticity." Due to computational speed advantages, the aerodynamic forces are derived by means of strip theory. The control forces for the flight dynamics problem are obtained by an "inverse" process. On the other hand, the feedback control forces for the extended aeroelasticity problem are derived by means of LQG theory. A numerical example corresponding to steady level flight and steady level turn maneuver is included.

Dedication

To my mother and father, İnayet and Adnan Tuzcu

my sisters, Yasemin and Ümran

my brothers, Erdoğan, Ertuğrul and Alpaslan

Acknowledgment

I am particularly grateful to my advisor, Dr. Leonard Meirovitch, for his technical support, leadership and professional guidance as well as his encouragement and mentoring during my study and research. I especially appreciate his patience and understanding. My special thanks goes to Dr. Daniel J. Inman for serving as the co-chair in my advisory committee and for his assistance and guidance. Dr. Inman has always been very helpful, nice and available for my concerns and questions. I would like also to thank Dr. Mehdi Ahmadian, Dr. Liviu Librescu and Dr. Alfred L. Wicks for their interest in my research and the council and advise provided.

The present study was supported by the NASA Langley Research Center through grant No. NCC-1-346 awarded to Dr. L. Meirovitch. The technical support and useful suggestions by Mr. Martin R. Waszak, NASA Langley Research Center, are gratefully acknowledged.

I would like to thank Norma B. Guynn for her excellent job in typing this dissertation. I also wish to express my gratitude to my colleagues and friends for their support and friendship. Among these, I would like to mention Dr. Ramazan Asmatulu, Dr. Sean Fahey, Dr. Adel Benhaj Jilani, Ferman Konukman, Dr. Piergiovanni Marzocca, Dr. Semih Olcmen and Dr. Ismail Yildirim.

Finally, I am deeply grateful to my family for their ever-lasting love and support; I dedicate this work to them.

Contents

List of Figures

List of Tables

Chapter 1

Introduction

1.1 Overview

This investigation is concerned with a dynamic formulation capable of simulating the flight of flexible aircraft. It integrates in a single and consistent mathematical formulation all the necessary material from the pertinent disciplines, namely, analytical dynamics, structural dynamics, aerodynamics and controls. The unified formulation is based on fundamental principles and incorporates in a natural manner both the rigid body motions and the elastic deformations, and the couplings thereof, as well as the aerodynamic, propulsion, control and gravity forces. In essence, the formulation not only unifies flight dynamics and aeroelasticity, traditionally treated as separate disciplines, but also permits a computer simulation of the response of flying flexible aircraft to external stimuli.

In describing the motion of *rigid bodies* in space, it is convenient to attach a set of axes to the body, where the axes are commonly known as body axes, and express the motions in terms of components along these body axes. It is quite common to describe the motion of rigid bodies in terms of the translation of the origin of the body axes and the rotation of the body axes; the corresponding variables, particularly the rotations, are referred to as quasi-coordinates. If the origin of this reference frame coincides with the mass center of the body, the translation and rotation are independent of each other. Moreover, if the body axes themselves coincide with the principal axes of the body, then the products of inertia are zero, so that the inertia matrix is diagonal.

The situation is more complicated for *flexible bodies*, in which case there are basically two types of reference frames:

i. **Fixed in the undeformed body** - In this case, it is convenient to define the translation of the origin of the reference frame and the rotation of the reference frame as the rigid body translation and rotation of the body, and regard any displacement relative to the reference frame as elastic deformation.

ii. **Moving relative to the undeformed body** - In this case, it is common to choose the reference axes so that the linear momentum and angular momentum vectors due to elastic deformations vanish; axes satisfying these conditions are called *mean axes*. Because the elastic deformations depend in general on time, the mean axes are continuously moving relative to the undeformed body. Moreover, if the origin of the reference frame coincides with the mass center at all times, then the first moments of inertia of the deformed body vanish, and the rigid body translations are decoupled inertially from the rigid body rotations. The rigid body translations are also decoupled from the elastic displacements. However, decoupling between the rigid body rotations and the elastic displacements can only occur if the elastic displacements appearing in the inertia matrix are ignored. Under all these assumptions, the rigid body translations, the rigid body rotations and the elastic displacements are all inertially decoupled. Finally, if the reference frame coincides with the principal axes, the inertia matrix is diagonal.

Whereas the use of mean axes for flexible bodies in vacuum can produce some inertial decouplings, in the case of aircraft any such benefits are questionable, because the equations of motion remain coupled through the aerodynamic forces. Moreover, if one insists on the use of mean axes, then the aerodynamic forces must also be expressed in terms of components along the same mean axes, which is a very tedious task at best.

The motion of *force-free rigid bodies* in space is unstable. Under certain circumstances, the motion of rigid bodies can be stabilized by imparting to them some spin about the axis of either the minimum or the maximum moment of inertia. On the other hand, *flexible bodies* cannot be stabilized if the spin is about the axis of minimum moment of inertia. The preceding statements imply that the motion takes place in vacuum, such as in the case of a spacecraft. Matters are entirely different for flexible aircraft, which are neither force-free, nor do they operate in vacuum. In fact, aircraft are subjected to aerodynamic and wind forces, and any stabilization is done by active means, namely, by the engine throttle and control surfaces, where the latter consist of the aileron, elevator and rudder.

The flight of an aircraft tends to be quite diverse, ranging from steady level cruise to complex

maneuvers, and stabilization requires the use of controls permitting the aircraft to carry out the intended maneuver while suppressing any deviations from it, whether in the form of rigid body displacements or elastic deformations. Both flight dynamics and aeroelasticity are concerned with aircraft stability. But, whereas flight dynamics is concerned mainly with rigid body motions, aeroelasticity is concerned with vibration and flutter.

A stability analysis tends to be limited in scope, in the sense that it can only yield a qualitative statement about the nature of motion in the neighborhood of an equilibrium state of a system. More specifically, it can state whether the equilibrium is merely stable, asymptotically stable, or unstable. The time plays no role in a stability analysis. In fact, stability analyses tend to be limited to cases in which the time variable can be eliminated, such as when the equations of motion can be reduced to an eigenvalue problem. The stability of time-dependent maneuvers can only be evaluated numerically.

To obtain information going beyond stability statements, such as the time response of aircraft to external stimuli, it is necessary to undertake a simulation of the equations of motion, which amounts to the integration of the equations of motion. Such a dynamic simulation can be used for parametric studies in preliminary design. Moreover, it can be used to determine aircraft performance, thus reducing the time required for flight testing by "flying the aircraft on a computer."

The choice in this dissertation is to work with a reference frame attached to the undeformed aircraft, which has many advantages over mean axes. But, because the elastic deformations prevent the origin of a frame attached to the undeformed body from coinciding with the mass center and the axes themselves from coinciding with the principal axes for all times, there is no preferred choice of a reference frame; we base the choice on geometric considerations. In particular, we attach a set of body axes to the undeformed fuselage, where one of the axes is along the symmetry axis. For convenience, sets of body axes are also attached to the other flexible components, such as the wing and the empennage. Ultimately, however, all motions are referred to the fuselage body axes, which act as a reference frame for the whole aircraft.

The mathematical formulation is based on equations of motion in terms of quasi-coordinates derived earlier by Meirovitch for flexible spacecraft and later adapted by him to flexible aircraft. (see **1.2 Literature Review**) The formulation is hybrid in nature, in the sense that it consists of ordinary differential equations for the rigid body translations and rotations of the aircraft as a whole and boundary-value problems for the elastic deformations for the

flexible components of the aircraft, namely, the fuselage, wing and empennage. For practical reasons, the distributed variables describing the boundary-value problems for the individual components are discretized in space, obtaining a relatively large set of second-order ordinary differential equations for the whole aircraft. The discretization process amounts to representing the distributed variables as finite series of known space-dependent shape functions multiplied by time-dependent generalized coordinates. The derivation of the equations of motion in conjunction with the extended Hamilton principle requires expressions for the kinetic energy, potential energy and virtual work, all scalar quantities. In turn, the kinetic energy requires the velocity of every point of the aircraft, which can be obtained by means of an orderly kinematical synthesis, going from the fuselage to the wing and to the empennage. The potential energy is merely equal to the strain energy. Moreover, the aerodynamic, propulsion, control and gravity forces are accounted for through the virtual work. Rather than deriving first hybrid equations of motion and then discretizing them in space, it is perhaps more expeditious to carry out the discretization directly in the kinetic energy, potential energy and virtual work, thus obtaining the desired set of ordinary differential equations for the whole flexible aircraft without the need to derive boundary-value problems. For integration of the differential equations and for control design, it is necessary to transform the set of second-order differential equations into a set of first-order differential equations, namely, into a set of state equations. It turns out that, for the problem at hand, it is more convenient to work with momenta rather than with velocities. Although the resulting first-order equations actually represent phase equations, we shall continue to refer to them as state equations.

The simulation of the flight of an aircraft amounts essentially to integration of the state equations. Because of various nonlinearities involved, such as those due to rigid body motions and aerodynamic forces, the integration must be carried out numerically on a computer. In one way or another, computer integration can only be done in discrete time, which raises the question of the size of the sampling period, or time step. Of course, the answer depends on the desired accuracy of the simulation, and it is intimately related to the dynamic characteristics of the system. If the aircraft is to be controlled by an autopilot, then the simulation must be carried out in real time. If the dynamic characteristics are such that the time step must be relatively short, perhaps of the order of 0.01s, most aerodynamic theories in current use must be ruled out, as the computation of the dynamic pressure over the entire aircraft is sure to take considerably longer time than that. Hence, a new method for computing the dynamic pressure must be developed, one characterized by high computational speed, even if some accuracy must be sacrificed. Moreover, the method for computing the dynamic pressure

must be compatible with the method for modeling the airframe. If the formulation is to be used for aircraft design, then real-time simulation may not really be necessary, although on-line simulation may. But, the size of the sampling period, which is determined by the system dynamic characteristics, remains the same regardless of whether the simulation is in real time or only on-line. The implication is that the computation of the dynamic pressure must still be relatively fast. Indeed, a mere 10 s simulation requires 1,000 time steps. Hence if the computation of the dynamic pressure takes one hour, the simulation requires over 40 days. This demonstrates the need for a method for computing the dynamic pressure in a very short time period. In this regard, a reasonably accurate approximate method may be acceptable.

As indicated above, the equations of motion for a flying flexible aircraft are nonlinear, where the nonlinearity is due to the rigid body motions and the aerodynamic forces. Moreover, the equations tend to be of high order, the order depending on the discretization procedure employed. Hence, one can expect difficulties both with a stability analysis and with control design. In addition, difficulties can be experienced in the integration process, because some of the variables describing the aircraft rigid body motions tend to be large and the variables describing the elastic displacements tend to be small. A perturbation approach to the solution can obviate many of these difficulties. More specifically, the solution can be represented as the sum of a zero-order part for the large rigid body variables and a first-order part for the small elastic variables and perturbations in the rigid body variables, where the zero-order quantities are larger than the first-order quantities by at least one order of magnitude. Then, the equations of motion can be separated into a *zero-order problem* for the rigid body motions alone and a *first-order problem* for the elastic displacements and the perturbations in the rigid body motions. The state equations for the zero-order problem are of order 12 at most; they can be identified as the equations of *flight dynamics* and can be used to describe aircraft maneuvers. On the other hand, the state equations for the first-order problem are of order $12 + 2n_e$, where n_e is the number of elastic degrees of freedom; they represent the *extended aeroelasticity* equations, where "extended" is in the sense that they include not only the elastic displacements but also perturbations in the rigid body variables, where the latter are sometimes referred to as "body freedoms."

The flight dynamics equations are in general *nonlinear* and describe the translations and rotations of the aircraft as if it were rigid. They can be used to design given maneuvers of an aircraft, which amounts to solving an "inverse" problem. In the commonly encountered

direct problems in dynamics of rigid bodies, the forces are given and the equations of motion are solved for the state, i.e., for the positions and velocities. In the context of the present formulation unifying flight dynamics and aeroelasticity, however, the state representing a desired maneuver is given and the problem amounts to determining the engine thrust and the control surface forces permitting the realization of the maneuver; this represents an inverse problem. On the other hand, the extended aeroelasticity equations are *linear*, but they contain the state and forces from the flight dynamics problem as coefficients and as an input. Hence, *there is a set of extended aeroelasticity equations for every conceivable aircraft maneuver*. If the flight dynamics problem represents steady level cruise or a steady level turn maneuver, then the zero-order state and forces are constant and the system of extended aeroelasticity equations is linear time-invariant. In this case, the state equations lend themselves to a standard stability check, such as one based on the roots of the eigenvalue problem, to control design by commonly used techniques, such as the LQG method, and to ready integration for simulation of the aircraft response to external stimuli. If the flight dynamics problem represents a time-dependent maneuver, such as the transition from one steady state to another, then the zero-order state and forces depend on time and the extended aeroelasticity state equations are linear time-varying, which precludes a standard stability analysis. However, the state equations still permit control design and response simulation.

1.2 Literature Review

The following literature review should help relate the present research to previous investigations: Although flight dynamics and aeroelasticity have been developed traditionally as separate disciplines, the need for considering interacting efforts was recognized quite early.[1-3] Still, relatively few attempts have been made to link the two disciplines, and when such attempts were made almost invariably the scope was quite limited. This lack of interest in linking flight dynamics and aeroelasticity can be attributed to a reluctance to increase the complexity of the problem to a significant extent at a time when powerful computers capable of solving such problems were not available. As a result, problems combining flight dynamics and aeroelasticity effects have tended to be subjected to many simplifying assumptions designed to permit largely analytical solutions. In one of the first references on the subject, Bisplinghoff and Ashley[4] derived scalar equations of motion for an unrestrained flexible vehicle. The equations consisted of three inertially decoupled sets, one for the rigid body translations, one for the rigid body rotations and one for the elastic deformations, the latter

expressed in terms of aircraft structural natural modes. Although not stated explicitly, this implies the use of principal mean axes with the origin at the vehicle mass center. Moreover, the inertia matrix was assumed to be constant, which implies that the contributions from the elastic deformations to the inertia matrix were ignored. Aerodynamic forces for the case of small disturbed motions from steady rectilinear flight were given in terms of an influence function for an unrestrained aircraft. An integrated analytical treatment of the equilibrium and stability of flexible aircraft was presented by Milne.[5] In Part I, he derived linearized equations of motion about a steady state, assuming not only that the elastic deformations but also the rigid body translations and rotations were small. Although the constraint equations defining the mean axes were given, the formulation seems to have used body axes attached to the undeformed aircraft. The equations are expressed in a vector-dyadic form that does not permit a ready check for missing terms and, more importantly, does not lend itself to ready computer solutions. In Part II, the general analysis was applied to the study of equilibrium and longitudinal stability about equilibrium of an aircraft having longitudinal flexibility only. A monograph by Taylor and Woodcock[6] consists of two parts representing different approaches to the same problem. In Part I, Taylor presents a very lucid summary of the equations of motion for deformable aircraft derived by Bisplinghoff and Ashley[4] and by Milne.[5] Following a reduction to scalar form, the equations are simplified to permit the study of some special cases. In Part II, Woodcock uses an unorthodox form of Lagrange's equations to derive scalar perturbation equations of motion about a given "datum motion," not necessarily corresponding to steady level rectilinear flight; the equations are in terms of body-fixed axes. The question of aerodynamics receives scant attention in both parts. An extensive report by Dusto et al.,[7] resulting in a computer program known as FLEXSTAB, integrates flexible body mechanics with a low frequency aerodynamics employing linear influence coefficients. The flexible aircraft mechanics uses free vibration modes superimposed on rigid body dynamics. Aerodynamic influence coefficients are derived using a paneling scheme lending itself to empirical corrections. The equations are expressed in terms of steady perturbations about a reference motion to determine dynamic stability by characteristic roots or by time histories following an initial perturbation or some gust disturbance. There are two major concerns. The first consists of the fact that the structural dynamics formulation is in terms of mean axes and the aerodynamics is in terms of a different set of axes, namely, "fluid axes," where the latter move with a steady velocity relative to the undeformed aircraft body axes; using two different sets of axes in the same formulation, without making the necessary transformation from one set to another, is a very questionable

proposition. The second source of concern is the time required to run FLEXSTAB (see Ref. 24). Several analytical methods for mathematical modeling of aircraft active control system design are described by Roger,[8] placing the emphasis on aerodynamics. Inconsistencies in control configured vehicles are highlighted by Schwanz.[9] He suggests that familiarity of flight control specialists with a broad spectrum of pertinent disciplines, including aerodynamics, structures, modern dynamics and control, can minimize and perhaps avoid altogether these inconsistencies. Free-free dynamic analyses of forward swept wing aircraft by Miller, Wykes and Brosnan[10] have shown that the static aeroelastic divergence exhibited by a cantilevered forward swept wing is replaced by a low-frequency flutter mode due to coupling between the wing divergent mode and the aircraft short-period mode. This coupling is shown to have detrimental effects on flying qualities, ride qualities and gust loads, but these effects can be minimized by an active flutter control system. In the same spirit, Weisshaar and Zeiler[11] discuss the importance of including aircraft rigid-body modes in the aeroelastic analysis of forward swept wing aircraft. They show that body-freedom flutter and aircraft aeroelastic divergence, not wing divergence, are the primary aeroelastic instabilities. Rodden and Love[12] point out that equations of motion derived using mean axes for the inertial terms and axes attached to the undeformed structure for the flexibility terms are likely to be incorrect; such flexibility terms are obtained when using structural influence coefficients. Cerra, Calico and Noll [13] developed a linear model of an elastic aircraft providing the capability of analyzing the coupling between the rigid body motions and the elastic motions. The model can be used for stability and control analyses. As in Ref. 4, the rigid body translations, rigid body rotations and elastic deformations are assumed to be inertially decoupled. A framework for constructing simulation models for flexible aircraft is described by Arbuckle, Buttrill and Zeiler.[14] The objectives are to increase simulation model fidelity and to reduce the time required for developing and modifying these models. The framework has been applied to the development of an open-loop F/A-18 simulation model. Buttrill, Zeiler and Arbuckle[15] considered a mathematical model integrating nonlinear rigid body mechanics and linear aeroelasticity in conjunction with Lagrangian mechanics to derive the equations of motion for flexible aircraft. Undamped vibration modes satisfying first-order mean axes constraints were used as generalized coordinates. Considering a model of an F/A-18 aircraft, elastic modes significantly affected by inertial coupling were found to be aerodynamically decoupled from the rest of the model. Zeiler and Buttrill[16] used the extended Hamilton principle to derive equations of motion for a flexible body. The equations include inertial terms due to flexibility, as well as terms coupling rigid body and flexible momenta. In addition, a nonlin-

ear strain-displacement relation permits centrifugal stiffening to be taken into account. The equations are used to simulate the motion of a structure spinning initially about an unstable principal axis in gravity-free vacuum. Using Lagrange's equations, Waszak and Schmidt[17] derived the equations of motion for a flexible aircraft. The strip theory was used to obtain closed-form integral expressions for the generalized aerodynamic forces. Moreover, the use of mean axes permitted inertial decoupling of the rigid body translations, rigid body rotations and elastic deformations, the latter being expressed in terms of aircraft vibration modes. The modeling method was applied to a generic elastic aircraft, and the model was used for a parametric study of the flexibility effects. Nonlinear equations of motion for elastic panels in an aircraft executing a pull-up maneuver of given velocity and angular velocity were derived by Sipcic and Morino.[18] The effect of the maneuver on the flutter speed and on the limit cycle amplitude was discussed for various load conditions. Accurate modeling of aeroelastic vehicles, with emphasis on the rigid body and elastic degrees of freedom, was discussed by Waszak, Buttrill and Schmidt.[19] A comparison of the approach of Ref. 17 on the one hand and that of Refs. 15 and 16 on the other hand was presented and various model reduction techniques were reviewed. An integrated analytical framework for modeling elastic hypersonic flight vehicles was developed by Bilimoria and Schmidt.[20] A Lagrangian approach was used to derive equations of motion including rigid body motions and elastic deformations, as well as effects due to fluid flow, rotating machinery, wind and a spherical rotating Earth. The elastic deformations are represented in terms of modal coordinates relative to mean axes. A paper by Olsen[21] reveals new insights in the aeroelasticity and flight mechanics of flexible aircraft by obtaining and solving the equations of motion for an accelerating, rotating aircraft. General equations in terms of quasi-coordinates are first obtained and then reduced to the case of a "flat" airplane. The influence of gusts on the dynamics of large flexible aircraft is analyzed by Teufel, Hanel and Well,[22] who present an integrated flight and aeroelastic control law reducing gust sensitivity. Moreover, the control laws, designed by μ-synthesis, are such that flight maneuvers do not excite elastic motions. König and Schuler[23] describe how an integral model for large flexible aircraft can be derived and how an integral control, covering flight control, load control and structural mode control, can be designed by multiobjective parameter optimization. Samareh and Bhatia[24] presented a unified three-dimensional approach that reduces the number of interactions among various disciplines by using a computer-aided design model. Results were presented for a blended wing body and a high-speed civil transport. Schmidt and Raney[25] considered the effects of flexibility on the flight dynamics of large flexible aircraft. In particular, when the fre-

quencies of the lower elastic modes approach those of the rigid body modes the handling characteristics can suffer and the flight control system design tends to become significantly more complex. Expressing the motion in terms of components along mean axes, they add the flexible degrees of freedom to an existing simulation model of the vehicle's rigid body dynamics. The NASA Langley Research Center simulation facility was used to obtain the dynamic response of two different aircraft.

With some exceptions, the equations of motion in Refs. 3-23,25 were derived either by means of Newtonian mechanics or by means of standard Lagrange's equations. These approaches are more suitable when the motions are expressed in terms of inertial axes and/or when the rotations are in terms of Euler's angles. Yet, in the case of aircraft it is more convenient to express the motion in terms of components along body axes. In this regard, we should point out that this is common practice in flight dynamics, in which case the angular velocities in terms of body axes are the well-known roll, pitch and yaw. Of course, equations in terms of inertial axes and/or Eulerian angles can always be transformed into equations in terms of body axes through coordinate transformations. It is appreciably simpler, however, to derive the equations of motion directly in terms of body axes, which can be done through the use of Lagrange's equations in terms of quasi-coordinates.[26]

Motivated by problems in dynamics of spacecraft with flexible appendages, Meirovitch and Nelson[27] derived for the first time hybrid (ordinary and partial) differential equations of motion coupling rigid body rotations and elastic deformations. The elastic deformations were measured relative to a set of body axes attached to the undeformed spacecraft and the rotational motions were in terms of quasi-coordinates. The explicit formulation of Ref. 27 was extended by Meirovitch[28] to a generic whole flexible body by deriving a set of hybrid equations of motion in terms of quasi-coordinates, treating for the first time translational velocities as quasi-velocities; the equations were then cast in state form. The equations of motion in terms of quasi-coordinates of Ref. 27 were used by Platus[29] to derive coupled equations of motion governing the aeroelastic stability of spinning flexible missiles. The coupling between the elastic deflections and rigid-body motions was nonlinear, but the equations were linearized so as to permit a stability analysis. The developments of Ref. 28 were extended by Meirovitch[30] and Meirovitch and Stemple[31] to flexible multibody systems. Then, the approach of Refs. 28, 30 and 31 was used by Meirovitch[32] to produce a definitive unified theory for the flight dynamics and aeroelasticity of whole aircraft. Generic state equations describing the flight of flexible aircraft were first derived in hybrid form and subsequently

discretized in space. Then, using a perturbation approach, the discrete state equations were separated into a set of nonlinear flight dynamics equations for the rigid body variables and a set of linear extended aeroelasticity equations for the elastic variables and perturbations in the rigid body variables. Nydick and Friedmann[33] applied the equations of motion in terms of quasi-coordinates derived in Ref. 28 to the analysis of a hypersonic vehicle in free flight. To this end, they simplified the equations by considering only the pitch and plunge rigid body degrees of freedom and small elastic displacements. The nonlinear equations were linearized about a trim state obtained by using a rigid body trim model and steady hypersonic aerodynamics. Flutter derivatives were calculated by means of piston theory. The generic formulation of Ref. 32 was used by Meirovitch and Tuzcu[34] to carry out the derivation of explicit equations of motion in terms of quasi-coordinates for a flexible aircraft model and to cast the equations in a special state form suitable for simulation on a computer. Due to computational speed advantages, the aerodynamic forces were derived by means of strip theory. Finally, equations for flight dynamics and extended aeroelasticity were derived.

The present dissertation represents an extension of the developments in Ref. 34. In addition to some modeling refinements, the paper contains a numerical example for a model of a flexible aircraft containing 76 states, 12 rigid body states and 64 elastic states. Several flight dynamics problems are considered, such as the steady level cruise, a steady level turn maneuver and a pull-up maneuver. The corresponding extended aeroelasticity problems are derived and used to design feedback controls guaranteeing the vanishing of the rigid body perturbations and the elastic vibration, and hence the stability of the maneuver and the comfort of the flight. The control design consists of a linear quadratic regulator in conjunction with a stochastic observer.

Chapter 2

Equations of Motion

2.1 Hybrid State Equations in Terms of Quasi-Coordinates

We regard the aircraft model shown in Fig. 1 as a flexible multibody system subjected to gravity, aerodynamic, propulsion and control forces, where the bodies can be broadly identified as the fuselage, wing and empennage. The motion of the aircraft can be conveniently described by attaching a reference frame $x_f y_f z_f$ to the undeformed fuselage (Fig. 1), as well as corresponding reference frames $x_w y_w z_w$ and $x_e y_e z_e$ to the wing and empennage, where the various reference frames represent respective body axes. Then, the motion can be described by six rigid body degrees of freedom of the fuselage body axes, three translations and three rotations, and by the elastic deformation of every point of each flexible component relative to the respective body axes.

From Ref. 32, and making provisions for members in torsion, as well as for structural damping, the hybrid equations of motion for the whole flexible aircraft in terms of quasi-

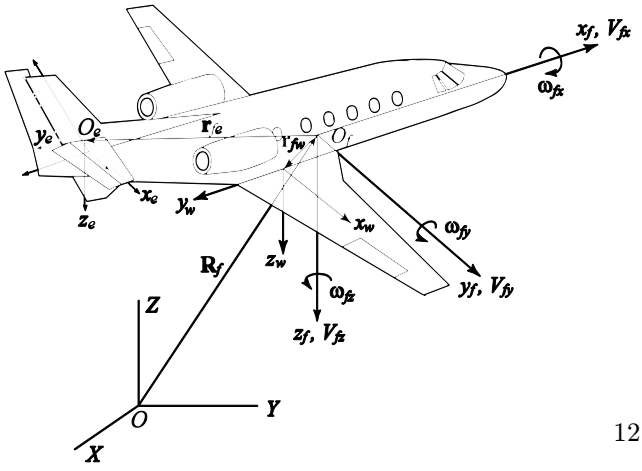

Figure 1. Flexible Aircraft Model

coordinates have the generic form

$$\begin{aligned}
&\frac{d}{dt}\left(\frac{\partial L}{\partial \mathbf{V}_f}\right)+\tilde{\omega}_f\frac{\partial L}{\partial \mathbf{V}_f}-C_f\frac{\partial L}{\partial \mathbf{R}_f}=\mathbf{F}\\
&\frac{d}{dt}\left(\frac{\partial L}{\partial \boldsymbol{\omega}_f}\right)+\tilde{V}_f\frac{\partial L}{\partial \mathbf{V}_f}+\tilde{\omega}_f\frac{\partial L}{\partial \boldsymbol{\omega}_f}-(E_f^T)^{-1}\frac{\partial L}{\partial \boldsymbol{\theta}_f}=\mathbf{M}\\
&\frac{\partial}{\partial t}\left(\frac{\partial \hat{L}_i}{\partial \mathbf{v}_i}\right)-\frac{\partial \hat{L}_i}{\partial \mathbf{u}_i}+\frac{\partial \hat{\mathcal{F}}_{ui}}{\partial \dot{\mathbf{u}}_i}+\mathcal{L}_{ui}\mathbf{u}_i=\hat{\mathbf{U}}_i,\quad \frac{\partial}{\partial t}\left(\frac{\partial \hat{L}_i}{\partial \boldsymbol{\alpha}_i}\right)+\frac{\partial \hat{\mathcal{F}}_{\alpha i}}{\partial \dot{\boldsymbol{\psi}}_i}+\mathcal{L}_{\psi i}\boldsymbol{\psi}_i=\hat{\boldsymbol{\Psi}}_i,\\
&\qquad\qquad\qquad\qquad\qquad\qquad\qquad\qquad\qquad\qquad i=f\ (\text{fuselage}),\ w\ (\text{wing}),\ e\ (\text{empennage})
\end{aligned}\tag{2.1}$$

where

L = Lagrangian for the whole aircraft

$\mathbf{V}_f, \boldsymbol{\omega}_f$ = vector of translational, angular quasi-velocities of $x_f y_f z_f$

$\tilde{V}_f, \tilde{\omega}_f$ = skew symmetric matrices derived from $\mathbf{V}_f,\ \boldsymbol{\omega}_f$

C_f = matrix of direction cosines between $x_f y_f z_f$ and XYZ (inertial axes)

$\mathbf{R}_f = \mathbf{R}_f(X_f, Y_f, Z_f)$ = position vector of origin O_f of $x_f y_f z_f$ relative to XYZ

E_f = matrix relating Eulerian velocities to angular quasi-velocities

$\boldsymbol{\theta}_f$ = symbolic vector of Eulerian angles between $x_f y_f z_f$ and XYZ

$\mathbf{u}_i, \mathbf{v}_i$ = elastic displacement, velocity vectors for body i

$\boldsymbol{\psi}_i, \boldsymbol{\alpha}_i$ = elastic angular displacement, velocity vectors for body i

$\hat{L}_i$ = Lagrangian density for body i exclusive of strain energy

$\hat{\mathcal{F}}_{ui}, \hat{\mathcal{F}}_{\psi i}$ = Rayleigh's dissipation function[35] densities for body i

$\mathcal{L}_{ui}, \mathcal{L}_{\psi i}$ = matrices of stiffness differential operators for body i

$\mathbf{F}, \mathbf{M}$ = resultant of gravity, aerodynamic, propulsion and control force, moment vectors acting on the whole aircraft in terms of fuselage body axes components

$\hat{\mathbf{U}}_i, \boldsymbol{\Psi}_i$ = resultant of gravity, aerodynamic, propulsion and control force, moment density vectors for body i

Assuming that axes $x_f y_f z_f$ are obtained from axes XYZ through the sequence of rotations ψ about Z to axes $x_1 y_1 z_1$, θ about y_1 to $x_2 y_2 z_2$ and ϕ about x_2 to $x_f y_f z_f$, the matrices C_f

and E_f have the form[35]

$$C_f = \begin{bmatrix} \mathrm{c}\psi\mathrm{c}\theta & \mathrm{s}\psi\mathrm{c}\theta & -\mathrm{s}\theta \\ \mathrm{c}\psi\mathrm{s}\theta\mathrm{s}\phi - \mathrm{s}\psi\mathrm{c}\phi & \mathrm{s}\psi\mathrm{s}\theta\mathrm{s}\phi + \mathrm{c}\psi\mathrm{c}\phi & \mathrm{c}\theta\mathrm{s}\phi \\ \mathrm{c}\psi\mathrm{s}\theta\mathrm{c}\phi + \mathrm{s}\psi\mathrm{s}\phi & \mathrm{s}\psi\mathrm{s}\theta\mathrm{c}\phi - \mathrm{c}\psi\mathrm{s}\phi & \mathrm{c}\theta\mathrm{c}\phi \end{bmatrix}$$
$$E_f = \begin{bmatrix} 1 & 0 & -\mathrm{s}\theta \\ 0 & \mathrm{c}\phi & \mathrm{c}\theta\mathrm{s}\phi \\ 0 & -\mathrm{s}\phi & \mathrm{c}\theta\mathrm{c}\phi \end{bmatrix} \tag{2.2}$$

in which s = sin, c = cos. The elastic displacement vectors $\mathbf{u}_i$ and $\boldsymbol{\psi}_i$ are subject to given boundary conditions at the interface between bodies. Equations (2.1) involve the Lagrangian $L = T - V$, in which T is the kinetic energy and V the potential energy, the Rayleigh dissipation function densities $\hat{\mathcal{F}}_{ui}$ and $\hat{\mathcal{F}}_{\psi i}$, which contain the information about the structural damping, and the stiffness operators $\mathcal{L}_{ui}$ and $\mathcal{L}_{\psi i}$, which are related to the strain energy. Before more explicit equations of motion can be derived, it is necessary to produce these quantities. The kinetic energy for the whole aircraft can be written as

$$T = T_f + T_w + T_e \tag{2.3}$$

where

$$T_i = \tfrac{1}{2}\int \bar{\mathbf{V}}_i^T \bar{\mathbf{V}}_i dm_i, \;\; i = f, w, e \tag{2.4}$$

are kinetic energies of the individual components, in which $\bar{\mathbf{V}}_i$ are velocity vectors of typical points in the components and dm_i are corresponding mass differential elements. The velocity of a point in the fuselage can be written as

$$\begin{aligned} \bar{\mathbf{V}}_f(\mathbf{r}_f, t) &= \mathbf{V}_f(t) + [\tilde{r}_f + \tilde{u}_f(\mathbf{r}_f, t)]^T [\boldsymbol{\omega}_f(t) + \boldsymbol{\alpha}_f(\mathbf{r}_f, t)] + \mathbf{v}_f(\mathbf{r}_f, t) \\ &\cong \mathbf{V}_f + (\tilde{r}_f + \tilde{u}_f)^T \boldsymbol{\omega}_f + \tilde{r}_f^T \boldsymbol{\alpha}_f + \mathbf{v}_f \end{aligned} \tag{2.5}$$

where $\mathbf{r}_f$ is the nominal position of the mass element dm_f, $\tilde{r}_f$ and $\tilde{u}_f$ are skew symmetric matrices[26] corresponding to $\mathbf{r}_f$ and $\mathbf{u}_f$ and $\mathbf{v}_f$ and $\boldsymbol{\alpha}_f$ are elastic displacements associated with bending and torsion, respectively. Then, denoting by C_w the matrix of direction cosines between $x_w y_w z_w$ and $x_f y_f z_f$, the velocity of a point on the wing has the expression

$$\begin{aligned} \bar{\mathbf{V}}_w(\mathbf{r}_w, t) &= C_w \bar{\mathbf{V}}_f(\mathbf{r}_{fw}, t) + \tilde{r}_w^T C_w [\boldsymbol{\Omega}_f(\mathbf{r}_{fw}, t) + \boldsymbol{\alpha}_f(\mathbf{r}_{fw}, t)] + [\tilde{r}_w + \tilde{u}_w(\mathbf{r}_w, t)]^T [\boldsymbol{\omega}_w(t) \\ &\quad + \boldsymbol{\alpha}_w(\mathbf{r}_w, t)] + \mathbf{v}_w(\mathbf{r}_w, t) \\ &\cong C_w \mathbf{V}_f + [C_w(\tilde{r}_{fw} + \tilde{u}_{fw})^T + (\tilde{r}_w + \tilde{u}_w)^T C_w] \boldsymbol{\omega}_f + \tilde{r}_w^T C_w (\boldsymbol{\Omega}_{fw} + \boldsymbol{\alpha}_{fw}) \\ &\quad + C_w(\mathbf{v}_{fw} + \tilde{r}_{fw}^T \boldsymbol{\alpha}_{fw}) + \tilde{r}_w^T \boldsymbol{\alpha}_w + \mathbf{v}_w \end{aligned} \tag{2.6}$$

in which $\mathbf{r}_{fw}$ is the radius vector from the origin of $x_f y_f z_f$ to the origin of $x_w y_w z_w$,

$$\mathbf{\Omega}_{fw} = [0 \quad -\partial \dot{u}_{fz}/\partial x_f \quad \partial \dot{u}_{fy}/\partial x_f]\big|_{\mathbf{r}_{fw}}^{T} \tag{2.7}$$

is the angular velocity of the fuselage at $\mathbf{r}_{fw}$ due to bending and $\boldsymbol{\alpha}_{fw} = [\alpha_{fw} \;\; 0 \;\; 0]\big|_{\mathbf{r}_{fw}}^{T}$ is the elastic velocity of the fuselage at $\mathbf{r}_{fw}$ due to torsion. The velocity $\bar{\mathbf{V}}_e(\mathbf{r}_e, t)$ of a point on the empennage can be obtained from Eq. (2.6) by simply replacing w by e. The total kinetic energy can be expressed in the general form

$$T = \tfrac{1}{2}\int \bar{\mathbf{V}}_f^T \bar{\mathbf{V}}_f dm_f + \tfrac{1}{2}\int \bar{\mathbf{V}}_w^T \bar{\mathbf{V}}_w dm_w + \tfrac{1}{2}\int \bar{\mathbf{V}}_e^T \bar{\mathbf{V}}_e dm_e \tag{2.8}$$

The potential energy can be expressed in terms of the operators $\mathcal{L}_{ui},\ \mathcal{L}_{\psi i}$ $(i = f, w, e)$, but is more conveniently expressed as the strain energy. Moreover, the Rayleigh dissipation function densities can be expressed in the form

$$\hat{\mathcal{F}}_{ui} = \tfrac{1}{2} c_{ui} EI_i \frac{\partial^2 \dot{\mathbf{u}}_i^T}{\partial x_i^2}\frac{\partial^2 \dot{\mathbf{u}}_i}{\partial x_i^2},\ \hat{\mathcal{F}}_{\psi i} = \tfrac{1}{2} c_{\psi i} GJ_i \frac{\partial \dot{\boldsymbol{\psi}}_i^T}{\partial x_i}\frac{\partial \dot{\boldsymbol{\psi}}_i}{\partial x_i},\ i = f, w, e \tag{2.9}$$

where $c_{ui},\ c_{\psi i}$ are damping functions and $EI_i,\ GJ_i$ are flexural and torsional rigidities $(i = f, w, e)$.

Equation (2.8), the potential energy V, the functions $\hat{\mathcal{F}}_{ui}$ and $\hat{\mathcal{F}}_{\psi i}$ and the operators $\mathcal{L}_{ui}$ and $\mathcal{L}_{\psi i}$, when inserted into Eqs. (2.1), permit the derivation of explicit hybrid equations of motion. Because for all practical purposes it is not feasible to work with hybrid equations, we do not pursue this subject any farther, and approximate instead the partial differential equations by sets of ordinary differential equations.

2.2 Spatial Discretization of the Distributed Variables

For the most part, aircraft are modeled as discrete systems, either by regarding the inertia and stiffness properties as lumped from the onset or by describing their elastic motions in terms of aircraft structural modes. For undamped structures in vacuum, the use of structural modes yields complete decoupling, i.e., it yields a set of independent modal equations of motion. In the case of aircraft, however, complete decoupling is not possible, even when aircraft structural modes are used, as the aerodynamic forces guarantee that the equations of motion remain coupled. Spatial discretization using aircraft structural modes not only does not offer any particular advantage but also has the disadvantage that some geometric details of the aircraft are lost in the process. Hence, a discretization procedure that does

not require the structural modes, which may not be readily available and/or may not be compatible with the rest of the formulation, and retains some sense of the aircraft geometry seems desirable. Consistent with this, we consider spatial discretization of the individual aircraft components separately. To this end, we use either the Galerkin method or the finite element method[36] and introduce the expansions

$$\mathbf{u}_i(\mathbf{r}_i,t)=\Phi_{ui}(\mathbf{r}_i)\mathbf{q}_{ui}(t),\ \boldsymbol{\psi}_i(\mathbf{r}_i,t)=\Phi_{\psi i}(\mathbf{r}_i)\mathbf{q}_{\psi i}(t),\ i=f,w,e \tag{2.10}$$

where Φ_{ui} and $\Phi_{\psi i}$ are matrices of shape functions and $\mathbf{q}_{ui}$ and $\mathbf{q}_{\psi i}$ are corresponding vectors of generalized coordinates. Note that the choice of shape functions is very important. Indeed, for accurate modeling, the shape functions must reflect the mass and stiffness characteristics of the components. Some guidelines concerning the choice of shape functions can be found in Ref. 36. Moreover, we denote the associated generalized velocities by

$$\mathbf{s}_{ui}(t)=\dot{\mathbf{q}}_{ui}(t),\ \mathbf{s}_{\psi i}(t)=\dot{\mathbf{q}}_{\psi i}(t),\ i=f,w,e \tag{2.11}$$

In anticipation of later needs, we write the velocity vectors for points on the individual components in the two discrete forms

$$\begin{aligned}\bar{\mathbf{V}}_f(\mathbf{r}_f,t)&=\mathbf{V}_f+(\tilde{r}_f+\widetilde{\Phi_{uf}\mathbf{q}_{uf}})^T\boldsymbol{\omega}_f+\Phi_{uf}\mathbf{s}_{uf}+\tilde{r}_f^T\Phi_{\psi f}\mathbf{s}_{\psi f}\\&=\mathbf{V}_f+\tilde{r}_f^T\boldsymbol{\omega}_f+\tilde{\omega}_f\Phi_{uf}\mathbf{q}_{uf}+\Phi_{uf}\mathbf{s}_{uf}+\tilde{r}_f^T\Phi_{\psi f}\mathbf{s}_{\psi f}\end{aligned}$$

$$\begin{aligned}\bar{\mathbf{V}}_w(\mathbf{r}_w,t)&=C_w\mathbf{V}_f+[C_w(\tilde{r}_{fw}+\widetilde{\Phi_{ufw}\mathbf{q}_{uf}})^T+(\tilde{r}_w+\widetilde{\Phi_{uw}\mathbf{q}_{uw}})^TC_w]\boldsymbol{\omega}_f\\&\quad+(\tilde{r}_w^TC_w\Delta\Phi_{ufw}+C_w\Phi_{ufw})\mathbf{s}_{uf}+\Phi_{uw}\mathbf{s}_{uw}\\&\quad+(\tilde{r}_w^TC_w\Phi_{\psi fw}+C_w\tilde{r}_{fw}^T\Phi_{\psi fw})\mathbf{s}_{\psi f}+\tilde{r}_w^T\Phi_{\psi w}\mathbf{s}_{\psi w}\\&=C_w\mathbf{V}_f+(C_w\tilde{r}_{fw}^T+\tilde{r}_w^TC_w)\boldsymbol{\omega}_f+C_w\tilde{\omega}_f\Phi_{ufw}\mathbf{q}_{uf}+\widetilde{C_w\boldsymbol{\omega}_f}\Phi_{uw}\mathbf{q}_{uw}\\&\quad+(\tilde{r}_w^TC_w\Delta\Phi_{ufw}+C_w\Phi_{ufw})\mathbf{s}_{uf}+\Phi_{uw}\mathbf{s}_{uw}\\&\quad+(\tilde{r}_w^TC_w\Phi_{\psi fw}+C_w\tilde{r}_{fw}^T\Phi_{\psi fw})\mathbf{s}_{\psi f}+\tilde{r}_w^T\Phi_{\psi w}\mathbf{s}_{\psi w}\end{aligned} \tag{2.12}$$

in which

$$\Delta=\begin{bmatrix}0&0\\0&-\partial/\partial x_f\\\partial/\partial x_f&0\end{bmatrix},\ \Phi_{uf}=\begin{bmatrix}\boldsymbol{\phi}_{ufy}^T&\mathbf{0}^T\\\mathbf{0}^T&\boldsymbol{\phi}_{ufz}^T\end{bmatrix},\ \Phi_{ufw}=\Phi_{uf}(\mathbf{r}_{fw}) \tag{2.13}$$

Expression analogous to Φ_{uf} can be written for $\Phi_{\psi f}$ and $\Phi_{\psi fw}$. Moreover, $\bar{\mathbf{V}}_e(\mathbf{r}_e,t)$ can be obtained from $\bar{\mathbf{V}}_w(\mathbf{r}_w,t)$ by simply replacing w by e. Inserting Eqs. (2.12) into Eq. (2.8) and carrying out the indicated operations, we can write the kinetic energy in the compact form

$$T=\tfrac{1}{2}\int\bar{\mathbf{V}}_f^T\bar{\mathbf{V}}_f dm_f+\tfrac{1}{2}\int\bar{\mathbf{V}}_w^T\bar{\mathbf{V}}_w dm_w+\tfrac{1}{2}\int\bar{\mathbf{V}}_e^T\bar{\mathbf{V}}_e dm_e=\tfrac{1}{2}\mathbf{V}^TM\mathbf{V} \tag{2.14}$$

where $\mathbf{V} = [\mathbf{V}_f^T \ \boldsymbol{\omega}_f^T \ \mathbf{s}_{uf}^T \ \mathbf{s}_{uw}^T \ \mathbf{s}_{ue}^T \ \mathbf{s}_{\psi f}^T \ \mathbf{s}_{\psi w}^T \ \mathbf{s}_{\psi e}^T]^T = [\mathbf{V}_1^T \ \ \mathbf{V}_2^T \dots \mathbf{V}_8^T]^T$ is the discrete system velocity vector and $M = [M_{ij}]$ is the system mass matrix, a matrix that can be expressed in partitioned form with the submatrices

$$
\begin{aligned}
&M_{11} = mI, \ M_{12} = \tilde{S}^T, \\
&M_{13} = \int \Phi_{uf} dm_f + \int C_w^T (\tilde{r}_w^T C_w \Delta\Phi_{ufw} + C_w \Phi_{ufw}) dm_w + \int C_e^T (\tilde{r}_e^T C_e \Delta\Phi_{ufe} + C_e \Phi_{ufe}) dm_e \\
&M_{14} = C_w^T \int \Phi_{uw} dm_w, \ M_{15} = C_e^T \int \Phi_{ue} dm_e \\
&M_{16} = \int \tilde{r}_f^T \Phi_{\psi f} dm_f + C_w^T \int (\tilde{r}_w^T C_w \Phi_{\psi fw} + C_w \tilde{r}_{fw}^T \Phi_{\psi fw}) dm_w + C_e^T \int (\tilde{r}_e^T C_e \Phi_{\psi fe} \\
&\qquad + C_e \tilde{r}_{fe}^T \Phi_{\psi fe}) dm_e \\
&M_{17} = C_w^T \int \tilde{r}_w^T \Phi_{\psi w} dm_w, \ M_{18} = C_e^T \int \tilde{r}_e^T \Phi_{\psi e} dm_e \\
&M_{21} = M_{12}^T, \ M_{22} = J \\
&M_{23} = \int (\tilde{r}_f + \widetilde{\Phi_{uf} \mathbf{q}_{uf}}) \Phi_{uf} dm_f + \int [C_w (\tilde{r}_{fw} + \widetilde{\Phi_{ufw} \mathbf{q}_{uf}})^T + (\tilde{r}_w + \widetilde{\Phi_{uw} \mathbf{q}_{uw}})^T C_w]^T \\
&\qquad \times (\tilde{r}_w^T C_w \Delta\Phi_{ufw} + C_w \Phi_{ufw}) dm_w + \int [C_e (\tilde{r}_{fe} + \widetilde{\Phi_{ufe} \mathbf{q}_{uf}})^T + (\tilde{r}_e + \widetilde{\Phi_{ue} \mathbf{q}_{ue}})^T C_e]^T \\
&\qquad \times (\tilde{r}_e^T C_e \Delta\Phi_{ufe} + C_e \Phi_{ufe}) dm_e \\
&M_{24} = \int [C_w (\tilde{r}_{fw} + \widetilde{\Phi_{ufw} \mathbf{q}_{uf}})^T + (\tilde{r}_w + \widetilde{\Phi_{uw} \mathbf{q}_{uw}})^T C_w]^T \Phi_{uw} dm_w \\
&M_{25} = \int [C_e (\tilde{r}_{fe} + \widetilde{\Phi_{ufe} \mathbf{q}_{uf}})^T + (\tilde{r}_e + \widetilde{\Phi_{ue} \mathbf{q}_{ue}})^T C_e]^T \Phi_{ue} dm_e \\
&M_{26} = \int (\tilde{r}_f + \widetilde{\Phi_{uf} \mathbf{q}_{uf}}) \tilde{r}_f^T \Phi_{\psi f} dm_f + \int [C_w (\tilde{r}_{fw} + \widetilde{\Phi_{ufw} \mathbf{q}_{uf}})^T + (\tilde{r}_w + \widetilde{\Phi_{uw} \mathbf{q}_{uw}})^T C_w]^T \\
&\qquad \times (\tilde{r}_w^T C_w \Phi_{\psi fw} + C_w \tilde{r}_{fw}^T \Phi_{\psi fw}) dm_w + \int [C_e (\tilde{r}_{fe} + \widetilde{\Phi_{ufe} \mathbf{q}_{uf}})^T + (\tilde{r}_e + \widetilde{\Phi_{ue} \mathbf{q}_{ue}})^T C_e]^T \\
&\qquad \times (\tilde{r}_e^T C_e \Phi_{\psi fe} + C_e \tilde{r}_{fe}^T \Phi_{\psi fe}) dm_e \\
&M_{27} = \int [C_w (\tilde{r}_{fw} + \widetilde{\Phi_{ufw} \mathbf{q}_{uf}})^T + (\tilde{r}_w + \widetilde{\Phi_{uw} \mathbf{q}_{uw}})^T C_w]^T \tilde{r}_w^T \Phi_{\psi w} dm_w \\
&M_{28} = \int [C_e (\tilde{r}_{fe} + \widetilde{\Phi_{ufe} \mathbf{q}_{uf}})^T + (\tilde{r}_e + \widetilde{\Phi_{ue} \mathbf{q}_{ue}})^T C_e]^T \tilde{r}_e^T \Phi_{\psi e} dm_e \\
&M_{31} = M_{13}^T, \ M_{32} = M_{23}^T \\
&M_{33} = \int \Phi_{uf}^T \Phi_{uf} dm_f + \int (\tilde{r}_w^T C_w \Delta\Phi_{ufw} + C_w \Phi_{ufw})^T (\tilde{r}_w^T C_w \Delta\Phi_{ufw} + C_w \Phi_{ufw}) dm_w \\
&\qquad + \int (\tilde{r}_e^T C_e \Delta\Phi_{ufe} + C_e \Phi_{ufe})^T (\tilde{r}_e^T C_e \Delta\Phi_{ufe} + C_e \Phi_{ufe}) dm_e \\
&M_{34} = \int (\tilde{r}_w^T C_w \Delta\Phi_{ufw} + C_w \Phi_{ufw})^T \Phi_{uw} dm_w \\
&M_{35} = \int (\tilde{r}_e^T C_e \Delta\Phi_{ufe} + C_e \Phi_{ufe})^T \Phi_{ue} dm_e \\
&M_{36} = \int \Phi_{uf}^T \tilde{r}_f^T \Phi_{\psi f} dm_f + \int (\tilde{r}_w^T C_w \Delta\Phi_{ufw} + C_w \Phi_{ufw})^T (\tilde{r}_w^T C_w \Phi_{\psi fw} + C_w \tilde{r}_{fw}^T \Phi_{\psi fw}) dm_w \\
&\qquad + \int (\tilde{r}_e^T C_e \Delta\Phi_{ufe} + C_e \Phi_{ufe})^T (\tilde{r}_e^T C_e \Phi_{\psi fe} + C_e \tilde{r}_{fe}^T \Phi_{\psi fe}) dm_e
\end{aligned}
\tag{2.15}
$$

$$
\begin{aligned}
&M_{37} = \int (\tilde{r}_w^T C_w \Delta\Phi_{ufw} + C_w \Phi_{ufw})^T \tilde{r}_w^T \Phi_{\psi w} dm_w \\
&M_{38} = \int (\tilde{r}_e^T C_e \Delta\Phi_{ufe} + C_e \Phi_{ufe})^T \tilde{r}_e^T \Phi_{\psi e} dm_e \\
&M_{41} = M_{14}^T,\ M_{42} = M_{24}^T,\ M_{43} = M_{34}^T,\ M_{44} = \int \Phi_{uw}^T \Phi_{uw} dm_w,\ M_{45} = 0 \\
&M_{46} = \int \Phi_{uw}^T (\tilde{r}_w^T C_w \Phi_{\psi fw} + C_w \tilde{r}_{fw}^T \Phi_{\psi fw}) dm_w,\ M_{47} = \int \Phi_{uw}^T \tilde{r}_w^T \Phi_{\psi w} dm_w\ , M_{48} = 0 \\
&M_{51} = M_{15}^T,\ M_{52} = M_{25}^T,\ M_{53} = M_{35}^T,\ M_{54} = M_{45}^T,\ M_{55} = \int \Phi_{ue}^T \Phi_{ue} dm_e \\
&M_{56} = \int \Phi_{ue}^T (\tilde{r}_e^T C_e \Phi_{\psi fe} + C_e \tilde{r}_{fe}^T \Phi_{\psi fe}) dm_e,\ M_{57} = 0,\ M_{58} = \int \Phi_{ue}^T \tilde{r}_e^T \Phi_{\psi e} dm_e \\
&M_{61} = M_{16}^T,\ M_{62} = M_{26}^T,\ M_{63} = M_{36}^T,\ M_{64} = M_{46}^T,\ M_{65} = M_{56}^T \\
&M_{66} = \int \Phi_{\psi f}^T \tilde{r}_f \tilde{r}_f^T \Phi_{\psi f} dm_f + \int (\tilde{r}_w^T C_w \Phi_{\psi fw} + C_w \tilde{r}_{fw}^T \Phi_{\psi fw})^T (\tilde{r}_w^T C_w \Phi_{\psi fw} + C_w \tilde{r}_{fw}^T \Phi_{\psi fw}) dm_w \\
&\qquad + \int (\tilde{r}_e^T C_e \Phi_{\psi fe} + C_e \tilde{r}_{fe}^T \Phi_{\psi fe})^T (\tilde{r}_e^T C_e \Phi_{\psi fe} + C_e \tilde{r}_{fe}^T \Phi_{\psi fe}) dm_e \\
&M_{67} = \int (\tilde{r}_w^T C_w \Phi_{\psi fw} + C_w \tilde{r}_{fw}^T \Phi_{\psi fw})^T \tilde{r}_w^T \Phi_{\psi w} dm_w \\
&M_{68} = \int (\tilde{r}_e^T C_e \Phi_{\psi fe} + C_e \tilde{r}_{fe}^T \Phi_{\psi fe})^T \tilde{r}_e^T \Phi_{\psi e} dm_e \\
&M_{71} = M_{17}^T,\ M_{72} = M_{27}^T,\ M_{73} = M_{37}^T,\ M_{74} = M_{47}^T,\ M_{75} = M_{57}^T,\ M_{76} = M_{67}^T \\
&M_{77} = \int \Phi_{\psi w}^T \tilde{r}_w \tilde{r}_w^T \Phi_{\psi w} dm_w,\ M_{78} = 0 \\
&M_{81} = M_{18}^T,\ M_{82} = M_{28}^T,\ M_{83} = M_{38}^T,\ M_{84} = M_{48}^T,\ M_{85} = M_{58}^T,\ M_{86} = M_{68}^T,\ M_{87} = M_{78}^T \\
&M_{88} = \int \Phi_{\psi e}^T \tilde{r}_e \tilde{r}_e^T \Phi_{\psi e} dm_e
\end{aligned}
$$

in which m is the aircraft total mass,

$$
\begin{aligned}
\tilde{S} = &\int (\tilde{r}_f + \widetilde{\Phi_{uf}\mathbf{q}_{uf}}) dm_f + \int [(\tilde{r}_{fw} + \widetilde{\Phi_{ufw}\mathbf{q}_{uf}}) C_w^T + C_w^T (\tilde{r}_w + \widetilde{\Phi_{uw}\mathbf{q}_{uw}})] C_w dm_w \\
&+ \int [(\tilde{r}_{fe} + \widetilde{\Phi_{ufe}\mathbf{q}_{uf}}) C_e^T + C_e^T (\tilde{r}_e + \widetilde{\Phi_{ue}\mathbf{q}_{ue}})] C_e dm_e
\end{aligned} \tag{2.16}
$$

is the matrix of first moments of inertia of the *deformed* aircraft and

$$
\begin{aligned}
J = &\int (\tilde{r}_f + \widetilde{\Phi_{uf}\mathbf{q}_{uf}})^T (\tilde{r}_f + \widetilde{\Phi_{uf}\mathbf{q}_{uf}}) dm_f + \int [C_w (\tilde{r}_{fw} + \widetilde{\Phi_{ufw}\mathbf{q}_{uf}})^T + (\tilde{r}_w + \widetilde{\Phi_{uw}\mathbf{q}_{uw}})^T C_w]^T \\
&\times [C_w (\tilde{r}_{fw} + \widetilde{\Phi_{ufw}\mathbf{q}_{uf}})^T + (\tilde{r}_w + \widetilde{\Phi_{uw}\mathbf{q}_{uw}})^T C_w] dm_w + \int [C_e (\tilde{r}_{fe} + \widetilde{\Phi_{ufe}\mathbf{q}_{uf}})^T \\
&+ (\tilde{r}_e + \widetilde{\Phi_{ue}\mathbf{q}_{ue}})^T C_e]^T [C_e (\tilde{r}_{fe} + \widetilde{\Phi_{ufe}\mathbf{q}_{uf}})^T + (\tilde{r}_e + \widetilde{\Phi_{ue}\mathbf{q}_{ue}})^T C_e] dm_e
\end{aligned} \tag{2.17}
$$

is the inertia matrix of the deformed aircraft.

In a similar fashion, we insert Eqs. (2.10) into Eqs. (2.9), integrate over the respective components domains and obtain the generalized Rayleigh's dissipation functions

$$
\begin{aligned}
&\mathcal{F}_{ui} = \int_{D_i} \hat{\mathcal{F}}_{ui} dD_i = \tfrac{1}{2} \int_{D_i} c_{ui} E I_i \dot{\mathbf{q}}_{ui}^T \frac{d^2 \Phi_{ui}^T}{dx_i^2} \frac{d^2 \Phi_{ui}}{dx_i^2} \dot{\mathbf{q}}_{ui} dD_i = \tfrac{1}{2} \dot{\mathbf{q}}_{ui}^T C_{ui} \dot{\mathbf{q}}_{ui}, \\
&\mathcal{F}_{\psi i} = \int_{D_i} \hat{\mathcal{F}}_{\psi i} dD_i = \tfrac{1}{2} \int_{D_i} c_{\psi i} G J_i \dot{\mathbf{q}}_{\psi i}^T \frac{d\Phi_{\psi i}^T}{dx_i} \frac{d\Phi_{\psi i}}{dx_i} \dot{\mathbf{q}}_{\psi i} dD_i = \tfrac{1}{2} \dot{\mathbf{q}}_{\psi i}^T C_{\psi i} \dot{\mathbf{q}}_{\psi i},
\end{aligned} \qquad i = f, w, e \tag{2.18}
$$

where

$$C_{ui} = \int_{D_i} c_{ui} EI_i \frac{d^2\Phi_{ui}^T}{dx_i^2} \frac{d^2\Phi_{ui}}{dx_i^2} dD_i,\ C_{\psi i} = \int_{D_i} c_{\psi i} GJ_i \frac{d\Phi_{\psi i}^T}{dx_i} \frac{d\Phi_{\psi i}}{dx_i} dD_i,\ i = f, w, e \tag{2.19}$$

are damping matrices.

Next, we denote the momentum vector for the whole aircraft by $\mathbf{p} = [\mathbf{p}_{Vf}^T\ \mathbf{p}_{\omega f}^T\ \mathbf{p}_{uf}^T\ \mathbf{p}_{uw}^T\ \mathbf{p}_{ue}^T\ \mathbf{p}_{\psi f}^T\ \mathbf{p}_{\psi w}^T\ \mathbf{p}_{\psi e}^T]^T = [\mathbf{p}_1^T\ \mathbf{p}_2^T \dots \mathbf{p}_8^T]^T$, so that we can write

$$\mathbf{p} = \partial T / \partial \mathbf{V} = M\mathbf{V} \tag{2.20}$$

where the individual momenta are given by

$$\begin{aligned}
\mathbf{p}_{Vf} &= \partial T / \partial \mathbf{V}_f = \mathbf{p}_1 = \sum_{j=1}^{8} M_{1j}\mathbf{V}_j \\
\mathbf{p}_{\omega f} &= \partial T / \partial \boldsymbol{\omega}_f = \mathbf{p}_2 = \sum_{j=1}^{8} M_{2j}\mathbf{V}_j \\
\mathbf{p}_{uf} &= \partial T / \partial \mathbf{s}_{uf} = \mathbf{p}_3 = \sum_{j=1}^{8} M_{3j}\mathbf{V}_j \\
&\text{- -} \\
\mathbf{p}_{\psi e} &= \partial T / \partial \mathbf{s}_{\psi e} = \mathbf{p}_8 = \sum_{j=1}^{8} M_{8j}\mathbf{V}_j
\end{aligned} \tag{2.21}$$

Finally, adding some obvious kinematical identities to the discretized version of Eqs. (2.1), the state equations can be written in the special form

$$\begin{aligned}
&\dot{\mathbf{R}}_f = C_f^T \mathbf{V}_f,\ \dot{\boldsymbol{\theta}}_f = E_f^{-1} \boldsymbol{\omega}_f;\ \dot{\mathbf{q}}_{ui} = \mathbf{s}_{ui},\ \dot{\mathbf{q}}_{\psi i} = \mathbf{s}_{\psi i},\ i = f, w, e \\
&\dot{\mathbf{p}}_{Vf} = -\tilde{\omega}_f \mathbf{p}_{Vf} + \mathbf{F},\ \dot{\mathbf{p}}_{\omega f} = -\tilde{V}_f \mathbf{p}_{Vf} - \tilde{\omega}_f \mathbf{p}_{\omega f} + \mathbf{M} \\
&\left.\begin{aligned}
\dot{\mathbf{p}}_{ui} &= \partial T / \partial \mathbf{q}_{ui} - K_{ui}\mathbf{q}_{ui} - C_{ui}\mathbf{s}_{ui} + \mathbf{Q}_{ui} \\
\dot{\mathbf{p}}_{\psi i} &= -K_{\psi i}\mathbf{q}_{\psi i} - C_{\psi i}\mathbf{s}_{\psi i} + \mathbf{Q}_{\psi i}
\end{aligned}\right\}\ i = f, w, e
\end{aligned} \tag{2.22}$$

where, using Eq. (2.8) in conjunction with the second form of $\bar{\mathbf{V}}_f$, $\bar{\mathbf{V}}_w$ and $\bar{\mathbf{V}}_e$, Eqs. (2.12),

$$\begin{aligned}
\frac{\partial T}{\partial \mathbf{q}_{uf}} &= \frac{\partial \bar{\mathbf{V}}_f^T}{\partial \mathbf{q}_{uf}} \frac{\partial T}{\partial \bar{\mathbf{V}}_f} + \frac{\partial \bar{\mathbf{V}}_w^T}{\partial \mathbf{q}_{uf}} \frac{\partial T}{\partial \bar{\mathbf{V}}_w} + \frac{\partial \bar{\mathbf{V}}_e^T}{\partial \mathbf{q}_{uf}} \frac{\partial T}{\partial \bar{\mathbf{V}}_e} \\
&= \int \Phi_{uf}^T \tilde{\omega}_f^T \bar{\mathbf{V}}_f dm_f + \int \Phi_{ufw}^T \tilde{\omega}_f^T C_w^T \bar{\mathbf{V}}_w dm_w + \int \Phi_{ufe}^T \tilde{\omega}_f^T C_e^T \bar{\mathbf{V}}_e dm_e
\end{aligned} \tag{2.23}$$

$$\frac{\partial T}{\partial \mathbf{q}_{uw}} = \frac{\partial \bar{\mathbf{V}}_f^T}{\partial \mathbf{q}_{uw}}\frac{\partial T}{\partial \bar{\mathbf{V}}_f} + \frac{\partial \bar{\mathbf{V}}_w^T}{\partial \mathbf{q}_{uw}}\frac{\partial T}{\partial \bar{\mathbf{V}}_w} + \frac{\partial \bar{\mathbf{V}}_e^T}{\partial \mathbf{q}_{uw}}\frac{\partial T}{\partial \bar{\mathbf{V}}_e} = \int \Phi_{uw}^T \widetilde{C_w \boldsymbol{\omega}_f}^T \bar{\mathbf{V}}_w dm_w$$

$$\frac{\partial T}{\partial \mathbf{q}_{ue}} = \frac{\partial \bar{\mathbf{V}}_f^T}{\partial \mathbf{q}_{ue}}\frac{\partial T}{\partial \bar{\mathbf{V}}_f} + \frac{\partial \bar{\mathbf{V}}_w^T}{\partial \mathbf{q}_{ue}}\frac{\partial T}{\partial \bar{\mathbf{V}}_w} + \frac{\partial \bar{\mathbf{V}}_e^T}{\partial \mathbf{q}_{ue}}\frac{\partial T}{\partial \bar{\mathbf{V}}_e} = \int \Phi_{ue}^T \widetilde{C_e \boldsymbol{\omega}_f}^T \bar{\mathbf{V}}_e dm_e$$

Moreover,

$$K_{ui} = \int \Phi_{ui}^T \mathcal{L}_{ui} \Phi_{ui} dD_i,\ K_{\psi i} = \int \Phi_{\psi i}^T \mathcal{L}_{\psi i} \Phi_{\psi i} dD_i,\ i = f, w, e \tag{2.24}$$

are component stiffness matrices. In practice, K_{ui} and $K_{\psi i}$ $(i = f, w, e)$ can be obtained with greater ease from the strain energy directly.

2.3 Generalized Forces

The quantities $\mathbf{F}$, $\mathbf{M}$, $\mathbf{Q}_{ui}$ and $\mathbf{Q}_{\psi i}$ $(i = f, w, e)$ appearing in the state equations, Eqs. (2.22), represent generalized forces. They are related to the actual forces, which consist of the distributed force $\mathbf{f}_i(\mathbf{r}_i, t)$ over component i due to gravity, aerodynamics and controls and the engine thrust $\mathbf{F}_E \delta(\mathbf{r} - \mathbf{r}_E)$, where $\delta(\mathbf{r} - \mathbf{r}_E)$ is a spatial Dirac delta function,[36] in which $\mathbf{r}_E$ denotes the location of the engines. If some control forces are concentrated, they can also be treated as distributed, as in the case of the engine thrust. The relation between the generalized forces and the actual forces can be obtained by means of the virtual work, which can be expressed as

$$\delta \bar{W} = \textstyle\sum_i \int_{D_i} [\mathbf{f}_i^T + \mathbf{F}_E^T \delta(\mathbf{r} - \mathbf{r}_E)] \delta \bar{\mathbf{R}}_i^* dD_i \tag{2.25}$$

where $\delta \bar{\mathbf{R}}_i^*$ is the virtual quasi-displacement vector of a typical point on component i $(i = f, w, e)$. The vector $\delta \bar{\mathbf{R}}_i^*$ is related to the virtual quasi-displacement vectors corresponding to the quasi-velocities used to describe the motion of the aircraft components. Indeed, using Eqs. (2.12), we can write

$$\begin{aligned}
\delta \bar{\mathbf{R}}_f^* &= \delta \mathbf{R}_f^* + (\tilde{r}_f + \widetilde{\Phi_{uf} \mathbf{q}_{uf}})^T \delta \boldsymbol{\theta}_f^* + \Phi_{uf} \delta \mathbf{q}_{uf} + \tilde{r}_f^T \Phi_{\psi f} \delta \mathbf{q}_{\psi f} \\
\delta \bar{\mathbf{R}}_w^* &= C_w \delta \mathbf{R}_f^* + [C_w (\tilde{r}_{fw} + \widetilde{\Phi_{ufw} \mathbf{q}_{uf}})^T + (\tilde{r}_w + \widetilde{\Phi_{uw} \mathbf{q}_{uw}})^T C_w] \delta \boldsymbol{\theta}_f^* \\
&\quad + (\tilde{r}_w^T C_w \Delta \Phi_{ufw} + C_w \Phi_{ufw}) \delta \mathbf{q}_{uf} + \Phi_{uw} \delta \mathbf{q}_{uw} \\
&\quad + (\tilde{r}_w^T C_w \Phi_{\psi fw} + C_w \tilde{r}_{fw}^T \Phi_{\psi fw}) \delta \mathbf{q}_{\psi f} + \tilde{r}_w^T \Phi_{\psi w} \delta \mathbf{q}_{\psi w}
\end{aligned} \tag{2.26}$$

and we note that $\delta \bar{\mathbf{R}}_e^*$ can be obtained from $\delta \bar{\mathbf{R}}_w^*$ by replacing w by e. Inserting Eqs. (2.26) into Eq. (2.25), and collecting terms, we can write the virtual work in terms of virtual

generalized displacements as follows:

$$\delta\bar{W} = \mathbf{F}^T\delta\mathbf{R}_f^* + \mathbf{M}^T\delta\boldsymbol{\theta}_f^* + \textstyle\sum_i(\mathbf{Q}_{ui}^T\delta\mathbf{q}_{ui} + \mathbf{Q}_{\psi i}^T\delta\mathbf{q}_{\psi i}) \tag{2.27}$$

from which, assuming that the engines are mounted on the fuselage (Fig. 1), we obtain

$$\begin{aligned}
\mathbf{F} &= \textstyle\int_{D_f}[\mathbf{f}_f + \mathbf{F}_E\delta(\mathbf{r}-\mathbf{r}_E)]dD_f + C_w^T\int_{D_w}\mathbf{f}_w dD_w + C_e^T\int_{D_e}\mathbf{f}_e dD_e \\
\mathbf{M} &= \textstyle\int_{D_f}(\tilde{r}_f + \widetilde{\Phi_{uf}\mathbf{q}_{uf}})[\mathbf{f}_f + \mathbf{F}_E\delta(\mathbf{r}-\mathbf{r}_E)]dD_f + \int_{D_w}[(\tilde{r}_{fw} + \widetilde{\Phi_{ufw}\mathbf{q}_{uf}})C_w^T \\
&\quad + C_w^T(\tilde{r}_w + \widetilde{\Phi_{uw}\mathbf{q}_{uw}})]\mathbf{f}_w dD_w + \int_{D_e}[(\tilde{r}_{fe} + \widetilde{\Phi_{ufe}\mathbf{q}_{ue}})C_e^T + C_e^T(\tilde{r}_e + \widetilde{\Phi_{ue}\mathbf{q}_{ue}})]\mathbf{f}_e dD_e \\
\mathbf{Q}_{uf} &= \textstyle\int_{D_f}\Phi_{uf}^T[\mathbf{f}_f + \mathbf{F}_E\delta(\mathbf{r}-\mathbf{r}_E)]dD_f + \int_{D_w}(\tilde{r}_w^T C_w\Delta\Phi_{ufw} + C_w\Phi_{ufw})^T\mathbf{f}_w dD_w \\
&\quad + \textstyle\int_{D_e}(\tilde{r}_e^T C_e\Delta\Phi_{ufe} + C_e\Phi_{ufe})^T\mathbf{f}_e dD_e,
\end{aligned} \tag{2.28}$$

$$\begin{aligned}
\mathbf{Q}_{\psi f} &= \textstyle\int_{D_f}\Phi_{\psi f}^T\tilde{r}_f[\mathbf{f}_f + \mathbf{F}_E\delta(\mathbf{r}-\mathbf{r}_E)]dD_f + \int_{D_w}(\tilde{r}_w^T C_w\Phi_{\psi fw} + C_w\tilde{r}_{fw}^T\Phi_{\psi fw})^T\mathbf{f}_w dD_w \\
&\quad + \textstyle\int_{D_e}(\tilde{r}_e^T C_e\Phi_{\psi fe} + C_e\tilde{r}_{fe}^T\Phi_{\psi fe})^T\mathbf{f}_e dD_e \\
\mathbf{Q}_{ui} &= \textstyle\int_{D_i}\Phi_{ui}^T\mathbf{f}_i dD_i,\ \mathbf{Q}_{\psi i} = \int_{D_i}\Phi_{\psi i}^T\tilde{r}_i\mathbf{f}_i dD_i,\ i = w, e
\end{aligned}$$

To complete the state equations, Eqs. (2.22), it is necessary to derive the stiffness matrices K_{ui} and $K_{\psi i}$ $(i = f, w, e)$, the aerodynamic forces and the control forces.

2.4 The Aerodynamic and Gravity Forces

The forces acting on the aircraft can be identified as the aerodynamic, propulsion, control and gravity forces. Equations (2.28) give the generalized forces in terms of actual distributed and concentrated forces, where the first imply prescribing the forces at every point of the aircraft. Of the forces acting on an aircraft, the aerodynamic and control forces require special attention. We discuss the aerodynamic forces in this section and the control forces in a later section.

There are a number of aerodynamic theories available, some of them capable of prescribing the pressure distribution at every point of the aircraft. However, as pointed out in **1.1 overview**, any aerodynamic theory to be used in a dynamic simulation such as that described in this paper must satisfy certain requirements. Indeed, one of the requirements is that the aerodynamic forces be expressed in a form compatible with the present general dynamic formulation, which implies that they be in terms of the same variables and be referred to the same body axes attached to the undeformed aircraft as here. By far the

stringest requirement, however, is that the aerodynamic forces lend themselves to sufficiently fast computation as to permit time simulation of the aircraft behavior. Such computational efficiency does not appear to be within the state of the art. Hence, an aerodynamic theory capable of fitting within the framework of a computer simulation of the type envisioned here must yet be developed. Such a theory need not be unduly accurate, because a feedback control design tends to be sufficiently forgiving to tolerate small deviations from the actual aerodynamic forces. Until such a theory becomes reality, it is still possible to demonstrate how aerodynamics fits in the integration process by using an existing theory satisfying the requirement described above, namely, strip theory,[37] even though the theory may not be entirely suitable otherwise.

To derive the aerodynamic forces included in the distributed forces $\mathbf{f}_i$ $(i = f, \omega, e)$ acting on the aircraft by means of strip theory, we regard the fuselage, wing and empennage as two-dimensional aerodynamic surfaces. The lift force per unit span of fuselage can be written as[37]

$$\ell_f = q_f c_f C_{L\alpha f} \alpha_f = q_f c_f C_{Lf} \tag{2.29}$$

where c_f is the chord, $C_{L\alpha f}$ the slope of the lift curve, C_{Lf} the lift coefficient and

$$q_f = \tfrac{1}{2}\rho(\bar{V}_{fx}^2 + \bar{V}_{fz}^2),\ \alpha_f = \tan^{-1}(\bar{V}_{fz}/\bar{V}_{fx}) \tag{2.30}$$

are the dynamic pressure and angle of attack, respectively, in which ρ is the air density and $\bar{V}_{fx}$ and $\bar{V}_{fz}$ are components of the velocity vector $\bar{\mathbf{V}}_f$, Eq. (2.5). Similarly, the drag force per unit area of fuselage is given by

$$d_f = q_f c_f C_{Df} = q_f c_f (C_{Df0} + k_f C_{Lf}^2) = q_f c_f (C_{Df0} + k_f C_{L\alpha f}^2 \alpha_f^2) \tag{2.31}$$

where C_{Df0} is the drag coefficient corresponding to $\alpha_f = 0$ and k_f is a constant. The fuselage has also vertical surfaces subjected to aerodynamic forces. The lateral force per unit area can be expressed as

$$s_f = q_{sf} c_{sf} C_{s\beta f} \beta_f = q_{sf} c_{sf} C_{sf} \tag{2.32}$$

where c_{sf} is the lateral chord, $C_{s\beta f}$ the slope of the lateral force curve, C_{sf} the lateral force coefficient and

$$q_{sf} = \tfrac{1}{2}\rho(\bar{V}_{fx}^2 + \bar{V}_{fy}^2),\ \beta_f = \tan^{-1}(\bar{V}_{fy}/\bar{V}_{fx}) \tag{2.33}$$

are the dynamic pressure and the angle of attack of the lateral force, respectively, in which $\bar{V}_{fx}$ and $\bar{V}_{fy}$ are components of $\bar{\mathbf{V}}_f$. Hence, the aerodynamic forces on the fuselage can be

written in the vector form

$$\mathbf{f}_{af} = \begin{bmatrix} \ell_f \sin\alpha_f - d_f \cos\alpha_f \\ 0 \\ -\ell_f \cos\alpha_f - d_f \sin\alpha_f \end{bmatrix}, \ \mathbf{f}_{sf} = \begin{bmatrix} s_f \sin\beta_f \\ -s_f \cos\beta_f \\ 0 \end{bmatrix} \tag{2.34}$$

In a similar fashion, the lift and drag per unit span of wing are given by

$$\ell_w = q_w c_w (C_{L\alpha w}\alpha_w + C_{L\delta a}\delta_a), \ d_w = q_w c_w (C_{Dw0} + k_w C_{Lw}^2) = q_w c_w (C_{Dw0} + k_w C_{L\alpha w}^2 \alpha_w^2) \tag{2.35}$$

where c_w is the chord, δ_a an aileron rotation, $C_{L\delta a}$ a control effectiveness coefficient[17] and

$$q_w = \tfrac{1}{2}\rho(\bar{V}_{wy}^2 + \bar{V}_{wz}^2), \ \alpha_w = \tan^{-1}(\bar{V}_{wz}/\bar{V}_{wy}) + \psi_{wx} \tag{2.36}$$

in which the velocity components $\bar{V}_{wy}$ and $\bar{V}_{wz}$ of $\bar{\mathbf{V}}_w$ can be obtained from Eq. (2.6). Moreover, ψ_{wx} is the angular displacement of the wing about axis x_w due to torsion. There is no meaningful lateral force on the wing, so that

$$\mathbf{f}_{aw} = \begin{bmatrix} 0 \\ \ell_w \sin\alpha_w - d_w \cos\alpha_w \\ -\ell_w \cos\alpha_w - d_w \sin\alpha_w \end{bmatrix} \tag{2.37}$$

The empennage has both lift and lateral surfaces. The lift, drag and lateral forces per unit span of empennage are

$$\ell_e = q_e c_e (C_{L\alpha e}\alpha_e + C_{L\delta e}\delta_e), \ d_e = q_e c_e (C_{De0} + k_e C_{L\alpha e}^2 \alpha_e^2), \ s_e = q_{se} c_{se} (C_{s\beta e}\beta_e + C_{s\delta r}\delta_r) \tag{2.38}$$

where c_e and c_{se} are the chords, δ_e and δ_r are rotations of the elevator and ruder, $C_{L\delta e}$ and $C_{s\delta r}$ are respective control effectiveness coefficients and

$$\begin{aligned} q_e &= \tfrac{1}{2}\rho(\bar{V}_{ey}^2 + \bar{V}_{ez}^2), \ \alpha_e = \tan^{-1}(\bar{V}_{ez}/\bar{V}_{ey}) + \psi_{ex} \\ q_{se} &= \tfrac{1}{2}\rho(\bar{V}_{ey}^2 + \bar{V}_{ez}^2), \ \beta_e = \tan^{-1}(\bar{V}_{ez}/\bar{V}_{ey}) + \psi_{ex} \end{aligned} \tag{2.39}$$

Hence, the aerodynamic force vectors per unit span of empennage can be written as

$$\mathbf{f}_{ae} = \begin{bmatrix} 0 \\ \ell_e \sin\alpha_e - d_e \cos\alpha_e \\ -\ell_e \cos\alpha_e - d_e \sin\alpha_e \end{bmatrix}, \ \mathbf{f}_{se} = \begin{bmatrix} 0 \\ s_e \sin\beta_e \\ -s_e \cos\beta_e \end{bmatrix} \tag{2.40}$$

For a typical component, the lift, lateral force and drag per unit span are applied at the line of aerodynamic centers. Hence, in Eqs. (2.28), the domain of integration for the terms involving the aerodynamic forces is the line of aerodynamic centers. The gravity forces per unit volume of components are simply

$$\mathbf{f}_{gf} = C_f \begin{bmatrix} 0 \\ 0 \\ \rho_f g \end{bmatrix}, \ \mathbf{f}_{gw} = C_w C_f \begin{bmatrix} 0 \\ 0 \\ \rho_w g \end{bmatrix}, \ \mathbf{f}_{ge} = C_e C_f \begin{bmatrix} 0 \\ 0 \\ \rho_e g \end{bmatrix} \tag{2.41}$$

Note that the aerodynamic and gravity forces are in terms of respective component body axes.

Chapter 3

A Unified Theory for Flight Dynamics and Aeroelasticity

To complete the discussion of the forces acting on an aircraft, we turn our attention to the control forces. Aircraft control is carried out by means of control surfaces, as well as by the engine thrust. Before we consider the problem of control design, it will prove beneficial to examine the nature of the controls. Controls are of two general types, one designed to steer the aircraft as a whole and the other to suppress the effects of any undesirable disturbances. The first type involves rigid body motions of the aircraft, which are in general large, and traditionally lies in the domain of flight dynamics. On the other hand, the second type involves elastic deformations of the aircraft, which tend to be small compared to the rigid body motions, and traditionally lies in the domain of aeroelasticity. Hence, the formulation given by Eqs. (2.22) can be regarded as spanning the fields of flight dynamics and aeroelasticity.

From the above discussion, it appears that control of the aircraft as a whole is likely to be different in nature from control of disturbances. In this regard, we observe that the state equations, Eqs. (2.22), are in general nonlinear and of high dimension, where the nonlinearity can be traced to the large rigid body variables. On the other hand, the high dimensionality can be traced to the small elastic variables. In view of this, a solution by a perturbation approach seems indicated, which amounts to a separation of the problem into a *zero-order problem* for the large variables and a *first-order problem* for the small variables, where the difference between the large and small variables is one order of magnitude, or more. Physically, in the zero-order problem the aircraft executes a given maneuver as if it were rigid, in which case the mathematical formulation consists of a maximum of six

coupled, generally nonlinear ordinary differential equations, three for rigid body translations and three for rigid body rotations. They correspond to the equations commonly used in *flight dynamics*. On the other hand, the first-order problem involves the elastic deformations, as well as small perturbations in the rigid body variables. In view of the inclusion of the latter, the first-order problem defined here represents an *extended aeroelasticity theory*, in which the rigid body degrees of freedom are included in a natural manner. This is in contrast with some occasional practice,[38] in which "body freedoms" are included in an ad hoc manner. We note that the solution of the zero-order problem enters into the first-order problem, so that *this new theory provides one set of extended aeroelasticity equations for every conceivable rigid body maneuver of the aircraft*, rather than the single set of equations commonly associated with steady cruise. We express the perturbation solution as follows:

$$\begin{aligned} &\mathbf{R}_f = \mathbf{R}_f^{(0)} + \mathbf{R}_f^{(1)},\ \boldsymbol{\theta}_f = \boldsymbol{\theta}_f^{(0)} + \boldsymbol{\theta}_f^{(1)},\ \mathbf{V}_f = \mathbf{V}_f^{(0)} + \mathbf{V}_f^{(1)},\ \boldsymbol{\omega}_f = \boldsymbol{\omega}_f^{(0)} + \boldsymbol{\omega}_f^{(1)} \\ &\mathbf{p}_{Vf} = \mathbf{p}_{Vf}^{(0)} + \mathbf{p}_{Vf}^{(1)},\ \mathbf{p}_{\omega f} = \mathbf{p}_{\omega f}^{(0)} + \mathbf{p}_{\omega f}^{(1)},\ \mathbf{F} = \mathbf{F}^{(0)} + \mathbf{F}^{(1)},\ \mathbf{M} = \mathbf{M}^{(0)} + \mathbf{M}^{(1)} \end{aligned} \tag{3.1}$$

where the superscripts (0) and (1) denote orders of magnitude. All the quantities related to the elastic deformations are regarded as being of first order. Then, inserting Eqs. (3.1) into the state equations, Eqs. (2.22), and separating different orders of magnitude, we obtain the zero-order problem, or the *flight dynamics problem*

$$\begin{aligned} &\dot{\mathbf{R}}_f^{(0)} = C_f^{(0)T}\mathbf{V}_f^{(0)},\ \dot{\boldsymbol{\theta}}_f^{(0)} = (E_f^{(0)})^{-1}\boldsymbol{\omega}_f^{(0)} \\ &\dot{\mathbf{p}}_{Vf}^{(0)} = -\tilde{\omega}_f^{(0)}\mathbf{p}_{Vf}^{(0)} + \mathbf{F}^{(0)},\ \dot{\mathbf{p}}_{\omega f}^{(0)} = -\tilde{V}_f^{(0)}\mathbf{p}_{Vf}^{(0)} - \tilde{\omega}_f^{(0)}\mathbf{p}_{\omega f}^{(0)} + \mathbf{M}^{(0)} \end{aligned} \tag{3.2}$$

in which $C_f^{(0)}$ and $E_f^{(0)}$ can be obtained from C_f and E_f, Eqs. (2.2), by replacing ψ, θ and ϕ by $\psi^{(0)}$, $\theta^{(0)}$ and $\phi^{(0)}$, respectively. Moreover, from Eqs. (2.28), the zero-order generalized force and moment are given by

$$\begin{aligned} \mathbf{F}^{(0)} &= \textstyle\int_{D_f}[\mathbf{f}_f^{(0)} + \mathbf{F}_E^{(0)}\delta(\mathbf{r}-\mathbf{r}_E)]dD_f + C_w^T\int_{D_w}\mathbf{f}_w^{(0)}dD_w + C_e^T\int_{D_e}\mathbf{f}_e^{(0)}dD_e \\ \mathbf{M}^{(0)} &= \textstyle\int_{D_f}\tilde{r}_f[\mathbf{f}_f^{(0)} + \mathbf{F}_E^{(0)}\delta(\mathbf{r}-\mathbf{r}_E)]dD_f + \int_{D_w}(\tilde{r}_{fw}C_w^T + C_w^T\tilde{r}_w)\mathbf{f}_w^{(0)}dD_w \\ &\quad + \textstyle\int_{D_e}(\tilde{r}_{fe}C_e^T + C_e^T\tilde{r}_e)\mathbf{f}_e^{(0)}dD_e \end{aligned} \tag{3.3}$$

where the zero-order parts of the aerodynamic force densities contributing to $\mathbf{f}_f^{(0)}$, $\mathbf{f}_w^{(0)}$ and $\mathbf{f}_e^{(0)}$ are

$$\mathbf{f}_{af}^{(0)} = \begin{bmatrix} \ell_f^{(0)}\sin\alpha_f^{(0)} - d_f^{(0)}\cos\alpha_f^{(0)} \\ 0 \\ -\ell_f^{(0)}\cos\alpha_f^{(0)} - d_f^{(0)}\sin\alpha_f^{(0)} \end{bmatrix},\ \mathbf{f}_{sf}^{(0)} = \begin{bmatrix} s_f^{(0)}\sin\beta_f^{(0)} \\ -s_f^{(0)}\cos\beta_f^{(0)} \\ 0 \end{bmatrix} \tag{3.4}$$

$$\mathbf{f}_{ai}^{(0)} = \begin{bmatrix} 0 \\ \ell_i^{(0)} \sin\alpha_i^{(0)} - d_i^{(0)} \cos\alpha_i^{(0)} \\ -\ell_i^{(0)} \cos\alpha_i^{(0)} - d_i^{(0)} \sin\alpha_i^{(0)} \end{bmatrix},\ i = w, e;\ \mathbf{f}_{se}^{(0)} = \begin{bmatrix} 0 \\ s_e^{(0)} \sin\beta_e^{(0)} \\ -s_e^{(0)} \cos\beta_e^{(0)} \end{bmatrix}$$

in which the zero-order parts of the lift, drag and lateral forces per unit area are

$$\begin{aligned} &\ell_f^{(0)} = q_f^{(0)} c_f C_{L\alpha f} \alpha_f^{(0)},\ \ell_w^{(0)} = q_w^{(0)} c_w (C_{L\alpha w} \alpha_w^{(0)} + C_{L\delta a} \delta_a),\ \ell_e^{(0)} = q_e^{(0)} c_e (C_{L\alpha e} \alpha_e^{(0)} + C_{L\delta e} \delta_e) \\ &s_f^{(0)} = q_{sf}^{(0)} c_{sf} C_{s\beta f} \beta_f^{(0)},\ s_e^{(0)} = q_{se}^{(0)} c_{se} (C_{s\beta e} \beta_e^{(0)} + C_{s\delta r} \delta_r) \\ &d_i^{(0)} = q_i^{(0)} c_i [C_{Di0} + k_i C_{L\alpha i}^2 (\alpha_i^{(0)})^2],\ i = f, w, e \end{aligned} \tag{3.5}$$

where

$$\begin{aligned} q_f^{(0)} &= \tfrac{1}{2}\rho[(\bar{V}_{fx}^{(0)})^2 + (\bar{V}_{fz}^{(0)})^2],\ \alpha_f^{(0)} = \tan^{-1}(\bar{V}_{fz}^{(0)}/\bar{V}_{fx}^{(0)}),\ \beta_f^{(0)} = \tan^{-1}(\bar{V}_{fy}^{(0)}/\bar{V}_{fx}^{(0)}) \\ q_i^{(0)} &= \tfrac{1}{2}\rho[(\bar{V}_{iy}^{(0)})^2 + (\bar{V}_{iz}^{(0)})^2],\ \alpha_i^{(0)} = \tan^{-1}(\bar{V}_{iz}^{(0)}/\bar{V}_{iy}^{(0)}),\ \beta_i^{(0)} = \tan^{-1}(\bar{V}_{iz}^{(0)}/\bar{V}_{iy}^{(0)}),\ i = w, e \\ q_{sf}^{(0)} &= \tfrac{1}{2}\rho[(\bar{V}_{fx}^{(0)})^2 + (\bar{V}_{fy}^{(0)})^2],\ q_{se}^{(0)} = \tfrac{1}{2}\rho[(\bar{V}_{ey}^{(0)})^2 + (\bar{V}_{ez}^{(0)})^2] \end{aligned} \tag{3.6}$$

Moreover, the zero-order parts of the gravity force densities are

$$\mathbf{f}_{gf}^{(0)} = C_f^{(0)} [0\ 0\ \rho_f g]^T;\ \mathbf{f}_{gi}^{(0)} = C_i C_f^{(0)} [0\ 0\ \rho_i g]^T,\ i = w, e \tag{3.7}$$

The zero-order state is defined as $\mathbf{x}^{(0)} = [\mathbf{R}_f^{(0)T}\ \boldsymbol{\theta}_f^{(0)T}\ \mathbf{p}_{Vf}^{(0)T}\ \mathbf{p}_{\omega f}^{(0)T}]^T$, and Eqs. (3.2) contain in addition $\mathbf{V}_f^{(0)}$ and $\boldsymbol{\omega}_f^{(0)}$. However, $\mathbf{V}_f^{(0)}$ and $\boldsymbol{\omega}_f^{(0)}$ can be expressed in terms of $\mathbf{p}_{Vf}^{(0)}$ and $\mathbf{p}_{\omega f}^{(0)}$ by using Eqs. (2.21) and writing

$$\mathbf{p}_{Vf}^{(0)} = m\mathbf{V}_f^{(0)} + \tilde{S}^{(0)T} \boldsymbol{\omega}_f^{(0)},\ \mathbf{p}_{\omega f}^{(0)} = \tilde{S}^{(0)} \mathbf{V}_f^{(0)} + J^{(0)} \boldsymbol{\omega}_f^{(0)} \tag{3.8}$$

The solution of Eqs. (3.2) in conjunction with Eqs. (3.3)-(3.8) consists of the state $\mathbf{x}^{(0)}$ and it represents a given maneuver of the aircraft.

Inserting Eqs. (3.1) into Eqs. (2.22) and retaining the first-order terms, we obtain the *extended aeroelasticity problem* defined by

$$\begin{aligned} \dot{\mathbf{R}}_f^{(1)} &= C_f^{(0)T} \mathbf{V}_f^{(1)} + C_f^{(1)T} \mathbf{V}_f^{(0)},\ \dot{\boldsymbol{\theta}}_f^{(1)} = (E_f^{(0)})^{-1} \boldsymbol{\omega}_f^{(1)} - (E_f^{(0)})^{-1} E_f^{(1)} (E_f^{(0)})^{-1} \boldsymbol{\omega}_f^{(0)} \\ \dot{\mathbf{q}}_{ui} &= \mathbf{s}_{ui},\ \dot{\mathbf{q}}_{\psi i} = \mathbf{s}_{\psi i},\ i = f, w, e \\ \dot{\mathbf{p}}_{Vf}^{(1)} &= -\tilde{\omega}_f^{(1)} \mathbf{p}_{Vf}^{(0)} - \tilde{\omega}_f^{(0)} \mathbf{p}_{Vf}^{(1)} + \mathbf{F}^{(1)} \\ \dot{\mathbf{p}}_{\omega f}^{(1)} &= -\tilde{V}_f^{(1)} \mathbf{p}_{Vf}^{(0)} - \tilde{V}_f^{(0)} \mathbf{p}_{Vf}^{(1)} - \tilde{\omega}_f^{(1)} \mathbf{p}_{\omega f}^{(0)} - \tilde{\omega}_f^{(0)} \mathbf{p}_{\omega f}^{(1)} + \mathbf{M}^{(1)} \\ \dot{\mathbf{p}}_{uf} &= \int \Phi_{uf}^T (\tilde{\omega}_f^{(0)^T} \bar{\mathbf{V}}_f^{(1)} + \tilde{\omega}_f^{(1)^T} \mathbf{V}_f^{(0)}) dm_f + \int \Phi_{ufw}^T (\tilde{\omega}_f^{(0)^T} C_w^T \bar{\mathbf{V}}_w^{(1)} + \tilde{\omega}_f^{(1)^T} C_w^T \bar{\mathbf{V}}_w^{(0)}) dm_w \\ &\quad + \int \Phi_{ufe}^T (\tilde{\omega}_f^{(0)^T} C_e^T \bar{\mathbf{V}}_e^{(1)} + \tilde{\omega}_f^{(1)^T} C_e^T \bar{\mathbf{V}}_e^{(0)}) dm_e - K_{uf} \mathbf{q}_{uf} - C_{uf} \mathbf{s}_{uf} + \mathbf{Q}_{uf} \\ &\quad + \int \Phi_{uf}^T \tilde{\omega}_f^{(0)^T} \bar{\mathbf{V}}_f^{(0)} dm_f + \int \Phi_{ufw}^T \tilde{\omega}_f^{(0)^T} C_w^T \bar{\mathbf{V}}_w^{(0)} dm_w + \int \Phi_{ufe}^T \tilde{\omega}_f^{(0)^T} C_e^T \bar{\mathbf{V}}_e^{(0)} dm_e \end{aligned} \tag{3.9}$$

$$
\begin{aligned}
\dot{\mathbf{p}}_{\psi f} =& -K_{\psi f}\mathbf{q}_{\psi f} - C_{\psi f}\mathbf{s}_{\psi f} + \mathbf{Q}_{\psi f} \\
\dot{\mathbf{p}}_{ui} =& \int \Phi_{ui}^T(\widetilde{C_i\boldsymbol{\omega}_f^{(0)}}^T\bar{\mathbf{V}}_i^{(1)} + \widetilde{C_i\boldsymbol{\omega}_f^{(1)}}^T\bar{\mathbf{V}}_i^{(0)})dm_i - K_{ui}\mathbf{q}_{ui} - C_{ui}\mathbf{s}_{ui} + \mathbf{Q}_{ui} \\
&+ \int \Phi_{ui}^T\widetilde{C_i\boldsymbol{\omega}_f^{(0)}}^T\bar{\mathbf{V}}_i^{(0)}dm_i,\ i{=}w,e \\
\dot{\mathbf{p}}_{\psi i} =& -K_{\psi i}\mathbf{q}_{\psi i} - C_{\psi i}\mathbf{s}_{\psi i} + \mathbf{Q}_{\psi i},\ i = w,e
\end{aligned}
$$

where

$$
C_f^{(1)} = C_{f\psi}^{(0)}\psi^{(1)} + C_{f\theta}^{(0)}\theta^{(1)} + C_{f\phi}^{(0)}\phi^{(1)},\ E_f^{(1)} = E_{f\theta}^{(0)}\theta^{(1)} + E_{f\phi}^{(0)}\phi^{(1)} \tag{3.10}
$$

in which

$$
\begin{aligned}
C_{f\psi}^{(0)} &= \left.\frac{\partial C_f}{\partial \psi}\right|_{\psi^{(0)},\theta^{(0)},\phi^{(0)}} \\
&= \begin{bmatrix} -\mathrm{s}\psi^{(0)}\mathrm{c}\theta^{(0)} & \mathrm{c}\psi^{(0)}\mathrm{c}\theta^{(0)} & 0 \\ -\mathrm{s}\psi^{(0)}\mathrm{s}\theta^{(0)}\mathrm{s}\phi^{(0)} - \mathrm{c}\psi^{(0)}\mathrm{c}\phi^{(0)} & \mathrm{c}\psi^{(0)}\mathrm{s}\theta^{(0)}\mathrm{s}\phi^{(0)} - \mathrm{s}\psi^{(0)}\mathrm{c}\phi^{(0)} & 0 \\ -\mathrm{s}\psi^{(0)}\mathrm{s}\theta^{(0)}\mathrm{c}\phi^{(0)} + \mathrm{c}\psi^{(0)}\mathrm{s}\phi^{(0)} & \mathrm{c}\psi^{(0)}\mathrm{s}\theta^{(0)}\mathrm{c}\phi^{(0)} + \mathrm{s}\psi^{(0)}\mathrm{s}\phi^{(0)} & 0 \end{bmatrix} \\
C_{f\theta}^{(0)} &= \left.\frac{\partial C_f}{\partial \theta}\right|_{\psi^{(0)},\theta^{(0)},\phi^{(0)}} \\
&= \begin{bmatrix} -\mathrm{c}\psi^{(0)}\mathrm{s}\theta^{(0)} & -\mathrm{s}\psi^{(0)}\mathrm{s}\theta^{(0)} & -\mathrm{c}\theta^{(0)} \\ \mathrm{c}\psi^{(0)}\mathrm{c}\theta^{(0)}\mathrm{s}\phi^{(0)} & \mathrm{s}\psi^{(0)}\mathrm{c}\theta^{(0)}\mathrm{s}\phi^{(0)} & -\mathrm{s}\theta^{(0)}\mathrm{s}\phi^{(0)} \\ \mathrm{c}\psi^{(0)}\mathrm{c}\theta^{(0)}\mathrm{c}\phi^{(0)} & \mathrm{s}\psi^{(0)}\mathrm{c}\theta^{(0)}\mathrm{c}\phi^{(0)} & -\mathrm{s}\theta^{(0)}\mathrm{c}\phi^{(0)} \end{bmatrix} \\
C_{f\phi}^{(0)} &= \left.\frac{\partial C_f}{\partial \phi}\right|_{\psi^{(0)},\theta^{(0)},\phi^{(0)}} \\
&= \begin{bmatrix} 0 & 0 & 0 \\ \mathrm{c}\psi^{(0)}\mathrm{s}\theta^{(0)}\mathrm{c}\phi^{(0)} + \mathrm{s}\psi^{(0)}\mathrm{s}\phi^{(0)} & \mathrm{s}\psi^{(0)}\mathrm{s}\theta^{(0)}\mathrm{c}\phi^{(0)} - \mathrm{c}\psi^{(0)}\mathrm{s}\phi^{(0)} & \mathrm{c}\theta^{(0)}\mathrm{c}\phi^{(0)} \\ -\mathrm{c}\psi^{(0)}\mathrm{s}\theta^{(0)}\mathrm{s}\phi^{(0)} + \mathrm{s}\psi^{(0)}\mathrm{c}\phi^{(0)} & -\mathrm{s}\psi^{(0)}\mathrm{s}\theta^{(0)}\mathrm{s}\phi^{(0)} - \mathrm{c}\psi^{(0)}\mathrm{c}\phi^{(0)} & -\mathrm{c}\theta^{(0)}\mathrm{s}\phi^{(0)} \end{bmatrix} \\
E_{f\theta}^{(0)} &= \left.\frac{\partial E_f}{\partial \theta}\right|_{\theta^{(0)},\phi^{(0)}} = \begin{bmatrix} 0 & 0 & -\mathrm{c}\theta^{(0)} \\ 0 & 0 & -\mathrm{s}\theta^{(0)}\mathrm{s}\phi^{(0)} \\ 0 & 0 & -\mathrm{s}\theta^{(0)}\mathrm{c}\phi^{(0)} \end{bmatrix} \\
E_{f\phi}^{(0)} &= \left.\frac{\partial E_f}{\partial \phi}\right|_{\theta^{(0)},\phi^{(0)}} = \begin{bmatrix} 0 & 0 & 0 \\ 0 & -\mathrm{s}\phi^{(0)} & \mathrm{c}\theta^{(0)}\mathrm{c}\phi^{(0)} \\ 0 & -\mathrm{c}\phi^{(0)} & -\mathrm{c}\theta^{(0)}\mathrm{s}\phi^{(0)} \end{bmatrix}
\end{aligned} \tag{3.11}
$$

and

$$
\begin{aligned}
&\bar{\mathbf{V}}_f^{(0)} = \mathbf{V}_f^{(0)} + \tilde{r}_f^T\boldsymbol{\omega}_f^{(0)},\ \bar{\mathbf{V}}_f^{(1)} = \mathbf{V}_f^{(1)} + \tilde{r}_f^T\boldsymbol{\omega}_f^{(1)} + \widetilde{\Phi_{uf}\mathbf{q}_{uf}}^T\boldsymbol{\omega}_f^{(0)} + \Phi_{uf}\mathbf{s}_{uf} + \tilde{r}_f^T\Phi_{\psi f}\mathbf{s}_{\psi f} \\
&\bar{\mathbf{V}}_w^{(0)} = C_w\mathbf{V}_f^{(0)} + (C_w\tilde{r}_{fw}^T + \tilde{r}_w^TC_w)\boldsymbol{\omega}_f^{(0)} \\
&\bar{\mathbf{V}}_w^{(1)} = C_w\mathbf{V}_f^{(1)} + (C_w\tilde{r}_{fw}^T + \tilde{r}_w^TC_w)\boldsymbol{\omega}_f^{(1)} + (C_w\widetilde{\Phi_{ufw}\mathbf{q}_{uf}}^T + \widetilde{\Phi_{uw}\mathbf{q}_{uw}}^TC_w)\boldsymbol{\omega}_f^{(0)} \\
&\quad + (\tilde{r}_w^TC_w\Delta\Phi_{ufw} + C_w\Phi_{ufw})\mathbf{s}_{uf} + \Phi_{uw}\mathbf{s}_{uw} + (\tilde{r}_w^TC_w\Phi_{\psi fw} + C_w\tilde{r}_{fw}^T\Phi_{\psi fw})\mathbf{s}_{\psi f} + \tilde{r}_w^T\Phi_{\psi w}\mathbf{s}_{\psi w}
\end{aligned} \tag{3.12}
$$

Then, from Eqs. (2.28), the first-order generalized forces are

$$
\begin{aligned}
\mathbf{F}^{(1)} &= \textstyle\int_{D_f}[\mathbf{f}_f^{(1)} + \mathbf{F}_E^{(1)}\delta(\mathbf{r}-\mathbf{r}_E)]dD_f + C_w^T\int_{D_w}\mathbf{f}_w^{(1)}dD_w + C_e^T\int_{D_e}\mathbf{f}_e^{(1)}dD_e \\
\mathbf{M}^{(1)} &= \textstyle\int_{D_f}\{\tilde{r}_f[\mathbf{f}_f^{(1)} + \mathbf{F}_E^{(1)}\delta(\mathbf{r}-\mathbf{r}_E)] + \widetilde{\Phi_{uf}\mathbf{q}_{uf}}[\mathbf{f}_f^{(0)} + \mathbf{F}_E^{(0)}\delta(\mathbf{r}-\mathbf{r}_E)]\}dD_f + \int_{D_w}[(\tilde{r}_{fw}C_w^T \\
&\quad + C_w^T\tilde{r}_w)\mathbf{f}_w^{(1)} + (\widetilde{\Phi_{ufw}\mathbf{q}_{uf}}C_w^T + C_w^T\widetilde{\Phi_{uw}\mathbf{q}_{uw}})\mathbf{f}_w^{(0)}]dD_w + \int_{D_e}[(\tilde{r}_{fe}C_e^T + C_e^T\tilde{r}_e)\mathbf{f}_e^{(1)} \\
&\quad + (\widetilde{\Phi_{ufe}\mathbf{q}_{uf}}C_e^T + C_e^T\widetilde{\Phi_{ue}\mathbf{q}_{ue}})\mathbf{f}_e^{(0)}]dD_e \\
\mathbf{Q}_{uf} &= \textstyle\int_{D_f}\Phi_{uf}^T[\mathbf{f}_f^{(0)} + \mathbf{f}_f^{(1)} + \mathbf{F}_E^{(0)}\delta(\mathbf{r}-\mathbf{r}_E) + \mathbf{F}_E^{(1)}\delta(\mathbf{r}-\mathbf{r}_E)]dD_f + \int_{D_w}(\tilde{r}_w^TC_w\Delta\Phi_{ufw} \\
&\quad + C_w\Phi_{ufw})^T(\mathbf{f}_w^{(0)} + \mathbf{f}_w^{(1)})dD_w + \int_{D_e}(\tilde{r}_e^TC_e\Delta\Phi_{ufe} + C_e\Phi_{ufe})^T(\mathbf{f}_e^{(0)} + \mathbf{f}_e^{(1)})dD_e \\
\mathbf{Q}_{\psi f} &= \textstyle\int_{D_f}\Phi_{\psi f}^T\tilde{r}_f[\mathbf{f}_f^{(0)} + \mathbf{f}_f^{(1)} + \mathbf{F}_E^{(0)}\delta(\mathbf{r}-\mathbf{r}_E) + \mathbf{F}_E^{(1)}\delta(\mathbf{r}-\mathbf{r}_E)]dD_f + \int_{D_w}(\tilde{r}_w^TC_w\Phi_{\psi fw} \\
&\quad + C_w\tilde{r}_{fw}^T\Phi_{\psi fw})^T(\mathbf{f}_w^{(0)}+\mathbf{f}_w^{(1)})dD_w + \int_{D_e}(\tilde{r}_e^TC_e\Phi_{\psi fe}+C_e\tilde{r}_{fe}^T\Phi_{\psi fe})^T(\mathbf{f}_e^{(0)}+\mathbf{f}_e^{(1)})dD_e \\
\mathbf{Q}_{ui} &= \textstyle\int_{D_i}\Phi_{ui}^T(\mathbf{f}_i^{(0)} + \mathbf{f}_i^{(1)})dD_i,\ \mathbf{Q}_{\psi i} = \int_{D_i}\Phi_{\psi i}^T\tilde{r}_i(\mathbf{f}_i^{(0)} + \mathbf{f}_i^{(1)})dD_i,\ i = w, e
\end{aligned}
\tag{3.13}
$$

where the first-order parts of the aerodynamic force densities contributing to $\mathbf{f}_f^{(1)}$, $\mathbf{f}_w^{(1)}$ and $\mathbf{f}_e^{(1)}$ are

$$
\begin{aligned}
\mathbf{f}_{af}^{(1)} &= \begin{bmatrix} \ell_f^{(1)}\sin\alpha_f^{(0)} - d_f^{(1)}\cos\alpha_f^{(0)} + (\ell_f^{(0)}\cos\alpha_f^{(0)} + d_f^{(0)}\sin\alpha_f^{(0)})\alpha_f^{(1)} \\ 0 \\ -\ell_f^{(1)}\cos\alpha_f^{(0)} - d_f^{(1)}\sin\alpha_f^{(0)} + (\ell_f^{(0)}\sin\alpha_f^{(0)} - d_f^{(0)}\cos\alpha_f^{(0)})\alpha_f^{(1)} \end{bmatrix} \\
\mathbf{f}_{sf}^{(1)} &= \begin{bmatrix} s_f^{(1)}\sin\beta_f^{(0)} + s_f^{(0)}\beta_f^{(1)}\cos\beta_f^{(0)} \\ -s_f^{(1)}\cos\beta_f^{(0)} + s_f^{(0)}\beta_f^{(1)}\sin\beta_f^{(0)} \\ 0 \end{bmatrix}
\end{aligned}
\tag{3.14}
$$

$$
\begin{aligned}
\mathbf{f}_{ai}^{(1)} &= \begin{bmatrix} 0 \\ \ell_i^{(1)}\sin\alpha_i^{(0)} - d_i^{(1)}\cos\alpha_i^{(0)} + (\ell_i^{(0)}\cos\alpha_i^{(0)} + d_i^{(0)}\sin\alpha_i^{(0)})\alpha_i^{(1)} \\ -\ell_i^{(1)}\cos\alpha_i^{(0)} - d_i^{(1)}\sin\alpha_i^{(0)} + (\ell_i^{(0)}\sin\alpha_i^{(0)} - d_i^{(0)}\cos\alpha_i^{(0)})\alpha_i^{(1)} \end{bmatrix} \\
\mathbf{f}_{si}^{(1)} &= \begin{bmatrix} 0 \\ s_e^{(1)}\sin\beta_e^{(0)} + s_e^{(0)}\beta_e^{(1)}\cos\beta_e^{(0)} \\ -s_e^{(1)}\cos\beta_e^{(0)} + s_e^{(0)}\beta_e^{(1)}\sin\beta_e^{(0)} \end{bmatrix},\ i = w, e
\end{aligned}
$$

in which the first-order parts of the lift, drag and lateral forces per unit area are

$$
\begin{aligned}
&\ell_f^{(1)} = c_fC_{L\alpha f}(q_f^{(1)}\alpha_f^{(0)} + q_f^{(0)}\alpha_f^{(1)}),\ \ell_w^{(1)} = q_w^{(1)}c_w(C_{L\alpha w}\alpha_w^{(0)} + C_{L\delta a}\delta_a) + q_w^{(0)}c_wC_{L\alpha w}\alpha_w^{(1)} \\
&\ell_e^{(1)} = q_e^{(1)}c_e(C_{L\alpha e}\alpha_e^{(0)} + C_{L\delta e}\delta_e) + q_e^{(0)}c_eC_{L\alpha e}\alpha_e^{(1)},\ s_f^{(1)} = c_{sf}C_{s\beta f}(q_{sf}^{(1)}\beta_f^{(0)} + q_{sf}^{(0)}\beta_f^{(1)}) \\
&s_e^{(1)} = q_{se}^{(1)}c_{se}(C_{s\beta e}\beta_e^{(0)} + C_{s\delta r}\delta_r) + q_{se}^{(0)}c_{se}C_{s\beta e}\beta_e^{(1)} \\
&d_i^{(1)} = q_i^{(1)}c_i[C_{Di0} + k_iC_{L\alpha i}^2(\alpha_i^{(0)})^2] + 2q_i^{(0)}c_ik_iC_{L\alpha i}^2\alpha_i^{(0)}\alpha_i^{(1)},\ i = f, w, e
\end{aligned}
\tag{3.15}
$$

where

$$
\begin{aligned}
q_f^{(1)} &= \rho(\bar{V}_{fx}^{(0)}\bar{V}_{fx}^{(1)} + \bar{V}_{fz}^{(0)}\bar{V}_{fz}^{(1)}),\ \alpha_f^{(1)} = \tan^{-1}\left(\frac{\bar{V}_{fx}^{(0)}V_{fz}^{(1)} - \bar{V}_{fx}^{(1)}\bar{V}_{fz}^{(0)}}{(\bar{V}_{fx}^{(0)})^2 + (\bar{V}_{fz}^{(0)})^2}\right)\\
q_{sf}^{(1)} &= \rho(\bar{V}_{fx}^{(0)}\bar{V}_{fx}^{(1)} + \bar{V}_{fy}^{(0)}\bar{V}_{fy}^{(1)}),\ \beta_f^{(1)} = \tan^{-1}\left(\frac{\bar{V}_{fx}^{(0)}\bar{V}_{fy}^{(1)} - \bar{V}_{fx}^{(1)}\bar{V}_{fy}^{(0)}}{(\bar{V}_{fx}^{(0)})^2 + (\bar{V}_{fy}^{(0)})^2}\right)\\
q_i^{(1)} &= \rho(\bar{V}_{iy}^{(0)}\bar{V}_{iy}^{(1)} + \bar{V}_{iz}^{(0)}\bar{V}_{iz}^{(1)}),\ \alpha_i^{(1)} = \tan^{-1}\left(\frac{\bar{V}_{iy}^{(0)}V_{iz}^{(1)} - \bar{V}_{iy}^{(1)}\bar{V}_{iz}^{(0)}}{(\bar{V}_{iy}^{(0)})^2 + (\bar{V}_{iz}^{(0)})^2}\right) + \psi_{ix},\ i = w, e\\
q_{se}^{(1)} &= \rho(\bar{V}_{ey}^{(0)}\bar{V}_{ey}^{(1)} + \bar{V}_{ez}^{(0)}\bar{V}_{ez}^{(1)}),\ \beta_e^{(1)} = \tan^{-1}\left(\frac{\bar{V}_{ey}^{(0)}\bar{V}_{ez}^{(1)} - \bar{V}_{ey}^{(1)}\bar{V}_{ez}^{(0)}}{(\bar{V}_{ey}^{(0)})^2 + (\bar{V}_{ez}^{(0)})^2}\right) + \psi_{ex}
\end{aligned}
\tag{3.16}
$$

Moreover, the first-order parts of the gravity force densities are

$$
\mathbf{f}_{gf}^{(1)} = C_f^{(1)}\,[0\ 0\ \rho_f g]^T;\ \mathbf{f}_{gi}^{(1)} = C_i C_f^{(1)}\,[0\ 0\ \rho_i g]^T,\ i = w, e \tag{3.17}
$$

Equations (3.9)-(3.17) must be solved for the state $\mathbf{x}^{(1)} = [\mathbf{R}_f^{(1)T}\boldsymbol{\theta}_f^{(1)T}\mathbf{q}_{uf}^T\ \mathbf{q}_{uw}^T \dots \mathbf{q}_{\psi e}^T\ \mathbf{p}_{Vf}^{(1)T}\mathbf{p}_{\omega f}^{(1)T}$ $\mathbf{p}_{uf}^T\ \ \mathbf{p}_{uw}^T \dots \mathbf{p}_{\psi e}^T]^T$ in conjunction with

$$
\begin{aligned}
\mathbf{p}_{Vf}^{(1)} &= m\mathbf{V}_f^{(1)} + \tilde{S}^{(1)^T}\boldsymbol{\omega}_f^{(0)} + \tilde{S}^{(0)^T}\boldsymbol{\omega}_f^{(1)} + M_{13}^{(0)}\mathbf{s}_{uf} + M_{14}^{(0)}\mathbf{s}_{uw} + M_{15}^{(0)}\mathbf{s}_{ue} + M_{16}^{(0)}\mathbf{s}_{\psi f}\\
&\quad + M_{17}^{(0)}\mathbf{s}_{\psi w} + M_{18}^{(0)}\mathbf{s}_{\psi e}\\
\mathbf{p}_{\omega f}^{(1)} &= \tilde{S}^{(1)}\mathbf{V}_f^{(0)} + \tilde{S}^{(0)}\mathbf{V}_f^{(1)} + J^{(1)}\boldsymbol{\omega}_f^{(0)} + J^{(0)}\boldsymbol{\omega}_f^{(1)} + M_{23}^{(0)}\mathbf{s}_{uf} + M_{24}^{(0)}\mathbf{s}_{uw} + M_{25}^{(0)}\mathbf{s}_{ue}\\
&\quad + M_{26}^{(0)}\mathbf{s}_{\psi f} + M_{27}^{(0)}\mathbf{s}_{\psi w} + M_{28}^{(0)}\mathbf{s}_{\psi e}\\
\mathbf{p}_{uf} &= M_{31}^{(0)}\mathbf{V}_f^{(1)} + M_{31}^{(1)}\mathbf{V}_f^{(0)} + M_{32}^{(0)}\boldsymbol{\omega}_f^{(1)} + M_{32}^{(1)}\boldsymbol{\omega}_f^{(0)} + M_{33}^{(0)}\mathbf{s}_{uf} + M_{34}^{(0)}\mathbf{s}_{uw} + M_{35}^{(0)}\mathbf{s}_{ue}\\
&\quad + M_{36}^{(0)}\mathbf{s}_{\psi f} + M_{37}^{(0)}\mathbf{s}_{\psi w} + M_{38}^{(0)}\mathbf{s}_{\psi e}\\
\mathbf{p}_{uw} &= M_{41}^{(0)}\mathbf{V}_f^{(1)} + M_{41}^{(1)}\mathbf{V}_f^{(0)} + M_{42}^{(0)}\boldsymbol{\omega}_f^{(1)} + M_{42}^{(1)}\boldsymbol{\omega}_f^{(0)} + M_{43}^{(0)}\mathbf{s}_{uf} + M_{44}^{(0)}\mathbf{s}_{uw} + M_{45}^{(0)}\mathbf{s}_{ue}\\
&\quad + M_{46}^{(0)}\mathbf{s}_{\psi f} + M_{47}^{(0)}\mathbf{s}_{\psi w} + M_{48}^{(0)}\mathbf{s}_{\psi e}\\
\mathbf{p}_{ue} &= M_{51}^{(0)}\mathbf{V}_f^{(1)} + M_{51}^{(1)}\mathbf{V}_f^{(0)} + M_{52}^{(0)}\boldsymbol{\omega}_f^{(1)} + M_{52}^{(1)}\boldsymbol{\omega}_f^{(0)} + M_{53}^{(0)}\mathbf{s}_{uf} + M_{54}^{(0)}\mathbf{s}_{uw} + M_{55}^{(0)}\mathbf{s}_{ue}\\
&\quad + M_{56}^{(0)}\mathbf{s}_{\psi f} + M_{57}^{(0)}\mathbf{s}_{\psi w} + M_{58}^{(0)}\mathbf{s}_{\psi e}\\
\mathbf{p}_{\psi f} &= M_{61}^{(0)}\mathbf{V}_f^{(1)} + M_{61}^{(1)}\mathbf{V}_f^{(0)} + M_{62}^{(0)}\boldsymbol{\omega}_f^{(1)} + M_{62}^{(1)}\boldsymbol{\omega}_f^{(0)} + M_{63}^{(0)}\mathbf{s}_{uf} + M_{64}^{(0)}\mathbf{s}_{uw} + M_{65}^{(0)}\mathbf{s}_{ue}\\
&\quad + M_{66}^{(0)}\mathbf{s}_{\psi f} + M_{67}^{(0)}\mathbf{s}_{\psi w} + M_{68}^{(0)}\mathbf{s}_{\psi e}\\
\mathbf{p}_{\psi w} &= M_{71}^{(0)}\mathbf{V}_f^{(1)} + M_{71}^{(1)}\mathbf{V}_f^{(0)} + M_{72}^{(0)}\boldsymbol{\omega}_f^{(1)} + M_{72}^{(1)}\boldsymbol{\omega}_f^{(0)} + M_{73}^{(0)}\mathbf{s}_{uf} + M_{74}^{(0)}\mathbf{s}_{uw} + M_{75}^{(0)}\mathbf{s}_{ue}\\
&\quad + M_{76}^{(0)}\mathbf{s}_{\psi f} + M_{77}^{(0)}\mathbf{s}_{\psi w} + M_{78}^{(0)}\mathbf{s}_{\psi e}\\
\mathbf{p}_{\psi e} &= M_{81}^{(0)}\mathbf{V}_f^{(1)} + M_{81}^{(1)}\mathbf{V}_f^{(0)} + M_{82}^{(0)}\boldsymbol{\omega}_f^{(1)} + M_{82}^{(1)}\boldsymbol{\omega}_f^{(0)} + M_{83}^{(0)}\mathbf{s}_{uf} + M_{84}^{(0)}\mathbf{s}_{uw} + M_{85}^{(0)}\mathbf{s}_{ue}\\
&\quad + M_{86}^{(0)}\mathbf{s}_{\psi f} + M_{87}^{(0)}\mathbf{s}_{\psi w} + M_{88}^{(0)}\mathbf{s}_{\psi e}
\end{aligned}
\tag{3.18}
$$

where $M_{ij}^{(0)}$ and $M_{ij}^{(1)}$ are the zero-order part and first-order part of M_{ij}, Eqs. (2.15). Equations (3.18) are to be solved for $\mathbf{V}_f^{(1)},\ \boldsymbol{\omega}_f^{(1)},\ \mathbf{s}_{uf},\ \mathbf{s}_{uw},\ \ldots,\ \mathbf{s}_{\psi e}$ in terms of $\mathbf{p}_{Vf}^{(1)},\ \mathbf{p}_{\omega f}^{(1)},\ \mathbf{p}_{uf},\ \mathbf{p}_{uw},\ \ldots,\ \mathbf{p}_{\psi e},\ \mathbf{V}_f^{(0)}$ and $\boldsymbol{\omega}^{(0)}$ and the result inserted in Eqs. (3.9).

The zero-order problem, or flight dynamics problem, represents an inverse problem, which amounts to determining the controls permitting realization of a given rigid body maneuver. The first-order equations representing the extended aeroelasticity problem are linear and tend to be of high order. Moreover, they contain the zero-order variables $\mathbf{V}_f^{(0)}$ and $\boldsymbol{\omega}_f^{(0)}$, representing a given maneuver, as coefficients and as an input. If $\mathbf{V}_f^{(0)}$ and $\boldsymbol{\omega}_f^{(0)}$ are constant, then the system is time-invariant, and if $\mathbf{V}_f^{(0)}$ and $\boldsymbol{\omega}_f^{(0)}$ depend on time, then the system is time-varying. In either case, controls can be designed by various methods. In the time-invariant case, a stability analysis for the closed-loop system can be carried out by solving an eigenvalue problem. Such a stability analysis is precluded in the time-varying case. Simulation of the response of the closed-loop system to external excitations, such as gusts, can be obtained in both the time-invariant case and time-varying case.

Chapter 4

Control of Flexible Aircraft

4.1 Control Design

Flying aircraft are subjected to various disturbances tending to drive them from the intended maneuver and to cause vibration. If the system is controllable, these effects can be suppressed through controls, which are carried out by means of actuators; in the case of aircraft they consist of the engine thrust and the control surfaces. A system is said to be controllable if there exists a piecewise continuous input that will drive the initial state to any final state within a finite time interval. System controllability can be determined by checking the rank of a so-called controllability matrix,[39] which may not be feasible if the system order is large. In practice, controllability can be ascertained on physical grounds by making sure that the input forces, namely, the forces due to the engine thrust and control surfaces, affect all the state variables.

As indicated in earlier sections, there are two types of controls, one type designed to permit the aircraft to execute a desired maneuver as if it were rigid and the other type to reduce any deviations from the rigid body maneuver to zero, which amounts to suppressing vibration and perturbations in the rigid body motions of the aircraft. The first is associated with the flight dynamics problem and the second with the extended aeroelasticity problem. In general, the engine thrust and control surfaces are designed so as to ensure that the aircraft is able to carry out the required maneuvers, as well as to suppress any undesirable disturbances, thus addressing the needs of both the flight dynamics problem and extended aeroelasticity problem.

Using Eqs. (3.2), we write the flight dynamics problem, or the zero-order problem, in the

compact state form

$$\dot{\mathbf{x}}^{(0)}(t) = \mathbf{f}[\mathbf{x}^{(0)}(t),\ \mathbf{V}_{rb}^{(0)}(t)] + B^{(0)}[\mathbf{V}_{rb}^{(0)}(t)]\mathbf{u}^{(0)}(t) \tag{4.1}$$

which, from Eqs. (3.8), must be considered in conjunction with

$$\mathbf{p}_{rb}^{(0)}(t) = M^{(0)}\mathbf{V}_{rb}^{(0)}(t) \tag{4.2}$$

where the zero-order quantities are identified as follows: $\mathbf{x}^{(0)} = [\mathbf{R}_f^{(0)^T}\ \ \boldsymbol{\theta}_f^{(0)^T}\ \ \mathbf{p}_{Vf}^{(0)^T}\ \ \mathbf{p}_{\omega f}^{(0)^T}]^T$ is the state vector, $\mathbf{f}$ is a nonlinear function of the state vector and the zero-order rigid body velocity vector $\mathbf{V}_{rb}^{(0)} = [\mathbf{V}_f^{(0)^T}\ \ \boldsymbol{\omega}_f^{(0)^T}]^T$, $B^{(0)}$ is a coefficient matrix, $\mathbf{u}^{(0)} = [F_E^{(0)}\ \ \delta_a^{(0)}\ \ \delta_e^{(0)}\ \ \delta_r^{(0)}]^T$ is the control vector, in which $F_E^{(0)}$, $\delta_a^{(0)}$, $\delta_e^{(0)}$ and $\delta_r^{(0)}$ are the engine thrust and control surfaces angles, $\mathbf{p}_{rb}^{(0)} = [\mathbf{p}_{Vf}^{(0)^T}\ \ \mathbf{p}_{\omega f}^{(0)^T}]^T$ is the rigid body momentum vector and

$$M^{(0)} = \begin{bmatrix} mI & \tilde{S}^{(0)^T} \\ \tilde{S}^{(0)} & J^{(0)} \end{bmatrix} \tag{4.3}$$

is the rigid-body mass matrix. In the context of the present integrated approach, Eqs. (4.1) and (4.2) represent an inverse problem, in the sense that a state vector $\mathbf{x}^{(0)}$ describing a desired maneuver is postulated and a force vector $\mathbf{u}^{(0)}$ permitting a realization of the given maneuver is determined.

Next, we assume that $\mathbf{x}^{(0)}(t)$ and $\mathbf{V}_{rb}^{(0)}(t)$ are known and use Eqs. (3.9) and (3.18) to express the extended aeroelasticity problem, or first-order problem, in the form

$$\dot{\mathbf{x}}^{(1)}(t) = A(t)\mathbf{x}^{(1)}(t) + B\mathbf{u}^{(1)}(t) + [0\ \ I]^T\mathbf{F}_{\text{ext}}(t) \tag{4.4}$$

and

$$\mathbf{p}^{(1)}(t) = M^{(0)}\mathbf{V}^{(1)}(t) + M^{(1)}(t)\mathbf{V}^{(0)}(t) \tag{4.5}$$

respectively, in which $\mathbf{x}^{(1)} = [\mathbf{R}_f^{(1)^T}\ \ \boldsymbol{\theta}_f^{(1)T}\ \ \mathbf{q}_{uf}^T\ \ \mathbf{q}_{uw}^T \dots \mathbf{q}_{\psi e}^T\ \ \mathbf{p}_{Vf}^{(1)^T}\ \ \mathbf{p}_{\omega f}^{(1)^T}\ \ \mathbf{p}_{uf}^T\ \ \mathbf{p}_{uw}^T \dots \mathbf{p}_{\psi e}^T]^T$ is the first-order state vector, $A(t) = A[\mathbf{x}^{(0)}(t),\ \mathbf{V}_{rb}^{(0)}(t)]$ and $B\ [\mathbf{x}^{(0)}(t), \mathbf{V}_{rb}^{(0)}(t)]$ are coefficient matrices, $\mathbf{u}^{(1)}(t) = [F_E^{(1)}\ \ \delta_a^{(1)}\ \ \delta_e^{(1)}\ \ \delta_r^{(1)}]^T$ is a first-order control vector, $\mathbf{F}_{\text{ext}}$ is an external disturbing force vector, such as due to gusts, $\mathbf{p}^{(1)} = [\mathbf{p}_{Vf}^{(1)^T}\ \ \mathbf{p}_{\omega f}^{(1)^T}\ \ \mathbf{p}_{uf}^T\ \ \mathbf{p}_{uw}^T \dots \mathbf{p}_{\psi e}^T]^T$ is the first-order momentum vector and

$$M^{(0)} = \begin{bmatrix} mI & \tilde{S}^{(0)^T} & M_{13}^{(0)} & \dots & M_{18}^{(0)} \\ \tilde{S}^{(0)} & J^{(0)} & M_{23}^{(0)} & \dots & M_{28}^{(0)} \\ M_{31}^{(0)} & M_{32}^{(0)} & M_{33}^{(0)} & \dots & M_{38}^{(0)} \\ \dots & \dots & \dots & \dots & \dots \\ M_{81}^{(0)} & M_{82}^{(0)} & M_{83}^{(0)} & \dots & M_{88}^{(0)} \end{bmatrix},\ M^{(1)} = \begin{bmatrix} 0 & \tilde{S}^{(1)^T} & 0 & \dots & 0 \\ \tilde{S}^{(1)} & J^{(1)} & M_{23}^{(1)} & \dots & M_{28}^{(1)} \\ 0 & M_{32}^{(1)} & 0 & \dots & 0 \\ \dots & \dots & \dots & \dots & \dots \\ 0 & M_{82}^{(1)} & 0 & \dots & 0 \end{bmatrix} \tag{4.6}$$

are zero-order and first-order extended mass matrices. Note that $\mathbf{F}_{\text{ext}}$ is regarded as a disturbing force of a transient nature whose effects will be eventually suppressed by the controls.

Equation (4.4) represents a set of linear equations, and the objective is to find a control vector $\mathbf{u}^{(1)}(t)$ that drives the state vector $\mathbf{x}^{(1)}$ to zero. To this end, we consider a linear regulator whereby the control vector is a linear function of the state vector. In particular, we consider a linear quadratic regulator (LQR) in which the objective is to determine an optimal control vector minimizing the quadratic performance measure[39]

$$J = \tfrac{1}{2}\mathbf{x}^{(1)^T}(t_f)H\mathbf{x}^{(1)}(t_f) + \tfrac{1}{2}\int_{t_0}^{t_f}[\mathbf{x}^{(1)^T}(t)\mathbf{Q}(t)\mathbf{x}^{(1)}(t) + \mathbf{u}^{(1)^T}(t)R(t)\mathbf{u}^{(1)}(t)]dt \tag{4.7}$$

where H and Q are real symmetric positive semidefinite matrices R is a real symmetric positive definite matrix, t_0 is the initial time (commonly assumed to be zero) and t_f is the final time. It is shown in Ref. 39 that the optimal feedback control vector is given by

$$\mathbf{u}^{(1)}(t) = -R^{-1}(t)B^T K(t)\mathbf{x}^{(1)}(t) = -G(t)\mathbf{x}^{(1)}(t) \tag{4.8}$$

where

$$G(t) = R^{-1}(t)B^T K(t) \tag{4.9}$$

is a control gain matrix, in which $K(t)$ is a real symmetric matrix satisfying the transient matrix Riccati equation

$$\dot{K} = -Q - A^T K - KA + KBR^{-1}B^T K, \quad K(t_f) = H(t_f) = H \tag{4.10}$$

a nonlinear equation which must be integrated backward in time from t_f to t_0. Rather than integrating a nonlinear matrix equation, it is advisable to transform the problem into a linear one. To this end, we consider the transformation

$$K(t) = E(t)F^{-1}(t) \tag{4.11}$$

where $E(t)$ and $F(t)$ can be obtained by solving the linear equation

$$\begin{bmatrix} \dot{E}(t) \\ \dot{F}(t) \end{bmatrix} = \begin{bmatrix} -A^T(t) & -Q(t) \\ -BR^{-1}(t)B^T & A(t) \end{bmatrix} \begin{bmatrix} E(t) \\ F(t) \end{bmatrix}, \quad \begin{bmatrix} E(t_f) \\ F(t_f) \end{bmatrix} = \begin{bmatrix} H \\ I \end{bmatrix} \tag{4.12}$$

which again must be integrated backward in time. Inserting Eq. (4.5) into Eq. (4.1), we obtain the closed-loop equation

$$\dot{\mathbf{x}}^{(1)}(t) = [A(t) - BG(t)]\mathbf{x}^{(1)}(t) + [0 \;\; I]\mathbf{F}_{\text{ext}}(t) \tag{4.13}$$

which can be integrated to simulate the system response.

The problem is considerably simpler when the zero-order solution is constant, such as in steady level flight, as in this case the coefficient matrix A is constant. Then, if the system is controllable, $H = 0$ and Q and R are constant, the Riccati matrix K approaches a constant value as t_f increases without bounds. In this case, Eq. (4.10) reduces to the steady-state matrix Riccati equation

$$-Q - A^T K - KA + KBR^{-1}B^T K = 0 \tag{4.14}$$

a nonlinear algebraic matrix equation, which can be solved by means of Potter's algorithm,[39] and the gain matrix G becomes constant. The closed-loop equation reduces to one with constant coefficients, or

$$\dot{\mathbf{x}}^{(1)}(t) = (A - BG)\mathbf{x}^{(1)}(t) + [0 \quad I]\mathbf{F}_{\text{ext}}(t) \tag{4.15}$$

which can be used for response simulation. For a stability analysis, we solve the associated eigenvalue problem

$$(A - BG - \lambda I)\mathbf{x} = \mathbf{0} \tag{4.16}$$

The closed-loop system is stable if all the eigenvalues are pure imaginary and/or complex with negative real part.

The control vector $\mathbf{u}^{(1)}$ is optimal in the sense that it minimizes the performance index J, but the physical merit of this optimality is debatable. In fact, it is often necessary to adjust the otherwise arbitrary weighting matrices Q and R to achieve a desirable system performance. The real value of the LQR algorithm is that it guarantees a stable closed-loop system.

4.2 Optimal State Observer

In Sec. 4.1, we carried out the control design in two stages. In the first stage, we postulated a desired aircraft maneuver $\mathbf{x}^{(0)}$ and used an inverse approach to determine the control vector $\mathbf{u}^{(0)}$ permitting realization of the maneuver. In the second stage, we designed a feedback control vector $\mathbf{u}^{(1)}$ ensuring stability of the maneuver, which amounts to driving the perturbation vector $\mathbf{x}^{(1)}$ to zero. The control vector is given by Eq. (4.8), in which G is the control gain matrix.

Implementation of the control law, Eq. (4.8), requires knowledge of the state vector $\mathbf{x}^{(1)}$, which can be obtained through measurement. This creates somewhat of a problem, as

measurements represent real quantities and our state vector consists of abstract generalized coordinates rather than real coordinates. Moreover, we feed back only perturbations from the maneuver variables. In the absence of external forces, the state equations describing the extended aeroelasticity problem have the vector form

$$\dot{\mathbf{x}}^{(1)}(t) = A\mathbf{x}^{(1)}(t) + B\mathbf{u}^{(1)}(t) \tag{4.17}$$

where the coefficient matrices A and B were defined in Sec. 4.1. Moreover, denoting the measurement vector by $\mathbf{y}(t)$, we can write

$$\mathbf{y}(t) = \mathbf{y}^{(0)}(t) + \mathbf{y}^{(1)}(t) \tag{4.18}$$

where $\mathbf{y}^{(0)}(t)$ is the contribution from the maneuver variables and $\mathbf{y}^{(1)}(t)$ is the contribution from the perturbations in the maneuver variables. We express the latter in the form

$$\mathbf{y}^{(1)}(t) = C\mathbf{x}^{(1)}(t) \tag{4.19}$$

and refer to $\mathbf{y}^{(1)}(t)$ as the output vector. The assumption is made here that the system is observable,[39] which implies that the initial state $\mathbf{x}^{(1)}(0)$ can be deduced from the outputs within a finite time period. Observability can be established by checking the rank of a so-called observability matrix,[39] a matrix involving the matrices A and C. For large-order systems, working with the observability matrix may not be feasible, and in practice the choice of sensors ensuring observability must be made on physical grounds. In particular, the choice must be such that the sensors signals permit reconstruction of the state at all times. The task of determining the matrix C relating the output vector to the state vector is discussed later in this section.

In reality, the state vector cannot be determined exactly from the output vector and must be estimated. A device permitting an estimate of the state vector is known as an observer[39] and can be expressed in the form

$$\dot{\hat{\mathbf{x}}}^{(1)}(t) = A\hat{\mathbf{x}}^{(1)}(t) + B\mathbf{u}^{(1)}(t) + K_o[\mathbf{y}^{(1)}(t) - C\hat{\mathbf{x}}^{(1)}(t)] \tag{4.20}$$

where K_o is an observer gain matrix. Subtracting Eq. (4.20) from Eq. (4.17), we obtain

$$\dot{\mathbf{e}}(t) = [A - K_o C]\mathbf{e}(t) \tag{4.21}$$

in which

$$\mathbf{e}(t) = \mathbf{x}^{(1)}(t) - \hat{\mathbf{x}}^{(1)}(t) \tag{4.22}$$

represents the observer error vector. The objective is to find a matrix K_o such that the vector $\mathbf{e}(t)$ approaches zero as t increases. In this case, $\hat{\mathbf{x}}(t) \to \mathbf{x}(t)$ with time. For a time-invariant system, this amounts to determine K_o so that all the eigenvalues of the matrix $A - K_o C$, known as the observer poles, lie in the left half of the complex plane. In implementing feedback controls, we must use the estimated state $\hat{\mathbf{x}}^{(1)}(t)$, because the initial state $\mathbf{x}^{(1)}(t)$ is not available. Hence, Eq. (4.8) must be replaced by

$$\mathbf{u}^{(1)}(t) = -G\hat{\mathbf{x}}^{(1)}(t) \tag{4.23}$$

One question of interest is how the choice of observer poles affect the choice of controller poles. To answer this question, we use Eqs. (4.22) and (4.23) and rewrite Eq. (4.17) in the form

$$\dot{\mathbf{x}}^{(1)}(t) = [A - BG]\mathbf{x}^{(1)}(t) + BG\mathbf{e}(t) \tag{4.24}$$

Equations (4.21) and (4.24) can be combined into

$$\begin{bmatrix} \dot{\mathbf{x}}^{(1)}(t) \\ \dot{\mathbf{e}}(t) \end{bmatrix} = \begin{bmatrix} A - BG & BG \\ 0 & A - K_o C \end{bmatrix} \begin{bmatrix} \mathbf{x}^{(1)}(t) \\ \mathbf{e}(t) \end{bmatrix} \tag{4.25}$$

Because the coefficient matrix in Eq. (4.25) is block-triangular, the poles of the combined system consist of the sum of the poles of $A - BG$ and the poles of $A - K_o C$, so that the observer poles can be chosen independently of the controller poles.

An optimal observer gain matrix can be obtained by adopting a stochastic approach, leading to the so-called Kalman-Bucy filter, in contrast to a deterministic observer known as a Luenberger observer. To this end, we rewrite Eqs. (4.17) and (4.19) in the form

$$\dot{\mathbf{x}}^{(1)}(t) = A\mathbf{x}^{(1)}(t) + B\mathbf{u}^{(1)}(t) + \mathbf{v}(t) \tag{4.26}$$

and

$$\mathbf{y}^{(1)}(t) = C\mathbf{x}^{(1)}(t) + \mathbf{w}(t) \tag{4.27}$$

where $\mathbf{v}(t)$ is known as the state excitation noise and $\mathbf{w}(t)$ as the observation noise, or sensor noise. It is customary to assume that $\mathbf{v}(t)$ and $\mathbf{w}(t)$ are white noise processes, with intensities $V(t)$ and $W(t)$, respectively, so that the correlation matrices have the form

$$E\{\mathbf{v}(t_1)\mathbf{v}^T(t_2)\} = V(t_1)\delta(t_2 - t_1),\ E\{\mathbf{w}(t_1)\mathbf{w}^T(t_2)\} = W(t_1)\delta(t_2 - t_1) \tag{4.28}$$

and that they are uncorrelated, so that

$$E\{\mathbf{v}(t_1)\mathbf{w}^T(t_2)\} = E\{\mathbf{w}(t_1)\mathbf{v}^T(t_2)\} = 0 \tag{4.29}$$

in which $E\{\cdot\}$ denotes the expected value.

The stochastic observer has the same form as that given by Eq. (4.20) in which the optimal gain matrix is determined by minimizing the performance measure

$$J_o = E\{\mathbf{e}^T(t)U(t)\mathbf{e}(t)\} \tag{4.30}$$

where $\mathbf{e}(t)$ is the observer error vector, Eq. (4.22), and $U(t)$ is a symmetric positive definite weighting matrix. From Ref. 39, the optimal observer gain matrix is given by

$$K_o^*(t) = Q(t)C^T W^{-1}(t) \tag{4.31}$$

where $Q(t)$ is the variance matrix of $\mathbf{e}(t)$ satisfying the Riccati equation

$$\dot{Q}(t) = AQ(t) + Q(t)A^T + V(t) - Q(t)C^T W^{-1}(t)CQ(t),\ Q(0) = Q_0 \tag{4.32}$$

In the time-invariant case, Eq. (4.32) reduces to an algebraic matrix Riccati equation yielding a steady-state optimal observer gain matrix. The main problem in implementing a Kalman-Bucy filter lies in the selection of the noise intensities $V(t)$ and $W(t)$.

At this point, we turn our attention to the determination of the matrix C defined by Eq. (4.19). To this end, we must first specify the measurement vector $\mathbf{y}^{(1)}(t)$, which in turn depends on the sensors used. In inertial navigation[40], which represents the process of determining the position and attitude of a moving vehicle from self-contained inertial measurements made on board of the vehicle, the system consists of a platform containing accelerometers sensing translational motions and gyroscopes sensing angular motions and a computer capable of integrating the sensors signals to generate the state. Inertial navigation is widely used for aircraft, in which case there are two accelerometers aligned with the North and East directions and three rate gyroscopes with the spin axes aligned with the North, East and zenith directions. To ensure that gravity does not contaminate the accelerometers signals, the platform is made to rotate continuously so as to remain normal to the local vertical. The vertical position of the aircraft is measured by means of an altimeter. In view of this, we can assume that the system measures the vectors $\mathbf{R}_f$ and $\boldsymbol{\theta}_f$ giving the position and attitude relative to axes XYZ. In this regard, it should be mentioned that we referred to axes XYZ as inertial, but in reality they represent earth-fixed axes. If the current formulation is used to describe relatively long flights, then proper allowance must be made for the rotation of the earth. Because the same process can be used to determine the zero-order position vectors $\mathbf{R}_f^{(0)}$ and $\boldsymbol{\theta}_f^{(0)}$, we can assume that the measurement system is capable of yielding $\mathbf{R}_f^{(1)}$ and $\boldsymbol{\theta}_f^{(1)}$.

The above process can be used to measure the perturbations in the rigid-body motions of the aircraft and the question remains as to how to measure the balance of the variables, namely, the elastic variables. To this end, we assume that there are N_i $(i = f, w, e)$ sensors measuring velocities at the points P_k $(k = 1, 2, \ldots, N_i)$ of the aircraft components and express the output vector in the form

$$\mathbf{y}^{(1)}(t) = [\mathbf{R}_f^{(1)^T} \;\; \boldsymbol{\theta}_f^{(1)^T} \;\; \mathbf{0}^T \;\; \mathbf{0}^T \ldots \mathbf{0}^T]^T + [\mathbf{y}_f^{(1)^T}(t) \;\; \mathbf{y}_w^{(1)^T}(t) \;\; \mathbf{y}_e^{(1)^T}(t)]^T \tag{4.33}$$

where

$$\mathbf{y}_i^{(1)^T} = [\bar{\mathbf{V}}_i^{(1)^T}(P_1, t) \;\; \bar{\mathbf{V}}_i^{(1)^T}(P_2, t) \;\; \ldots \;\; \bar{\mathbf{V}}_i^{(1)^T}(P_{N_i}, t)]^T, \;\; i = f, w, e \tag{4.34}$$

in which $\bar{\mathbf{V}}_i^{(1)}(P_k, t)$ are vectors of velocity measurements. From Eqs. (2.12) and (3.12), we can write

$$\begin{aligned}\bar{\mathbf{V}}_f^{(1)}(P_k, t) &= \mathbf{V}_f^{(1)}(t) + \tilde{r}_f^T(P_k)\boldsymbol{\omega}_f^{(1)} + \tilde{\omega}_f^{(0)}\Phi_{uf}(P_k)\mathbf{q}_{uf}(t) \\ &\quad + \Phi_{uf}(P_k)\mathbf{s}_{uf}(t) + \tilde{r}_f^T(P_k)\Phi_{\psi f}(P_k)\mathbf{s}_{\psi f}(t) \\ &= \text{block-diag } C_{fk} \begin{bmatrix} \mathbf{d}^{(1)}(t) \\ \mathbf{V}^{(1)}(t) \end{bmatrix}, \;\; k = 1, 2, \ldots, N_f \end{aligned} \tag{4.35}$$

where

$$\begin{aligned}\text{block-diag } C_{fk} = \text{block-diag}[&0 \;\; 0 \;\; \tilde{\omega}_f^{(0)}\Phi_{uf}(P_k) \;\; 0 \;\; 0 \;\; 0 \;\; 0 \;\; 0 \\ &I \;\; \tilde{r}_f^T(P_k) \;\; \Phi_{uf}(P_k) \;\; 0 \;\; 0 \;\; \tilde{r}_f^T(P_k)\Phi_{\psi f}(P_k) \;\; 0 \;\; 0]\end{aligned} \tag{4.36}$$

and $\mathbf{d}^{(1)} = [\mathbf{R}_f^{(1)^T} \;\; \boldsymbol{\theta}_f^{(1)^T} \;\; \mathbf{q}_{uf}^T \;\; \mathbf{q}_{uw}^T \;\; \mathbf{q}_{ue}^T \;\; \mathbf{q}_{\psi f}^T \;\; \mathbf{q}_{\psi w}^T \;\; \mathbf{q}_{\psi e}^T]^T$, $\mathbf{V}^{(1)} = [\mathbf{V}_f^{(1)^T} \;\; \boldsymbol{\omega}_f^{(1)^T} \;\; \mathbf{s}_{uf}^T \;\; \mathbf{s}_{uw}^T \;\; \mathbf{s}_{ue}^T \;\; \mathbf{s}_{\psi f}^T \;\; \mathbf{s}_{\psi w}^T \;\; \mathbf{s}_{\psi e}^T]^T$. Also from Eqs. (2.12) and (3.12), we can write

$$\begin{aligned}\bar{\mathbf{V}}_w^{(1)}(P_k, t) &= C_w\mathbf{V}_f^{(1)} + (C_w\tilde{r}_{fw}^T + \tilde{r}_w^T(P_k)C_w)\boldsymbol{\omega}_f^{(1)} + C_w\tilde{\omega}_f^{(0)}\Phi_{ufw}\mathbf{q}_{uf}(t) \\ &\quad + \widetilde{C_w\boldsymbol{\omega}_f^{(0)}}\Phi_{uw}(P_k)\mathbf{q}_{uw}(t) + (\tilde{r}_w^T(P_k)C_w\Delta\Phi_{ufw} + C_w\Phi_{ufw})\mathbf{s}_{uf} \\ &\quad + \Phi_{uw}(P_k)s_{uw}(t) + (\tilde{r}_w^T(P_k)C_w\Phi_{\psi fw} + C_w\tilde{r}_{fw}^T\Phi_{\psi fw})\mathbf{s}_{\psi f} \\ &\quad + \tilde{r}_w^T(P_k)\Phi_{\psi w}(P_k)\mathbf{s}_{\psi w} \\ &= \text{block-diag } C_{wk} \begin{bmatrix} \mathbf{d}^{(1)}(t) \\ \mathbf{V}^{(1)}(t) \end{bmatrix}, \;\; k = 1, 2, \ldots, N_w \end{aligned} \tag{4.37}$$

where

$$\begin{aligned}\text{block-diag } C_{wk} = \text{block-diag}[&0 \;\; 0 \;\; C_w\tilde{\omega}_f^{(0)}\Phi_{ufw} \;\; \widetilde{C_w\boldsymbol{\omega}_f^{(0)}}\Phi_{uw}(P_k) \;\; 0 \;\; 0 \;\; 0 \;\; 0 \\ &C_w \;\; (C_w\tilde{r}_{fw}^T + \tilde{r}_w^T(P_k)C_w) \;\; (\tilde{r}_w^T(P_k)C_w\Delta\Phi_{ufw} + C_w\Phi_{ufw}) \\ &\Phi_{uw}(P_k) \;\; 0 \;\; (\tilde{r}_w^T(P_k)C_w\Phi_{\psi fw} + C_w\tilde{r}_{fw}^T\Phi_{\psi fw}) \\ &\tilde{r}_w^T(P_k)\Phi_{\psi w}(P_k) \;\; 0]\end{aligned} \tag{4.38}$$

In a similar fashion, we can write

$$\bar{\mathbf{V}}_e^{(1)}(P_k,t) = \text{block-diag } C_{ek} \left[\begin{array}{c} \mathbf{d}^{(1)}(t) \\ \mathbf{V}^{(1)}(t) \end{array} \right],\ k = 1, 2, \ldots, N_e \tag{4.39}$$

where

$$\begin{aligned} \text{block-diag } C_{ek} = [0 \ \ 0 \ \ C_e\tilde{\omega}_f^{(0)}\Phi_{ufe} \ \ 0 \ \ \widetilde{C_e\boldsymbol{\omega}_f^{(0)}}\Phi_{uw}(P_k) \ \ 0 \ \ 0 \ \ 0 \\ C_e(C_e\tilde{r}_{fe}^T + \tilde{r}_e^T(P_k)C_e) \ \ (\tilde{r}_e^T(P_k)C_e\Delta\Phi_{ufe} + C_e\Phi_{ufe}) \ \ 0 \ \ \Phi_{ue}(P_k) \\ (\tilde{r}_e^T(P_k)C_e\Phi_{\psi fe} + C_e\tilde{r}_{fe}^T\Phi_{\psi fe}) \ \ 0 \ \ \tilde{r}_e^T(P_k)\Phi_{\psi e}(P_k)] \end{aligned} \tag{4.40}$$

Equations (4.35), (4.37) and (4.39) are in terms of $\mathbf{d}^{(1)}$ and $\mathbf{V}^{(1)}$. They can be transformed into expressions in terms of the state $\mathbf{x}^{(1)} = [\mathbf{d}^{(1)^T}\mathbf{p}^{(1)^T}]^T$ by considering Eq. (4.5). To this end, we observe that $M^{(1)} = M^{(1)}(\mathbf{q}_{uf},\ \mathbf{q}_{uw},\ \mathbf{q}_{ue})$, so that we can write

$$M^{(1)}\mathbf{V}^{(0)} = M_V\mathbf{d}^{(1)} \tag{4.41}$$

where M_V is a matrix depending on $\mathbf{V}^{(0)}$. Hence, using Eq. (4.5), we obtain

$$\mathbf{V}^{(1)} = (M^{(0)})^{-1}(\mathbf{p}^{(1)} - M_V\mathbf{d}^{(1)}) \tag{4.42}$$

so that

$$\left[\begin{array}{c} \mathbf{d}^{(1)} \\ \mathbf{V}^{(1)} \end{array} \right] = \left[\begin{array}{cc} I & 0 \\ -(M^{(0)})^{-1}M_V & (M^{(0)})^{-1} \end{array} \right] \mathbf{x}^{(1)} \tag{4.43}$$

Finally, using Eqs. (4.33), (4.34), (4.35), (4.37), (4.39) and (4.41), we conclude that

$$C = \left[\begin{array}{c} I \ \ 0 \ \ 0 \ \ \ldots \ \ 0 \\ 0 \ \ I \ \ 0 \ \ \ldots \ \ 0 \\ \text{block-diag } C_{f1} \\ \text{block-diag } C_{f2} \\ \ldots\ldots\ldots\ldots \\ \text{block-diag } C_{fN_f} \\ \text{block-diag } C_{w1} \\ \text{block-diag } C_{w2} \\ \ldots\ldots\ldots\ldots \\ \text{block-diag } C_{wN_w} \\ \text{block-diag } C_{e1} \\ \text{block-diag } C_{e2} \\ \ldots\ldots\ldots\ldots \\ \text{block-diag } C_{eN_e} \end{array} \right] \left[\begin{array}{cc} I & 0 \\ -(M^{(0)})^{-1}M_V & (M^{(0)})^{-1} \end{array} \right] \tag{4.44}$$

Chapter 5

Numerical Example

The flight of a flexible aircraft is fully described by Eqs. (3.2), (3.8), (3.9) and (3.18). A solution of these equations requires the aircraft geometry, the mass and stiffness distributions and the aerodynamic coefficients. Information pertaining to an actual aircraft was made available by an aircraft manufacturer and is listed in the **Appendix**.

The solution of the flight dynamics equations, Eqs. (3.2) and (3.8), requires the matrices $C_f^{(0)}$, $E_f^{(0)}$, the total aircraft mass m, the matrix $\tilde{S}^{(0)}$ of the first moments of inertia of the undeformed aircraft and the inertia matrix $J^{(0)}$ of the undeformed aircraft. The matrices $C_f^{(0)}$ and $E_f^{(0)}$ can be obtained from C_f and E_f, Eqs. (2.2), by simply replacing ψ, θ and ϕ by $\psi^{(0)}$, $\theta^{(0)}$ and $\phi^{(0)}$, respectively. The aerodynamic forces are given by Eqs. (3.5) and the required coefficients are given in the **Appendix**. Other data required is as follows: engine locations, $\mathbf{r}_{E1} = [-108.6176 \;\; 37.0 \;\; -13.96]^T$ in, $\mathbf{r}_{E2} = [-108.6176 \;\; -37.0 \;\; -13.96]^T$ in; total aircraft mass, $m = 33.5896$ lb $\cdot$ s^2/in; matrix of first moments of inertia and inertia matrix

$$\begin{aligned} \tilde{S}^{(0)} &= \begin{bmatrix} 0 & -134.6827 & 0 \\ 134.6827 & 0 & 0 \\ 0 & 0 & 0 \end{bmatrix} \text{lb} \cdot \text{s}^2 \\ J^{(0)} &= \begin{bmatrix} 183183.4257 & 4.7745 & -37624.9453 \\ & 566328.8970 & 81.1583 \\ \text{symm} & & 704218.5794 \end{bmatrix} \text{lb} \cdot \text{in} \cdot \text{s}^2 \end{aligned} \tag{5.1}$$

Some of the above quantities involve the matrices of direction cosines between the various components body axes and the fuselage body axes. These matrices are listed in the **Appendix**. The flight dynamics problem is essentially how to set the control surfaces and the engine thrust for a given aircraft maneuver, of which the steady cruise is a special case. It essentially amounts to the problem of "trimming" the aircraft. As far as this paper is

concerned, it provides the input $\mathbf{V}_f^{(0)}$, $\boldsymbol{\omega}_f^{(0)}$, $\mathbf{p}_{Vf}^{(0)}$ and $\mathbf{p}_{\omega f}^{(0)}$ to the extended aeroelasticity.

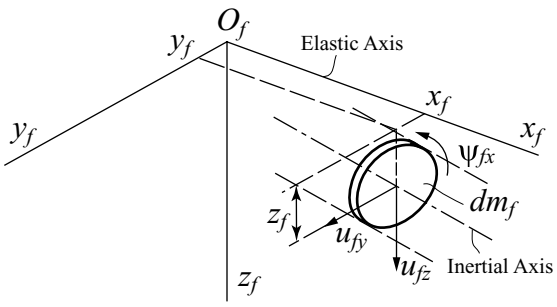

Figure 2. Mass Element for a Fuselage Undergoing Bending and Torsion

The solution of the extended aeroelasticity equations, Eqs. (3.9) and (3.18), requires an explicit choice of the structural model for the aircraft of Fig. 1. As a first approximation, the fuselage, wing, and both the horizontal and vertical stabilizers in the empennage are modeled as beams clamped at the origin of the respective body axes and undergoing bending and torsion. The fuselage undergoes the bending displacements u_{fy} and u_{fz} and the torsional displacement ψ_{fx}, as shown in Fig. 2, so that $\mathbf{u}_f = [0 \;\; u_{fy} \;\; u_{fz}]^T$ and $\boldsymbol{\psi}_f = [\psi_{fx} \;\; 0 \;\; 0]^T$. On the other hand, the wing and the stabilizers undergo only one bending and one torsional displacement each. Note that, as customary, displacements are measured relative to the elastic axis (Fig. 2). Each clamped beam is assumed to be discretized by the Galerkin method in conjunction with two shape functions per displacement component. For bending, the shape functions are chosen as the eigenfunctions of a uniform cantilever beam

$$\phi_{uir} = \sin\beta_r x_i - \sinh\beta_r x_i - \frac{\sin\beta_r L_i + \sinh\beta_r L_i}{\cos\beta_r L_i + \cosh\beta_r L_i}(\cos\beta_r x_i - \cosh\beta_r x_i), \;\; r = 1, 2 \qquad (5.2)$$

and for torsion, the eigenfunctions of a uniform clamped-free shaft

$$\phi_{\psi ir} = \sin(2r-1)\pi x_i / 2L_i, \;\; r = 1, 2 \qquad (5.3)$$

where L_i is the length of the cantilever beam. In this regard, we note that the fuselage is modeled as two cantilever beams clamped at O_f, one pointing to the aircraft nose and the other to the tail. New quantities entering into the first-order equation are $C_f^{(1)}$ and $E_f^{(1)}$, which can be obtained from C_f and E_f by using $\boldsymbol{\theta}_f = \boldsymbol{\theta}_f^{(0)} + \boldsymbol{\theta}_f^{(1)}$ and letting the components of $\boldsymbol{\theta}_f^{(1)}$ be small, $\mathbf{F}^{(1)}$, $\mathbf{M}^{(1)}$, $\mathbf{Q}_{ui}$ and $\mathbf{Q}_{\psi i}$ $(i = f, w, e)$, which are given by Eqs. (3.13), and Φ_{ui} and $\Phi_{\psi i}$, which contain ϕ_{uir} and $\phi_{\psi ir}$ as given above. Moreover, the stiffness matrices are obtained from the potential energy as follows:

$$\begin{aligned} V = {} & \tfrac{1}{2}\int_{D_f}\left[EI_{fz}\left(\partial^2 u_{fy}/\partial x_f^2\right)^2 + EI_{fy}\left(\partial^2 u_{fz}/\partial x_f^2\right)^2 + GJ_{fx}\left(\partial\psi_{fx}/\partial x_f\right)^2\right] dD_f \\ & + \int_{D_w}\left[EI_w\left(\partial^2 u_{wz}/\partial x_w^2\right)^2 + GJ_w\left(\partial\psi_{wx}/\partial x_w\right)^2\right] dD_w + \int_{D_e}\left[EI_e\left(\partial^2 u_{ez}/\partial x_e^2\right)^2\right. \\ & \left. + GJ_e\left(\partial\psi_{ex}/\partial x_{ex}\right)^2\right] dD_e = \tfrac{1}{2}[\mathbf{q}_{uf}^T K_{uf}\mathbf{q}_{uf} + \textstyle\sum_i(\mathbf{q}_{ui}^T K_{ui}\mathbf{q}_{ui} + \mathbf{q}_{\psi i}^T K_{\psi i}\mathbf{q}_{\psi i})] \end{aligned} \qquad (5.4)$$

where

$$\begin{aligned} &K_{uf} = \int_{D_f} (\Phi''_{uf})^T \text{diag}[EI_{fz} \;\; EI_{fy}] \Phi''_{uf} dD_f, \;\; K_{ui} = \int_{D_i} EI_i (\Phi''_{ui})^T \Phi''_{ui} dD_i \\ &K_{\psi i} = \int_{D_i} GJ_i (\Phi'_{\psi i})^T \Phi'_{\psi i} dD_i, \;\; i = f, w, e \end{aligned} \tag{5.5}$$

are the desired stiffness matrices, in which primes denote differentiations with respect to x_i.

Equations (4.4) for the model in question are of order 76, but the equations are linear. However, in the case of certain aircraft maneuvers, the systems is time-varying.

To demonstrate the ideas, we consider two cases, steady level flight and steady level turn maneuver.

5.1 Steady Level Flight

For steady level flight, the zero-order velocities are defined by

$$\mathbf{V}_f^{(0)} = C_f^{(0)} [V^{(0)} \;\; 0 \;\; 0]^T = \text{constant}, \;\; \boldsymbol{\omega}_f^{(0)} = \mathbf{0} \tag{5.6}$$

where $V^{(0)}$ is the forward velocity of the aircraft. From Eqs. (3.8), we conclude that the zero-order momenta are

$$\mathbf{p}_{Vf}^{(0)} = m\mathbf{V}_f^{(0)} = \text{constant}, \;\; \mathbf{p}_{\omega f}^{(0)} = \tilde{S}^{(0)} \mathbf{V}_f^{(0)} = \text{constant} \tag{5.7}$$

Hence, from the second line of Eqs. (3.2), we have

$$\mathbf{F}^{(0)} = \mathbf{0}, \;\; \mathbf{M}^{(0)} = \mathbf{0} \tag{5.8}$$

The implication of Eqs. (5.8) is that, for steady level flight, the forces and moments due to the engine thrust, aerodynamic forces, gravitational forces and control forces balance out to zero. The angle of attack can be expressed as

$$\alpha_f^{(0)} = \tan^{-1}(V_{fz}^{(0)} / V_{fx}^{(0)}) = \alpha_0 = \text{constant} \tag{5.9}$$

For level flight, we have $\psi^{(0)} = \phi^{(0)} = 0$, so that the pitch angle is equal to the angle of attack, or

$$\theta^{(0)} = \alpha_f^{(0)} \tag{5.10}$$

Moreover, because $V_{fy}^{(0)} = 0$, the sideslip angle is zero,

$$\beta_f^{(0)} = \tan^{-1}(V_{fy}^{(0)} / V_{fx}^{(0)}) = 0 \tag{5.11}$$

In view of this, and due to the symmetry of the gravitational and aerodynamic forces, the side force $F_y^{(0)}$ and the roll and yaw moments, $M_x^{(0)}$ and $M_z^{(0)}$, are automatically zero. We assume that $V^{(0)} = 5000$ in/s and consider a flight at a 25000 ft altitude, so that the speed of sound is 1016.1 ft/s and, hence, the Mach number is $5000/(1016.1 \times 12) = 0.41$. From Eq. (5.6) we have $\mathbf{V}_f^{(0)} = 5000[\cos\theta^{(0)} \quad 0 \quad \sin\theta^{(0)}]^T$. Then using Eqs. (3.3) in conjunction with Eqs. (3.4)-(3.7), Eqs. (5.8) yield

$$\begin{aligned}
F_x^{(0)} &= 2F_E^{(0)} - 695.3237\cos^2\theta^{(0)} - 12973\sin\theta^{(0)} + 2149.5358\delta_e^{(0)}\cos\theta^{(0)}\sin\theta^{(0)} \\
&\quad + \sin^2\theta^{(0)}(164224.6592 + 2149.5358\delta_e^{(0)}\tan\theta^{(0)} + 164919.9829\tan^2\theta^{(0)}) = 0 \\
F_z^{(0)} &= -2149.5358\delta_e^{(0)}\cos^2\theta^{(0)} + \cos\theta^{(0)}(12973 - 202450.4921\sin\theta^{(0)}) \\
&\quad + \sin^2\theta^{(0)}(-2149.5358\delta_e^{(0)} - 239285.6777\tan\theta^{(0)} - 36835.1856\tan^3\theta^{(0)}) = 0 \\
M_y^{(0)} &= -27.92F_E^{(0)} + (-16069.8929 - 553904.5798\delta_e^{(0)})\cos^2\theta^{(0)} \\
&\quad - 52019.1354\sin\theta^{(0)} + (-2.0058 \times 10^6 - 116986.5503\delta_e^{(0)})\cos\theta^{(0)}\sin\theta^{(0)} \\
&\quad + \sin^2\theta^{(0)}(3.0203 \times 10^6 - 553904.5798\delta_e^{(0)} + (-1.6634 \times 10^6 \\
&\quad - 116986.5503\delta_e^{(0)})\tan\theta^{(0)} + 3.0364 \times 10^6\tan^2\theta^{(0)} + 342353.8625\tan^3\theta^{(0)}) = 0
\end{aligned} \tag{5.12}$$

which can be solved for the pitch angle $\theta^{(0)}$, the engine thrust $F_E^{(0)}$ and the elevator angle $\delta_e^{(0)}$. Solving the nonlinear equations (5.12), we obtain $\theta^{(0)} = 0.0667$ rad, $F_E^{(0)} = 431.6465$ lb and $\delta_e^{(0)} = -0.2703$ rad, so that the zero-order control vector is given by $\mathbf{u}^{(0)} = [F_E^{(0)} \;\; 0 \;\; \delta_e^{(0)} \;\; 0]^T = [431.6465 \;\; 0 \;\; -0.2703 \;\; 0]^T$. Hence, the control force vector can be written in the matrix form

$$\begin{aligned}
\mathbf{F}_c^{(0)} = B^{(0)}\mathbf{u}^{(0)} &= \begin{bmatrix}
0 & 0 & 0 & 0 \\
0 & 0 & 0 & 0 \\
0 & 0 & 0 & 0 \\
0 & 0 & 0 & 0 \\
0 & 0 & 0 & 0 \\
0 & 0 & 0 & 0 \\
2 & 0 & 143.4894 & 0 \\
0 & 0 & 0 & -1905.7803 \\
0 & 0 & -2149.5358 & 0 \\
0 & 803506.9168 & 0 & -153855.5426 \\
-27.92 & 0 & -561713.8624 & 0 \\
0 & 53637.0429 & 0 & 529190.6764
\end{bmatrix}
\begin{bmatrix} 431.6465 \\ 0 \\ -0.2703 \\ 0 \end{bmatrix} \\
&= [0 \;\; 0 \;\; 0 \;\; 0 \;\; 0 \;\; 0 \;\; 824.5038 \;\; 0 \;\; 581.0801 \;\; 0 \;\; 139795.5057 \;\; 0]^T
\end{aligned} \tag{5.13}$$

In the case of steady level flight, the aircraft experiences static deformations due to zero-order

forces. Because static deformations are constant and deformations are first-order quantities, we denote all quantities involved by a subscript c and a superscript (1). Consistent with the zero-order results and using the first of Eqs. (3.9), we write

$$\mathbf{V}_{fc}^{(1)} = C_f^{(0)}\{[V^{(1)}0\ \ 0]^T - C_f^{(1)}\mathbf{V}_f^{(0)}\},\ \boldsymbol{\omega}_{fc}^{(1)} = \mathbf{0};\ \mathbf{s}_{uic} = \mathbf{0},\ \mathbf{s}_{\psi ic} = \mathbf{0},\ i = f, w, e \tag{5.14}$$

where $V^{(1)}$ is the first order forward velocity. Then, from Eqs. (3.18), the corresponding momenta are

$$\mathbf{p}_{Vfc}^{(1)} = m\mathbf{V}_{fc}^{(1)},\ \mathbf{p}_{\omega fc}^{(1)} = \tilde{S}_c^{(1)}\mathbf{V}_f^{(0)} + \tilde{S}^{(0)}\mathbf{V}_f^{(1)} \tag{5.15}$$

and, from Eqs. (3.9), we conclude that

$$\begin{aligned} &\mathbf{F}_c^{(1)} = \mathbf{0},\ \mathbf{M}_c^{(1)} = \mathbf{0} \\ &-K_{ui}\mathbf{q}_{uic} + \mathbf{Q}_{uic} = \mathbf{0},\ -K_{\psi i}\mathbf{q}_{\psi ic} + \mathbf{Q}_{\psi ic} = \mathbf{0},\ i = f, w, e \end{aligned} \tag{5.16}$$

which represent algebraic equations to be solved for the first-order pitch angle, the first-order elevator incident angle, the first-order engine thrust and the static generalized displacements $\mathbf{q}_{uic}$ and $\mathbf{q}_{\psi ic}$. We note that $\mathbf{F}_c^{(1)} = [F_{xc}^{(1)}\ \ 0\ \ F_{zc}^{(1)}]^T$, $\mathbf{M}_c^{(1)} = [0\ \ M_{yc}^{(1)}\ \ 0]^T$, $\mathbf{Q}_{uic}$ and $\mathbf{Q}_{\psi ic}$ are all functions of $\mathbf{q}_{uic}$ and $\mathbf{q}_{\psi ic}$ $(i = f, w, c)$.

The stiffness matrices are as follows:

$$\begin{aligned} K_{uf}^F &= \begin{bmatrix} 8687.0713 & -3181.9271 & 0 & 0 \\ -3181.9271 & 293633.2239 & 0 & 0 \\ 0 & 0 & 12883.4627 & -4643.2903 \\ 0 & 0 & -4643.2903 & 419984.1291 \end{bmatrix} \\ K_{uf}^A &= \begin{bmatrix} 8891.2109 & -28248.0864 & 0 & 0 \\ -28248.0864 & 231517.6212 & 0 & 0 \\ 0 & 0 & 13097.4380 & -36822.7531 \\ 0 & 0 & -36822.7531 & 363078.6024 \end{bmatrix} \\ K_{\psi f}^F &= \begin{bmatrix} 1.5462 & 1.0134 \\ 1.0134 & 9.0414 \end{bmatrix} \times 10^8,\ K_{\psi f}^A = \begin{bmatrix} 1.0781 & 1.9339 \\ 1.9339 & 6.7838 \end{bmatrix} \times 10^8 \\ K_{uw}^R = K_{\psi w}^L &= \begin{bmatrix} 581.3939 & -1488.0598 \\ -1488.0598 & 13050.3375 \end{bmatrix},\ K_{\psi w}^R = K_{\psi w}^L = \begin{bmatrix} 2.2974 & 3.6438 \\ 3.6438 & 13.5871 \end{bmatrix} \times 10^7 \\ K_{ue}^R = K_{ue}^L &= \begin{bmatrix} 406.2228 & -696.8287 \\ -696.8287 & 10685.4900 \end{bmatrix},\ K_{\psi e}^R = K_{\psi e}^L = \begin{bmatrix} 1.5455 & 1.4924 \\ 1.4924 & 10.0860 \end{bmatrix} \times 10^7 \\ K_{ue}^V &= \begin{bmatrix} 2126.9677 & -4303.4586 \\ -4303.4586 & 52929.3173 \end{bmatrix},\ K_{\psi e}^V = \begin{bmatrix} 5.0679 & 5.3834 \\ 5.3834 & 31.9145 \end{bmatrix} \times 10^6 \end{aligned} \tag{5.17}$$

where the superscripts F, A, R, L and V denote the fore part, aft part, right half, left half and vertical (stabilizer), respectively. Assuming that $V^{(1)} = –5$ in/s, so that $\mathbf{V}_f^{(1)} =$

$V^{(1)}[\cos\theta^{(0)} \;\; 0 \;\; \sin\theta^{(0)}]^T + V^{(0)}[-\theta^{(1)} s\theta^{(0)} \;\; 0 \;\; \theta^{(1)} c\theta^{(0)}]^T = [-4.6953 - 333.0272\theta^{(1)} \;\; 0 \;\; -4.7316 + 4988.8970\theta^{(1)}]^T$, we can solve Eqs. (5.16) and obtain

$$
\begin{aligned}
&\theta^{(1)} = \; -0.00088 \text{ rad}, \;\; F_E^{(1)} = -3.1169 \text{ lb}, \;\; \delta_e^{(1)} = -0.0047 \text{ rad} \\
&\mathbf{q}^F_{ufc} = [0 \;\; 0 \;\; 0.1206 \;\; -0.0015]^T \text{ in}, \;\; \mathbf{q}^F_{\psi fc} = [0 \;\; 0]^T \text{ rad} \\
&\mathbf{q}^A_{ufc} = [0 \;\; 0 \;\; 0.0585 \;\; 0.0038]^T \text{ in}, \;\; \mathbf{q}^A_{\psi fc} = [0 \;\; 0]^T \text{ rad} \\
&\mathbf{q}^R_{uwc} = \mathbf{q}^L_{uwc} = [-3.4537 \;\; -0.2918]^T \text{ in}, \;\; \mathbf{q}^R_{\psi wc} = \mathbf{q}^L_{\psi wc} = [0.0021 \;\; -0.0002]^T \text{ rad} \\
&\mathbf{q}^R_{uec} = \mathbf{q}^L_{uec} = [-0.0279 \;\; 0.0006]^T \text{ in}, \;\; \mathbf{q}^R_{\psi ec} = \mathbf{q}^L_{\psi ec} [0.0024 \;\; -0.0002]^T \text{ rad} \\
&\mathbf{q}^V_{uec} = [0 \;\; 0]^T \text{ in}, \;\; \mathbf{q}^V_{\psi ec} = [0 \;\; 0]^T
\end{aligned}
\tag{5.18}
$$

Assuming that the first-order state $\mathbf{x}^{(1)}$ is measured from the static elastic displacements position, the first-order state equations for steady level flight can be written in the customary form, Eq. (4.4), where A and B are constant coefficient matrices. This requires the mass matrices, defined by Eqs. (2.15). They can be computed as follows:

$$
\begin{aligned}
&M_{11} = mI, \\
&M_{12} = \tilde{S}^T = \begin{bmatrix} 0 & 131.1002 & 0 \\ -131.1002 & 0 & 0 \\ 0 & 0 & 0 \end{bmatrix} + \begin{bmatrix} 0 & 0 & -4.2385 \\ 0 & 0 & 0 \\ 4.2385 & 0 & 0 \end{bmatrix} q^F_{ufy1} \\
&\qquad + \begin{bmatrix} 0 & 0 & 3.2026 \\ 0 & 0 & 0 \\ -3.2026 & 0 & 0 \end{bmatrix} q^F_{ufy2} + \begin{bmatrix} 0 & 4.2385 & 0 \\ -4.2385 & 0 & \\ 0 & 0 & 0 \end{bmatrix} q^F_{ufz1} + \ldots \\
&\qquad + \begin{bmatrix} 0 & -0.0807 & -0.0128 \\ 0.0807 & 0 & 0 \\ 0.0128 & 0 & 0 \end{bmatrix} q^L_{ue2} + \begin{bmatrix} 0 & 0 & -0.1252 \\ 0 & 0 & 0 \\ 0.1252 & 0 & 0 \end{bmatrix} q^V_{ue1} \\
&\qquad + \begin{bmatrix} 0 & 0 & 0.0219 \\ 0 & 0 & 0 \\ -0.0219 & 0 & 0 \end{bmatrix} q^V_{ue2}, \\
&M^F_{13} = \begin{bmatrix} 0 & 0 & 0 & 0 \\ 4.2385 & -3.2026 & 0 & 0 \\ 0 & 0 & 4.2385 & -3.2026 \end{bmatrix}, \; \ldots, \\
&M_{22} = J = \begin{bmatrix} 182862.0586 & 4.7745 & -37732.0967 \\ 4.7745 & 566132.2704 & 81.1583 \\ -37732.0967 & 81.1583 & 704093.8389 \end{bmatrix} + \begin{bmatrix} 0 & -863.2814 & 0 \\ -863.2814 & 0 & -21.0393 \\ 0 & -21.0393 & 0 \end{bmatrix} q^F_{ufy1} \\
&\qquad + \begin{bmatrix} 0 & 367.2116 & 0 \\ 367.2116 & 0 & 7.3021 \\ 0 & 7.3021 & 0 \end{bmatrix} q^F_{ufy2} + \begin{bmatrix} 42.0786 & 0 & -863.2814 \\ 0 & 42.0786 & 0 \\ -863.2814 & 0 & 0 \end{bmatrix} q^F_{ufz1} + \ldots
\end{aligned}
\tag{5.19}
$$

$$
\begin{aligned}
&+\begin{bmatrix} 6.9600 & 3.2162 & -20.3065 \\ 3.2162 & 7.5428 & -1.2425 \\ -20.3065 & -1.2425 & -0.5828 \end{bmatrix} q^L_{ue2} + \begin{bmatrix} 0 & 35.9911 & 0 \\ 35.9911 & 0 & 12.8989 \\ 0 & 12.8989 & 0 \end{bmatrix} q^V_{ue1} \\
&+\begin{bmatrix} 0 & -4.0598 & 0 \\ -4.0598 & 0 & 4.0183 \\ 0 & 4.0183 & 0 \end{bmatrix} q^V_{ue2}, \\
M^F_{23} &= \begin{bmatrix} -21.0393 & 7.3021 & 0 & 0 \\ 0 & 0 & -863.2814 & 367.2116 \\ 863.2814 & -367.2116 & 0 & 0 \end{bmatrix} + \begin{bmatrix} 0 & 0 & 2.4862 & -0.7090 \\ 0 & 0 & 0 & 0 \\ 0 & 0 & 0 & 0 \end{bmatrix} q^F_{ufy1} + \dots \\
&+\begin{bmatrix} 0.7090 & -2.3655 & 0 & 0 \\ 0 & 0 & 0 & 0 \\ 0 & 0 & 0 & 0 \end{bmatrix} q^F_{ufz2}, \ \dots, \ M^V_{28} = \begin{bmatrix} 68.4129 & 72.7595 \\ 0 & 0 \\ -344.8056 & -402.1912 \end{bmatrix}, \ \dots, \\
M^A_{33} &= \begin{bmatrix} 2.2363 & -1.5318 & 0 & 0 \\ -1.5318 & 8.4942 & 0 & 0 \\ 0 & 0 & 2.0922 & -1.5310 \\ 0 & 0 & -1.5310 & 7.9257 \end{bmatrix}, \ \dots, \\
M^L_{88} &= \begin{bmatrix} 17.3669 & 10.8317 \\ 10.8317 & 32.5338 \end{bmatrix}, \ M^V_{88} = \begin{bmatrix} 34.1002 & 32.0129 \\ 32.0129 & 65.4667 \end{bmatrix}
\end{aligned}
$$

Before we can compute A and B, we must still generate the damping matrices C_{ui} and $C_{\psi i}$ $(i = f, w, e)$. To this end, we assume that the damping functions c_{ui} and $c_{\psi i}$ $(i = f, w, e)$ are all constant, so that the damping matrices, Eqs. (2.19), reduce to

$$C_{ui} = c_{ui} K_{ui}, \ C_{\psi i} = c_{\psi i} K_{\psi i}, \ i = f, w, e \tag{5.20}$$

Equations (5.20) state that the damping matrices are proportional to the stiffness matrices, which permits us to write the relations[36]

$$c_{ui} = 2\zeta/\Lambda^{1/2}_{ui}, \ c_{\psi i} = 2\zeta/\Lambda^{1/2}_{\psi i}, \ i = f, w, e \tag{5.21}$$

where ζ is a structural damping factor and $\Lambda^{1/2}_{ui}$ and $\Lambda^{1/2}_{\psi i}$ $(i = f, w, e)$ are the lowest natural frequencies of the respective components. We assume that $\zeta = 0.03$. Moreover, we obtain the component natural frequencies by solving the eigenvalue problems

$$
\begin{aligned}
&\det[K^F_{uf} - \Lambda^F_{uf} M^F_{33}] = 0, \ \det[K^A_{uf} - \Lambda^A_{uf} M^A_{33}] = 0, \ \det[K^R_{uw} - \Lambda^R_{uw} M^R_{44}] = 0 \\
&\det[K^L_{uw} - \Lambda^L_{uw} M^L_{44}] = 0, \ \dots, \ \det[K^L_{\psi e} - \Lambda^L_{\psi e} M^L_{88}] = 0, \ \det[K^V_{\psi e} - \Lambda^V_{\psi e} M^V_{88}] = 0
\end{aligned} \tag{5.22}
$$

with the results

$$
\begin{aligned}
&\sqrt{\Lambda^F_{uf}} = 59.1040 \text{ rad/s}, \ \sqrt{\Lambda^A_{uf}} = 52.2780 \text{ rad/s}, \ \sqrt{\Lambda^R_{uw}} = \sqrt{\Lambda^L_{uw}} = 36.2911 \text{ rad/s} \\
&\sqrt{\Lambda^R_{ue}} = \sqrt{\Lambda^L_{ue}} = 72.1276 \text{ rad/s}, \ \sqrt{\Lambda^V_{ue}} = 131.9557 \text{ rad/s},
\end{aligned} \tag{5.23}
$$

$$\sqrt{\Lambda^F_{\psi f}} = 221.8479 \text{ rad/s},\ \sqrt{\Lambda^A_{\psi f}} = 61.9940 \text{ rad/s},\ \sqrt{\Lambda^R_{\psi w}} = \sqrt{\Lambda^L_{\psi w}} = 253.9293 \text{ rad/s}$$
$$\sqrt{\Lambda^R_{\psi e}} = \sqrt{\Lambda^L_{\psi e}} = 294.1938 \text{ rad/s} \sqrt{\Lambda^V_{\psi e}} = 384.8014 \text{ rad/s}$$

Hence, using Eqs. (5.17), (5.20), (5.21) and (5.23), the damping matrices are

$$\begin{aligned}
C^F_{uf} &= \begin{bmatrix} 8.8187 & -3.2301 & 0 & 0 \\ -3.2301 & 298.0817 & 0 & 0 \\ 0 & 0 & 13.0786 & -4.7136 \\ 0 & 0 & -4.7136 & 426.3467 \end{bmatrix} \\
C^A_{uf} &= \begin{bmatrix} 10.2045 & -32.4206 & 0 & 0 \\ -32.4206 & 265.7150 & 0 & 0 \\ 0 & 0 & 15.0321 & -42.2618 \\ 0 & 0 & -42.2618 & 416.7088 \end{bmatrix} \\
C^F_{\psi f} &= \begin{bmatrix} 41818.3661 & 27408.5814 \\ 27408.5814 & 244530.1083 \end{bmatrix},\ C^A_{\psi f} = \begin{bmatrix} 104342.4068 & 187172.4172 \\ 187172.4172 & 656562.6583 \end{bmatrix} \\
C^R_{uw} &= C^L_{uw} = \begin{bmatrix} 0.9612 & -2.4602 \\ -2.4602 & 21.5761 \end{bmatrix},\ C^R_{\psi w} = C^L_{\psi w} = \begin{bmatrix} 5428.3762 & 8609.7859 \\ 8609.7859 & 32104.4936 \end{bmatrix} \\
C^R_{ue} &= C^L_{ue} = \begin{bmatrix} 0.3379 & -0.5797 \\ -0.5797 & 8.8888 \end{bmatrix},\ C^R_{\psi e} = C^L_{\psi e} = \begin{bmatrix} 315.1931 & 304.3728 \\ 304.3728 & 2056.9682 \end{bmatrix} \\
C^V_{ue} &= \begin{bmatrix} 0.9671 & -1.9568 \\ -1.9568 & 24.0669 \end{bmatrix},\ C^V_{\psi e} = \begin{bmatrix} 790.2110 & 839.4058 \\ 839.4058 & 4976.2592 \end{bmatrix}
\end{aligned} \tag{5.24}$$

Then, the coefficient matrices in Eq. (4.4) can be shown to be

$$A = \begin{bmatrix}
0 & 0 & 0 & 0 & 0 & 0 & \dots & -0.0005 & -0.00004 \\
0 & 0 & 0 & -333.0272 & 0 & 5000 & \dots & 0.0069 & 0.0007 \\
0 & 0 & 0 & 0 & -5000 & 0 & \dots & -0.0052 & -0.0005 \\
0 & 0 & 0 & 0 & 0 & 0 & \dots & 0.0001 & 0 \\
\dots & \dots & \dots & \dots & \dots & \dots & \dots & \dots & \dots \\
0 & 0 & 0 & 36.3883 & 19.0770 & 0 & \dots & -0.0086 & -0.0009 \\
0 & 0 & 0 & 40.8390 & 41.4025 & 0 & \dots & 0.4818 & 0.0566 \\
0 & 0 & 0 & 455.5429 & 0 & 0 & \dots & -31.9246 & -9.6705 \\
0 & 0 & 0 & 538.2891 & 0 & 0 & \dots & -62.7359 & -136.9900
\end{bmatrix} \tag{5.25}$$

$$B = \begin{bmatrix}
0 & 0 & 0 & 0 \\
0 & 0 & 0 & 0 \\
\dots & \dots & \dots & \dots \\
0 & 0 & 0 & 0 \\
2 & 0 & 143.4894 & 0 \\
0 & 0 & 0 & -1905.7803 \\
\dots & \dots & \dots & \dots \\
0 & 0 & 0 & -3097.7273
\end{bmatrix}$$

Moreover, the feedback control vector is

$$\mathbf{u}^{(1)} = [F_E^{(1)} \quad \delta_a^{(1)} \quad \delta_e^{(1)} \quad \delta_r^{(1)}]^T \tag{5.26}$$

in which it is assumed that the right and the left ailerons rotate by angles of the same magnitude $\delta_a^{(1)}$ but of opposite sense and that the right and left elevators rotate by angles of the same magnitude and sense.

Choosing the weighting matrices Q and R in the performance index, Eq. (4.7), as follows

$$Q = \begin{bmatrix} 1 & 0 & 0 & 0 & 0 & 0 & 0 & \dots & 0 \\ 0 & 1 & 0 & 0 & 0 & 0 & 0 & \dots & 0 \\ 0 & 0 & 1 & 0 & 0 & 0 & 0 & \dots & 0 \\ 0 & 0 & 0 & 1 & 0 & 0 & 0 & \dots & 0 \\ 0 & 0 & 0 & 0 & 1 & 0 & 0 & \dots & 0 \\ 0 & 0 & 0 & 0 & 0 & 1 & 0 & \dots & 0 \\ 0 & 0 & 0 & 0 & 0 & 0 & 0 & \dots & 0 \\ \dots & \dots & \dots & \dots & \dots & \dots & \dots & \dots & \dots \\ 0 & 0 & 0 & 0 & 0 & 0 & 0 & \dots & 0 \end{bmatrix} \quad R = \begin{bmatrix} 10 & 0 & 0 & 0 \\ 0 & 5 \times 10^8 & 0 & 0 \\ 0 & 0 & 10^8 & 0 \\ 0 & 0 & 0 & 10^8 \end{bmatrix} \tag{5.27}$$

solving the steady-state Riccati equation, Eq. (4.14), and using Eq. (4.9), we obtain the gain matrix

$$G = \begin{bmatrix} 0.2994 & 0 & 3.2141 \times 10^{-5} & 0 \\ 0 & 0.00004 & 0 & 1.3669 \times 10^{-5} \\ -0.1016 & 0 & 0.0001 & 0 \\ -0.0809 & 0.5222 & -0.0001 & 0.1024 \\ -1112.0572 & 1.3745 \times 10^{-5} & -1.8943 & 0.0001 \\ -0.0460 & 1.9349 & 0.00005 & 0.5107 \\ \dots & \dots & \dots & \dots \\ -0.0006 & 0 & 0 & 0 \\ 0.0001 & 0 & 0 & 0 \\ 0 & 0 & 0 & 0 \\ 0 & 0 & 0 & 0 \end{bmatrix}^T \tag{5.28}$$

Then, solving the closed-loop eigenvalue problem, Eq. (4.16), we obtain the closed-loop eigenvalues

$$\begin{aligned} &\lambda_{1,2} = -0.1038 \pm 0.0868\ i,\ \lambda_{3,4} = -0.1174 \pm 0.2033\ i,\ \lambda_5 = -0.2349, \\ &\lambda_{6,7} = -0.2919 \pm 0.3064\ i,\ \dots,\ \lambda_{69,70} = -40.5616 \pm 604.1438\ i, \\ &\lambda_{71,72} = -171.1032 \pm 587.8285\ i,\ \lambda_{73,74} = -83.6785 \pm 802.6200 i, \\ &\lambda_{75,76} = -229.1757 \pm 1076.8524\ i \end{aligned} \tag{5.29}$$

Clearly, all the eigenvalues are real and negative or complex with negative real part, so that the closed-loop first-order system is asymptotically stable. The implication is that any

disturbances from the steady level flight are driven to zero. This is in contrast with the open-loop eigenvalues, the eigenvalues of A, the first four of which are zero and the fifth is real and positive.

Finally we consider the response of a closed-loop system to a gust acting on the wing and having the linearly distributed form

$$\begin{aligned} \mathbf{f}_w^R(x_w^R,t) &= [0 \quad 0 \quad -0.5(3+x_w^R/L_w)\sin\pi t_{\prime\prime}(1-t)]^T,\ 0<x_w^R<L_w \\ \mathbf{f}_w^L(x_w^L,t) &= [0 \quad 0 \quad -0.5(3-x_w^L/L_w)\sin\pi t_{\prime\prime}(1-t)]^T,\ 0<x_w^L<L_w \end{aligned} \tag{5.30}$$

where $\sin\pi t_{\prime\prime}(1-t)$ represents a half-sine pulse, in which $_{\prime\prime}(1-t)$ is a rectangular function of unit length. Inserting Eq. (5.30) into Eqs. (3.13), we obtain the generalized force components of the disturbance vector $\mathbf{F}_{\text{ext}}$ entering into Eq. (4.15), which can be integrated to obtain the system response. Figures 3-5 show the response for the rigid body variables and a selected number of elastic variables, and Fig. 6 shows the control inputs.

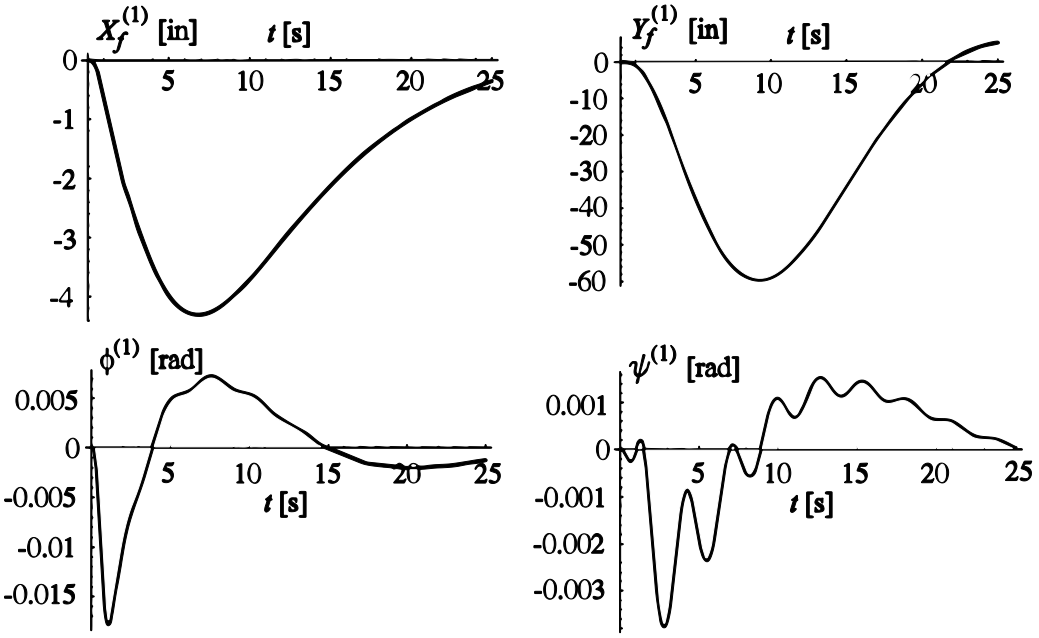

Figure 3. Rigid Body Displacements

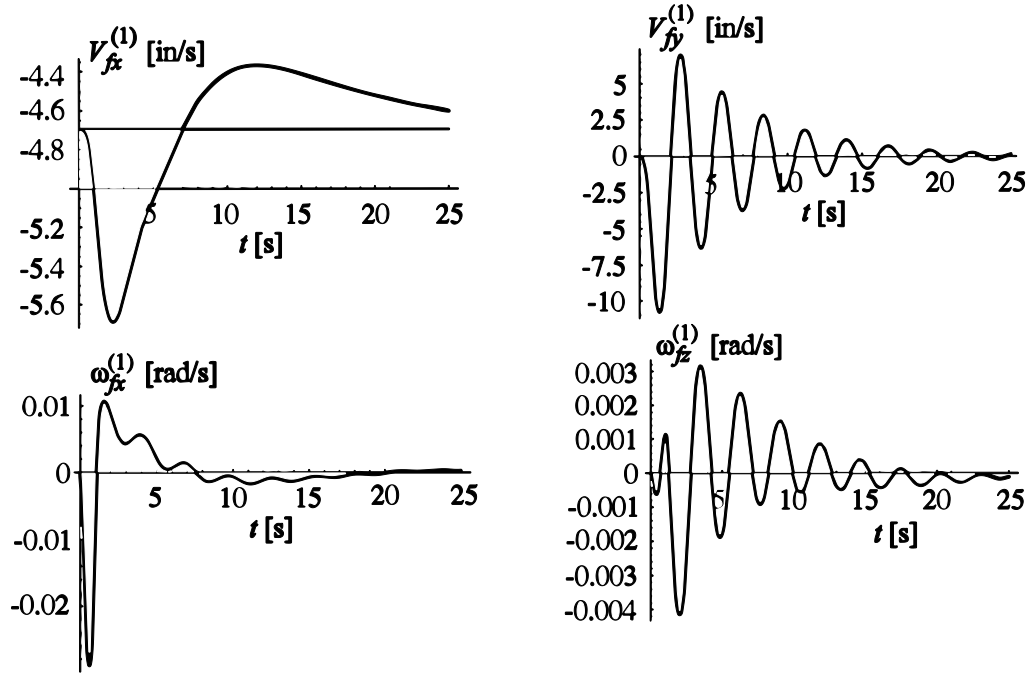

Figure 4. Rigid Body Velocities

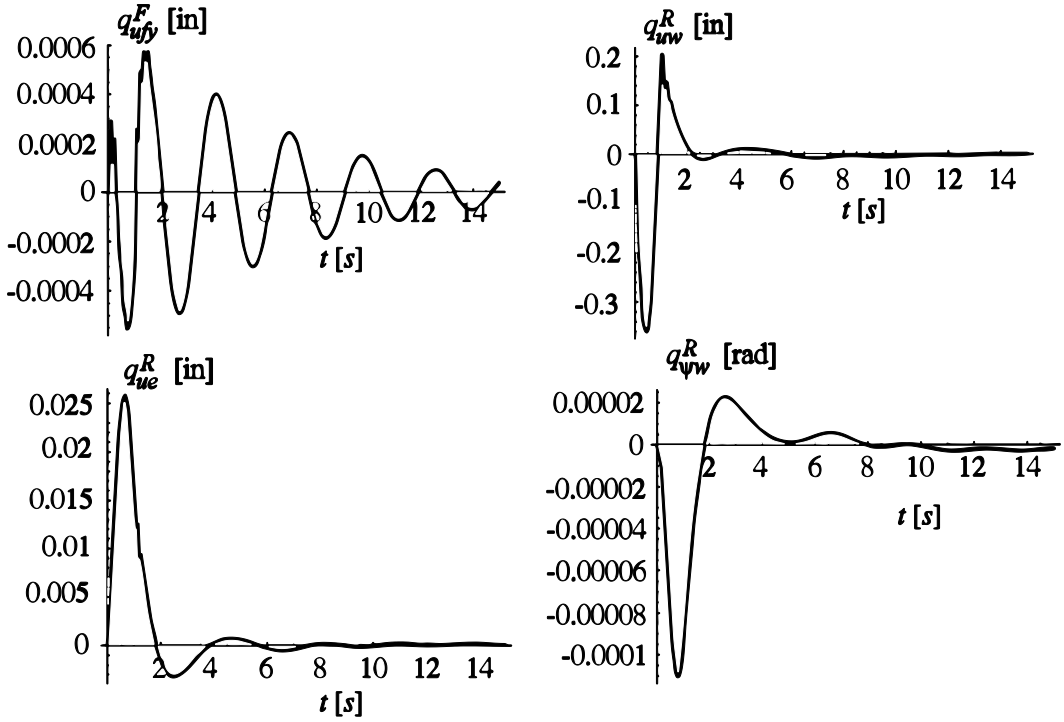

Figure 5. Generalized Elastic Displacements

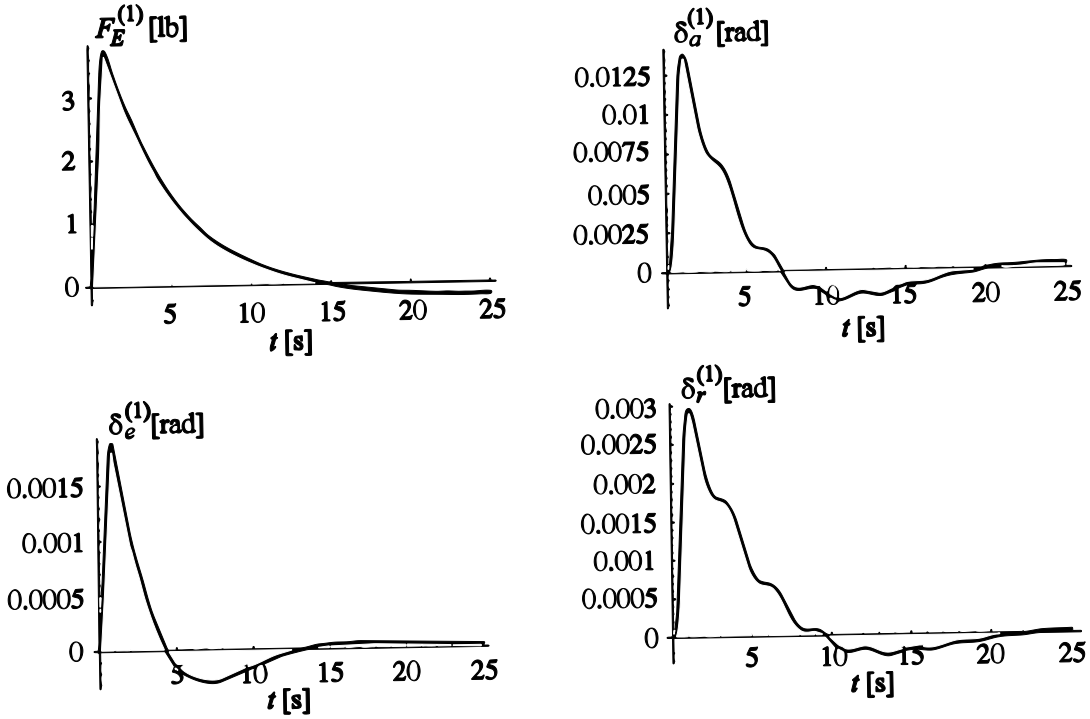

Figure 6. Control Inputs

Next, we turn our attention to the observer. To this end, we assume that $\mathbf{R}_f^{(1)}$ and $\boldsymbol{\theta}_f^{(1)}$ are available as part of the output of an inertial navigation system and that there are four sensors measuring velocities at the points P_k $(k = 1, 2, 3, 4)$ of each aircraft component. The coordinates x_x, y_x of P_k in component body axes, together with the type of velocities measured, are listed in Table 1. Moreover, the sensors locations are shown in Fig. A.

Table 1 - Sensor Locations and Type of Velocities Measured

	Fore Fuselage	Aft Fuselage	Right Wing	Left Wing	Right Horizontal Stabilizer	Left Horizontal Stabilizer	Vertical Stabilizer
$P_1 : x_1, y_1$ Velocities	111.21, 36.25 $\bar{V}_{fy}^{(1)}$ and $\bar{V}_{fz}^{(1)}$	111.92, 35.0 $\bar{V}_{fy}^{(1)}$ and $\bar{V}_{fz}^{(1)}$	120.35, 58.23 $\bar{V}_{wz}^{(1)}$	120.35, −58.23 $\bar{V}_{wz}^{(1)}$	50.54, 32.0 $\bar{V}_{ez}^{(1)}$	50.54, −32.0 $\bar{V}_{ez}^{(1)}$	50.0, 42.0 $\bar{V}_{ez}^{(1)}$
$P_2 : x_2, y_2$ Velocities	111.21, −36.25 $\bar{V}_{fz}^{(1)}$	111.92, −35.0 $\bar{V}_{fz}^{(1)}$	120.35, −28.0 $\bar{V}_{wz}^{(1)}$	120.35, 28.0 $\bar{V}_{wz}^{(1)}$	46.6, −20.0 $\bar{V}_{ez}^{(1)}$	46.6, 20.0 $\bar{V}_{ez}^{(1)}$	41.0, −28.0 $\bar{V}_{ez}^{(1)}$
$P_3 : x_3, y_3$ Velocities	277.21, 24.0 $\bar{V}_{fy}^{(1)}$ and $\bar{V}_{fz}^{(1)}$	279.79, 25.0 $\bar{V}_{fy}^{(1)}$ and $\bar{V}_{fz}^{(1)}$	327.66, 25.07 $\bar{V}_{wz}^{(1)}$	327.66, −25.07 $\bar{V}_{wz}^{(1)}$	127.0, 19.0 $\bar{V}_{ez}^{(1)}$	127.0, −19.0 $\bar{V}_{ez}^{(1)}$	112.0, 27.0 $\bar{V}_{ez}^{(1)}$
$P_4 : x_4, y_4$ Velocities	277.21, −24.0 $\bar{V}_{fz}^{(1)}$	279.79, −25.0 $\bar{V}_{fz}^{(1)}$	327.66, −10.0 $\bar{V}_{wz}^{(1)}$	327.66, 10.0 $\bar{V}_{wz}^{(1)}$	127.0, −12.0 $\bar{V}_{ez}^{(1)}$	127.0, 12.0 $\bar{V}_{ez}^{(1)}$	113.0, −16.0 $\bar{V}_{ez}^{(1)}$

To compute the matrix C, Eq. (4.44), relating the output vector to the state vector, we use

Eq. (4.41) and write

$$M_V = \begin{bmatrix} 0 & \dots & 0 & 0 & 0 & 0 \\ 0 & \dots & 0 & 0 & 0 & 0 \\ 0 & \dots & 0 & 0 & 0 & 0 \\ 0 & \dots & 0 & 1411.5402 & -1066.5377 & 0 \\ 0 & \dots & 0 & 0 & 0 & 21145.5039 \\ 0 & \dots & 0 & -21145.5039 & 15977.2118 & 0 \\ 0 & \dots & 0 & 0 & 0 & 0 \\ \dots & \dots & \dots & \dots & \dots & \dots \\ 0 & \dots & 0 & 0 & 0 & 0 \end{bmatrix}$$

$$\begin{bmatrix} \dots & 0 & 0 & 0 & 0 & \dots & 0 \\ \dots & 0 & 0 & 0 & 0 & \dots & 0 \\ \dots & 0 & 0 & 0 & 0 & \dots & 0 \\ \dots & 4.2544 & 41.7049 & -7.3013 & 0 & \dots & 0 \\ \dots & 2.3892 & 0 & 0 & 0 & \dots & 0 \\ \dots & -63.7322 & -624.7574 & 109.3773 & 0 & \dots & 0 \\ \dots & 0 & 0 & 0 & 0 & \dots & 0 \\ \dots & \dots & \dots & \dots & \dots & \dots & \dots \\ \dots & 0 & 0 & 0 & 0 & \dots & 0 \end{bmatrix} \tag{5.31}$$

Then, inserting Eq. (5.31) into Eq. (4.44), we obtain

$$C = \begin{bmatrix} 1 & 0 & 0 & 0 & 0 & 0 & 0 & 0 & 0 & \dots & 0 \\ \dots & \dots & \dots & \dots & \dots & \dots & \dots & \dots & \dots & \dots & \dots \\ 0 & 0 & 0 & 0 & 0 & 1 & 0 & 0 & 0 & 0 & 0 \\ 0 & 0 & 0 & 0 & 0 & 0 & 0.7164 & -0.5413 & -0.1528 & 0.1154 & 0 \\ 0 & 0 & 0 & 0 & 0 & 0 & 0.6671 & 0.5041 & 3.2735 & -2.4734 & 0 \\ 0 & 0 & 0 & 0 & 0 & 0 & 1.5558 & -1.1756 & 4.4292 & -3.3466 & 0 \\ \dots & \dots & \dots & \dots & \dots & \dots & \dots & \dots & \dots & \dots & \dots \\ 0 & 0 & 0 & 0 & 0 & 0 & -10.4119 & 7.8670 & -6.9155 & 5.2253 & 0 \\ 0 & 0 & 0 & 0 & 0 & 0 & -1.2636 & 0.9547 & 1.1015 & -0.8323 & 0 \\ 0 & 0 & 0 & 0 & 0 & 0 & 9.1203 & -6.8911 & 4.0257 & -3.0418 & 0 \end{bmatrix}$$

$$\begin{bmatrix} \dots & 0 & 0 & 0 & \dots & 0 & 0 \\ \dots & \dots & \dots & \dots & \dots & \dots & \dots \\ \dots & 0 & 0 & 0 & \dots & 0 & 0 \\ \dots & 0 & -0.00003 & 0.0123 & \dots & 0.0005 & 0.00006 \\ \dots & 0 & 0.0008 & 0.0320 & \dots & 0.0017 & 0.0002 \\ \dots & 0 & 0.0011 & -0.0373 & \dots & -0.0031 & -0.0003 \\ \dots & \dots & \dots & \dots & \dots & \dots & \dots \\ \dots & 0 & -0.0015 & 0.0871 & \dots & -0.4310 & -0.6603 \\ \dots & 0 & 0.0002 & -0.0260 & \dots & 2.1744 & -1.4009 \\ \dots & 0 & 0.0009 & -0.0385 & \dots & -1.4582 & 0.9927 \end{bmatrix} \tag{5.32}$$

We assume that the excitation noise $\mathbf{v}(t)$ and observation noise $\mathbf{w}(t)$ represent white noise processes with intensities V and W, respectively, and choose

$$\begin{aligned} V = \mathrm{diag}[&100000\ 100000\ 100000\ 100000\ 100000\ 100000\ 10^{-9}\ 10^{-9} \\ &10^{-9}\ 10^{-9}\ 10^{-9}\ 10^{-9}\ 10^{-9}\ 10^{-9}\ 10^{-9}\ 10^{-9}\ 10^{-9}\ 10^{-9}10^{-9}\ 10^{-9}\ 10^{-9}\ 10^{-9}\ 10^{-9}\ 10^{-9} \\ &10^{-9}\ 10^{-9}\ 10^{-9}\ 10^{-9}\ 10^{-9}\ 10^{-9}\ 10^{-9}\ 10^{-9}\ 10^{-9}\ 10^{-9}10^{-9}\ 10^{-9}\ 10^{-9}\ 10^{-9}\ 0\ \dots\ 0] \end{aligned} \tag{5.33}$$

and

$$W = \text{diag}[10^{-12}\ 10^{-12}\ 10^{-12}\ 10^{-6}\ 10^{-6}\ 10^{-6}\ 1\ \ldots\ 1] \tag{5.34}$$

so that, from Eq. (4.32), the steady-state Riccati equation

$$AQ + QA^T + V - QC^TW^{-1}CQ = 0 \tag{5.35}$$

yields

$$Q = \text{diag}\left[\begin{array}{cccccccccc} 0.0003 & 0.0003 & 0.0003 & 0.3162 & 0.3162 & 0.3162 & \ldots & 0 & 0 \end{array}\right] \tag{5.36}$$

Hence, from Eq. (4.31), the optimal observer gain matrix is

$$K_o = QC^TW^{-1} = \left[\begin{array}{ccccc}
3.1623\times10^{8} & 0 & 0 & 0 & 0 \\
0 & 3.1623\times10^{8} & 0 & -0.00033 & 0 \\
0 & 0 & 3.1623\times10^{8} & 0 & -0.0050 \\
0 & -332.6945 & -4.2121\times10^{-6} & 316227.7660 & 2.0270\times10^{-6} \\
-1.2224\times10^{-6} & -0.00001 & -4995.0051 & 2.0270\times10^{-6} & 316227.7661 \\
0 & 4995.0050 & 5.3401\times10^{-6} & -6.8126\times10^{-6} & 0 \\
0.3055 & -1.2621 & 3.2425 & -0.0253 & -0.0189 \\
-0.2309 & 0.9536 & -2.4500 & 0.0183 & 0.0142 \\
3.0011 & -2.3448 & 15.0393 & -0.0130 & -0.3660 \\
-2.2676 & 1.7718 & -11.3636 & 0.0100 & 0.2786 \\
0.2688 & -1.1104 & 2.8524 & -0.0222 & -0.0166 \\
\cdots & \cdots & \cdots & \cdots & \cdots \\
-0.0005 & 0.0069 & -0.0052 & 0.0006 & 0.00003 \\
-0.00004 & 0.0007 & -0.0005 & 5.5708\times10^{-6} & 2.6172\times10^{-6}
\end{array}\right.$$

$$\left.\begin{array}{ccccc}
0 & \ldots & 0 & 0 & 0 \\
0.0050 & \ldots & 0 & 0 & 0 \\
0 & \ldots & 0 & 0 & 0 \\
-6.8127\times10^{-6} & \ldots & 1.5948\times10^{-6} & -1.8328\times10^{-6} & -1.4351\times10^{-6} \\
0 & \ldots & 0.00001 & 0 & -7.8617\times10^{-6} \\
316227.7661 & \ldots & -7.3710\times10^{-6} & 0 & 6.4058\times10^{-6} \\
0.1431 & \ldots & -2.1299\times10^{-6} & 0 & 1.9001\times10^{-6} \\
-0.1085 & \ldots & 3.0634\times10^{-6} & 0 & -2.7693\times10^{-6} \\
0.0180 & \ldots & 0 & 0 & 0 \\
-0.0138 & \ldots & 0 & 0 & 0 \\
0.1258 & \ldots & 0 & 0 & 0 \\
\cdots & \cdots & \cdots & \cdots & \cdots \\
-0.00006 & \ldots & 0 & 0 & 0 \\
-4.3046\times10^{-6} & \ldots & 0 & 0 & 0
\end{array}\right] \tag{5.37}$$

Finally, solving the eigenvalue problem for $A - K_0C$, we obtain the observer eigenvalues

$$\begin{aligned}
&\lambda_1 = -0.0103,\ \lambda_{2,3} = -0.7808 \pm 1.6540i,\ \lambda_{4,5} = -0.4198 \pm 3.0843i,\\
&\lambda_6 = -5.7545,\ \lambda_{7,8} = -5.7225 \pm 36.9775i,\ \lambda_{9,10} = -3.5888 \pm 44.8820i,\\
&\lambda_{11,12} = -4.6600 \pm 60.6749i,\ \lambda_{13,14} = -4.2416 \pm 68.5048i, \dots ,\\
&\lambda_{63,64} = -40.4347 \pm 603.8843,\ \lambda_{65,66} = -177.2951 \pm 582.6928i,\\
&\lambda_{67,68} = -82.9854 \pm 802.0970i,\ \lambda_{69,70} = -229.1116 \pm 1077.0692i,\\
&\lambda_{71,72,73} = -316228,\ \lambda_{74,75,76} = -3.1623 \times 10^8
\end{aligned} \tag{5.38}$$

The performance of the observer design can be demonstrated by simulating the response of the combined system, defined by Eq. (4.25), to an initial state and initial observer error. To this end, we choose the values

$$\begin{aligned}
\mathbf{x}^{(1)}(0) = [&5\ \ 5\ \ 5\ \ 0.005\ \ 0.005\ \ 0.005\ \ 0.2\ \ 0.1\ \ 0.2\ \ 0.1\ \ 0.2\ \ 0.1\ \ -0.2\ \ -0.1\ \ -0.2\\
&-0.1\ \ -0.2\ \ -0.1\ \ -0.2\ \ -0.1\ \ -0.2\ \ -0.1\ \ -0.2\ \ -0.1\ \ 0.05\ \ 0.01\ \ -0.05\\
&-0.01\ \ 0.05\ \ 0.01\ \ -0.05\ \ -0.01\ \ 0.05\ \ 0.01\ \ -0.05\ \ -0.01\ \ 0.05\ \ 0.01\ \ 0 \dots\ 0]^T\\
\mathbf{e}(0) = &-0.15\mathbf{x}^{(1)}(0)
\end{aligned} \tag{5.39}$$

Figures 7-9 show the response for a selected number of rigid body and elastic variables and their observer estimates. Figure 10 shows the control inputs as given by Eq. (4.23).

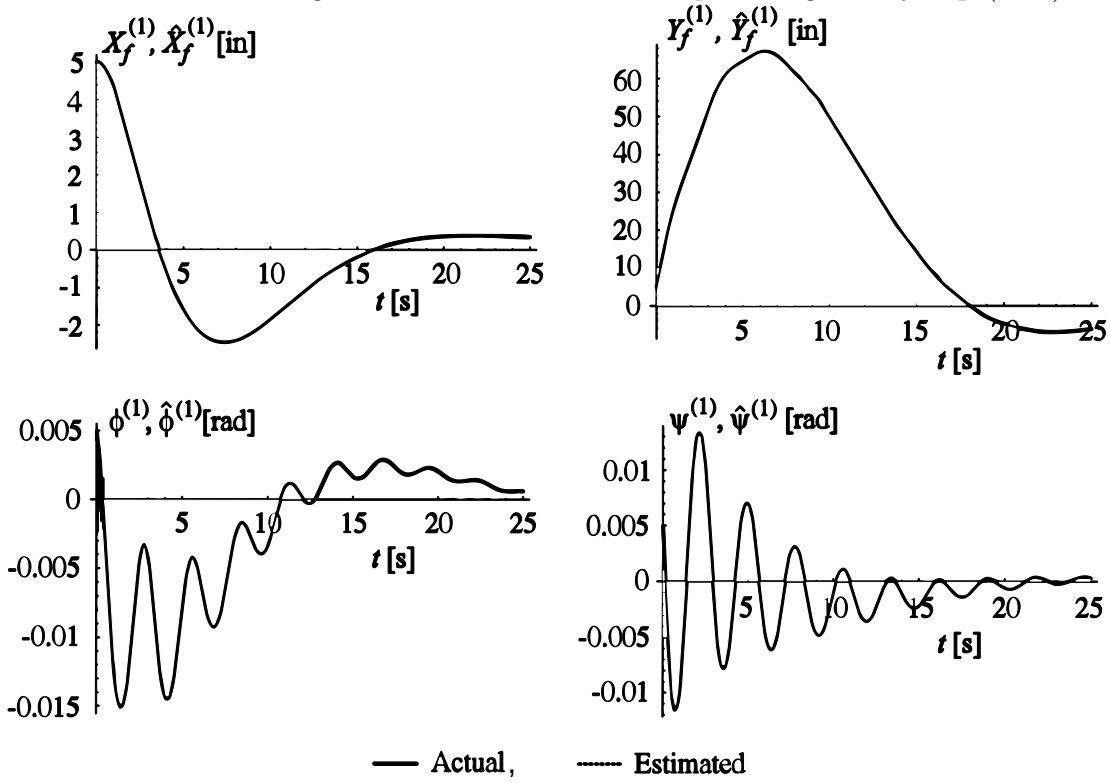

Figure 7. Rigid Body Displacements

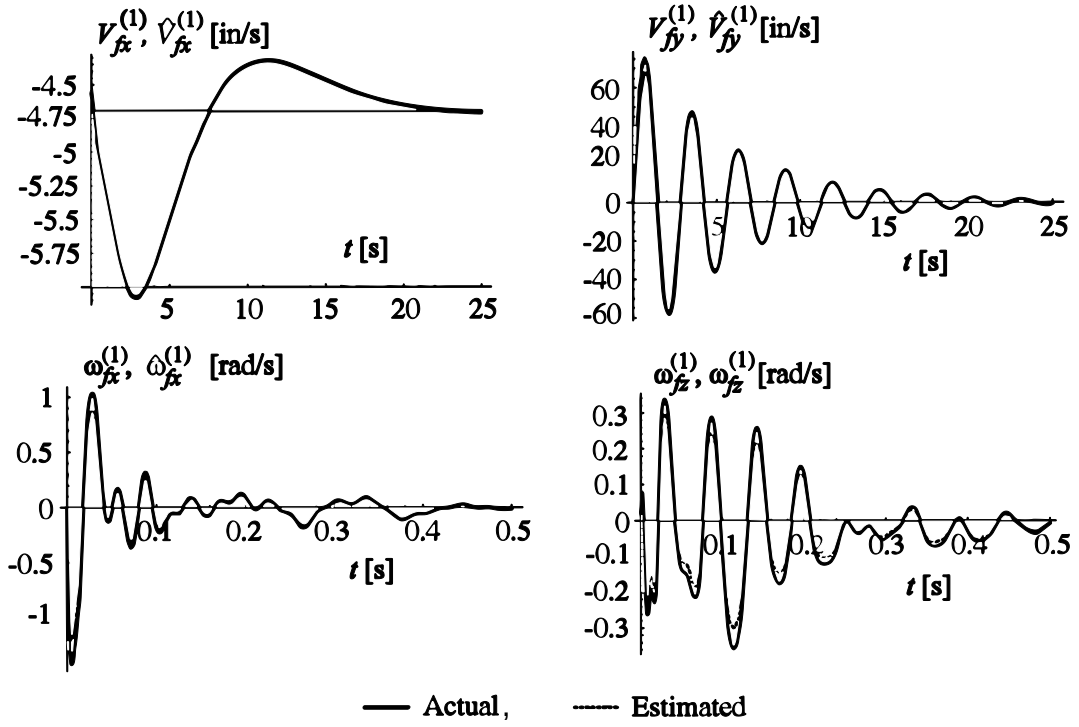

Figure 8. Rigid Body Velocities

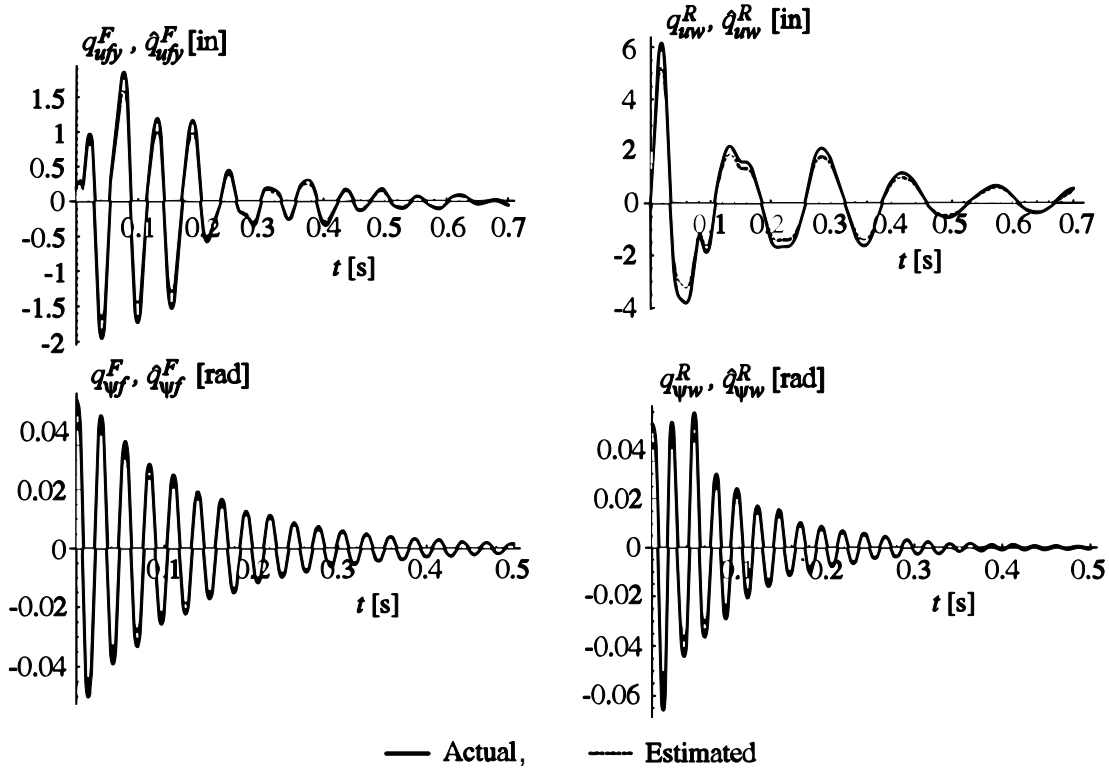

Figure 9. Generalized Elastic Displacements

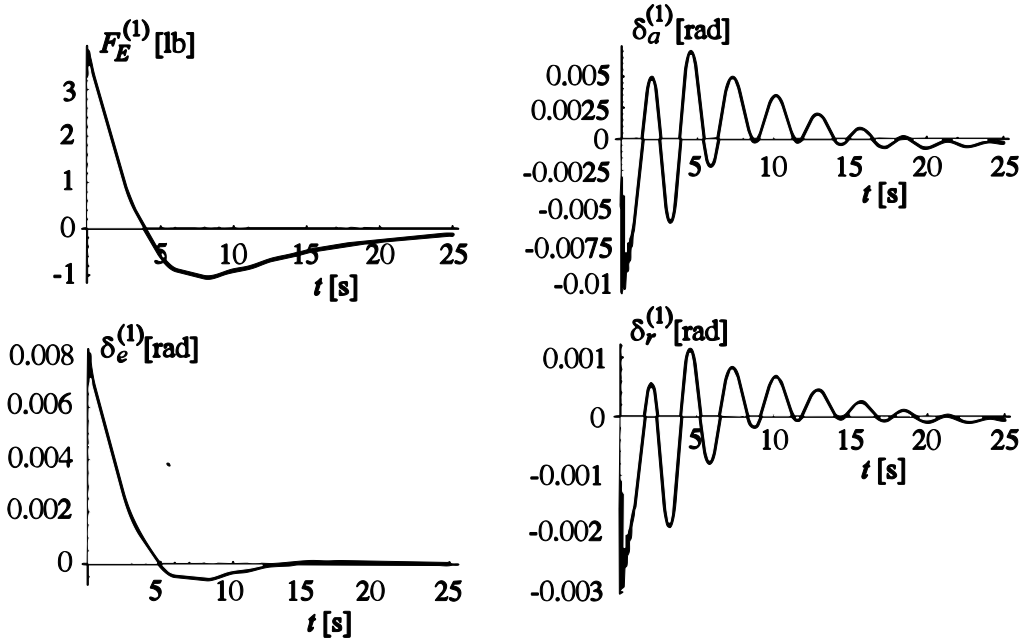

Figure 10. Control Inputs

5.2 Steady Level Turn Maneuver

We consider the case in which in the zero-order problem the aircraft flies at a constant velocity around a circular path of radius R in the horizontal X, Y-plane. In this case, it is convenient to refer the rigid body motions to a set of axes $x_1 y_1 z_1$ obtained through a rotation $\psi^{(0)}$ about Z, where $\dot{\psi}^{(0)} = \Omega = \text{constant}$. It is not difficult to see that axes x_1, y_1 and z_1 represent a set of cylindrical axes $t,\ n$ and Z, where t is tangent to the circle and n is normal to it. Denoting by $\dot{\bar{\mathbf{R}}}_f^{(0)}$ the velocity of O_f in terms of cylindrical components, the kinematical relation corresponding to the first of Eqs. (3.2) can be written as

$$\dot{\bar{\mathbf{R}}}_f^{(0)} = [\dot{R}_{ft}^{(0)} \quad \dot{R}_{fn}^{(0)} \quad \dot{Z}^{(0)}]^T = [R\Omega \quad 0 \quad 0]^T = \bar{C}_f^{(0)^T} \mathbf{V}_f^{(0)} \tag{5.40}$$

where

$$\bar{C}_f^{(0)} = \begin{bmatrix} \mathrm{c}\theta^{(0)} & 0 & -\mathrm{s}\theta^{(0)} \\ \mathrm{s}\theta^{(0)}\mathrm{s}\phi^{(0)} & \mathrm{c}\phi^{(0)} & \mathrm{c}\theta^{(0)}\mathrm{s}\phi^{(0)} \\ \mathrm{s}\theta^{(0)}\mathrm{c}\phi^{(0)} & -\mathrm{s}\phi^{(0)} & \mathrm{c}\theta^{(0)}\mathrm{c}\phi^{(0)} \end{bmatrix} \tag{5.41}$$

is the matrix of direction cosines between tnZ and the fuselage body axes $x_f y_f z_f$, obtained from C_f, the first of Eqs. (2.2), by letting $\psi = 0$ and replacing θ and ϕ by $\theta^{(0)}$ and $\psi^{(0)}$,

respectively. Similarly, the second of Eqs. (3.2) can be written as

$$\dot{\boldsymbol{\theta}}_f^{(0)} = [\dot{\phi}^{(0)} \;\; \dot{\theta}^{(0)} \;\; \dot{\psi}^{(0)}] = [0 \;\; 0 \;\; \Omega]^T = (E_f^{(0)})^{-1}\boldsymbol{\omega}_f^{(0)} \tag{5.42}$$

where $E_f^{(0)}$ can be obtained from E_f, the second of Eqs. (2.2), by replacing θ and ϕ by $\theta^{(0)}$ and $\psi^{(0)}$, respectively. Equations (5.40) and (5.41) yield

$$\mathbf{V}_f^{(0)} = [V_{fx}^{(0)} \;\; V_{fy}^{(0)} \;\; V_{fz}^{(0)}]^T = \bar{C}_f^{(0)}\dot{\bar{\mathbf{R}}}_f^{(0)} = R\Omega[\mathrm{c}\theta^{(0)} \;\; \mathrm{s}\theta^{(0)}\mathrm{s}\phi^{(0)} \;\; \mathrm{s}\theta^{(0)}\mathrm{c}\phi^{(0)}]^T = \text{constant} \tag{5.43}$$

and

$$\boldsymbol{\omega}_f^{(0)} = [\omega_{fx}^{(0)} \;\; \omega_{fy}^{(0)} \;\; \omega_{fz}^{(0)}]^T = E_f^{(0)}\dot{\boldsymbol{\theta}}_f^{(0)} = \Omega[-\mathrm{s}\theta^{(0)} \;\; \mathrm{c}\theta^{(0)}\mathrm{s}\phi^{(0)} \;\; \mathrm{c}\theta^{(0)}\mathrm{s}\phi^{(0)}]^T = \text{constant} \tag{5.44}$$

so that, from Eqs. (3.8), we have

$$\mathbf{p}_{Vf}^{(0)} = m\mathbf{V}_f^{(0)} + \tilde{S}^{(0)^T}\boldsymbol{\omega}_f^{(0)} = \text{constant}, \;\; \mathbf{p}_{\omega f}^{(0)} = \tilde{S}^{(0)}\mathbf{V}_f^{(0)} + J^{(0)}\boldsymbol{\omega}_f^{(0)} = \text{constant} \tag{5.45}$$

It follows that the equations of motion, the last two of Eqs. (3.2), reduce to

$$-\tilde{\omega}_f^{(0)}\mathbf{p}_{Vf}^{(0)} + \mathbf{F}^{(0)} = \mathbf{0}, \quad -\tilde{V}_f^{(0)}\mathbf{p}_{Vf}^{(0)} - \tilde{\omega}_f^{(0)}\mathbf{p}_{\omega f}^{(0)} + \mathbf{M}^{(0)} = \mathbf{0} \tag{5.46}$$

which are independent of time.

To determine the parameters defining the steady level turn maneuver, we choose the turn radius R and angular velocity Ω and solve Eqs. (5.46) for the bank angle $\phi^{(0)}$, pitch angle $\theta^{(0)}$ and control vector $\mathbf{u}^{(0)} = [F_e^{(0)} \;\; \delta_a^{(0)} \;\; \delta_e^{(0)} \;\; \delta_r^{(0)}]^T$. Hence, assuming the values $R = 1.5\,\mathrm{mi} = 95037\,\mathrm{in}$ and $\Omega = 0.0526\,\mathrm{rad/s}$, so that $R\Omega = 5000\,\mathrm{in/s}$, and using Eqs. (5.43) and (5.44), we have

$$\mathbf{V}_f^{(0)} = 5000\begin{bmatrix} \mathrm{c}\theta^{(0)} \\ \mathrm{s}\theta^{(0)}\mathrm{s}\phi^{(0)} \\ \mathrm{s}\theta^{(0)}\mathrm{c}\phi^{(0)} \end{bmatrix}, \;\; \boldsymbol{\omega}_f^{(0)} = 0.0526\begin{bmatrix} -\mathrm{s}\theta^{(0)} \\ \mathrm{c}\theta^{(0)}\mathrm{s}\phi^{(0)} \\ \mathrm{c}\theta^{(0)}\mathrm{c}\phi^{(0)} \end{bmatrix} \tag{5.47}$$

We consider a flight at a 25000 ft altitude, so that the speed of sound is 1016.1 ft/s and, hence, the Mach number for the flight is $5000/(1016.1 \times 12) = 0.41$. Inserting Eqs. (5.47) into Eqs. (5.46) in conjunction with Eqs. (5.45) and solving the resulting transcendental equations, we obtain

$$\begin{aligned} &\theta^{(0)} = 0.0986\,\mathrm{rad}, \;\; \phi^{(0)} = 0.6160\,\mathrm{rad} \\ &F_E^{(0)} = 468.7429\,\mathrm{lb}, \;\; \delta_a^{(0)} = 0.0028\,\mathrm{rad}, \;\; \delta_e^{(0)} = -0.3233\,\mathrm{rad}, \;\; \delta_r^{(0)} = -0.3445\,\mathrm{rad} \end{aligned} \tag{5.48}$$

Then, the zero-order control force vector can be written as

$$\mathbf{F}_c^{(0)} = B^{(0)}\mathbf{u}^{(0)} = \begin{bmatrix} 0 & 0 & 0 & 0 \\ 0 & 0 & 0 & 0 \\ 0 & 0 & 0 & 0 \\ 0 & 0 & 0 & 0 \\ 0 & 0 & 0 & 0 \\ 0 & 0 & 0 & 0 \\ 2 & 1.0370 & 178.2611 & 77.3023 \\ 0 & 0 & 0 & -1916.1116 \\ 0 & -13.7394 & -2875.1495 & 0 \\ 0 & 1.0746\times 10^6 & 1.4415 & -154689.6019 \\ -27.92 & -164.5690 & -750586.5476 & -6240.6944 \\ 0 & 65027.5713 & 11.7592 & 532059.4480 \end{bmatrix} \begin{bmatrix} 468.7429 \\ -0.0028 \\ -0.3233 \\ -0.3445 \end{bmatrix} = \begin{bmatrix} 0 \\ 0 \\ 0 \\ 0 \\ 0 \\ 0 \\ 844.5606 \\ 654.9960 \\ 962.9931 \\ 50641.1455 \\ 171482.9784 \\ -182061.4664 \end{bmatrix} \tag{5.49}$$

As in the case of steady level flight, the aircraft experiences static deformations in the steady level turn maneuver as well. Denoting the corresponding constant quantities by the superscript (1) and subscript c, using the first of Eqs. (3.9) and letting $\mathbf{V}^{(1)}$ be the cylindrical coordinates counterpart of $\dot{\mathbf{R}}_f^{(1)}$, we can write

$$\begin{aligned} &\mathbf{V}_{fc}^{(1)} = \bar{C}_f^{(0)}[\mathbf{V}^{(1)} - \bar{C}_f^{(1)T}\mathbf{V}_f^{(0)}] = \text{constant},\ \boldsymbol{\omega}_{fc}^{(1)} = \mathbf{0} \\ &\mathbf{s}_{uic} = \mathbf{0},\ \mathbf{s}_{\psi ic} = \mathbf{0},\ i = f, w, e \end{aligned} \tag{5.50}$$

The momenta are all constant and can be expressed in terms of the zero-order and first-order velocities and the static deformations using Eqs. (3.18).

A constant solution of the first-order equations, Eqs. (3.9), can be obtained by letting the left sides be equal to zero and solving for $\phi_c^{(1)}$, $\theta_c^{(1)}$, $\mathbf{u}_c^{(1)} = [F_{Ec}^{(1)} \ \ \delta_{ac}^{(1)} \ \ \delta_{ec}^{(1)} \ \ \delta_{rc}^{(1)}]^T$ and the static deformations $\mathbf{q}_{uic}$ and $\mathbf{q}_{\psi ic}$ $(i = f, w, e)$. Assuming that $\mathbf{V}^{(1)} = [-5 \ \ 0 \ \ 0]^T$ in/s and using the first of Eqs. (5.50), we obtain

$$\mathbf{V}_{fc}^{(1)} = \begin{bmatrix} -4.9754 - 492.1217\theta_c^{(1)} \\ -0.2843 + 2874.8121\theta_c^{(1)} + 486.4652\phi_c^{(1)} \\ -0.4017 + 4061.1909\theta_c^{(1)} - 344.3562\phi_c^{(1)} \end{bmatrix} \tag{5.51}$$

so that Eqs. (3.9) yield

$$
\begin{aligned}
&\phi_c^{(1)} = \ -0.0011\,\text{rad},\ \theta_c^{(1)} = -0.0013\,\text{rad}\\
&\mathbf{u}_c^{(1)} = [-4.0727 \quad -0.0002 \quad -0.0063 \quad 0.0001]^T\\
&\mathbf{q}_{ufc}^F = [-0.0005 \quad 0.0001 \quad 0.1458 \quad -0.0019]^T,\ \mathbf{q}_{\psi fc}^F = [-0.0001 \quad 0]^T\\
&\mathbf{q}_{ufc}^A = [-0.0408 \quad 0.0008 \quad 0.0827 \quad 0.0039]^T,\ \mathbf{q}_{\psi fc}^A = [0.0003 \quad -0.0001]^T\\
&\mathbf{q}_{uwc}^R = [-4.1523 \quad -0.3511]^T,\ \mathbf{q}_{\psi wc}^R = [0.0025 \quad -0.0003]^T\\
&\mathbf{q}_{uwc}^L = [-4.1765 \quad -0.3526]^T,\ \mathbf{q}_{\psi wc}^L = [-0.0025 \quad 0.0003]^T\\
&\mathbf{q}_{uec}^R = [-0.0473 \quad 0.0001]^T,\ \mathbf{q}_{\psi ec}^R = [0.0029 \quad -0.0002]^T\\
&\mathbf{q}_{uec}^L = [-0.0489 \quad 0.00008]^T,\ \mathbf{q}_{\psi ec}^L = [-0.0029 \quad 0.0002]^T\\
&\mathbf{q}_{uec}^V = [0.0032 \quad 0.0014]^T,\ \mathbf{q}_{\psi ec}^V = [0.0017 \quad -0.0001]^T
\end{aligned}
\tag{5.52}
$$

The mass matrices, Eqs. (2.15), for the steady turn case are as follows:

$$
\begin{aligned}
M_{12} = \tilde{S}^T = &\begin{bmatrix} 0 & 130.4114 & 0.1477 \\ -130.4114 & 0 & 0 \\ -0.1477 & 0 & 0 \end{bmatrix} + \begin{bmatrix} 0 & 0 & -4.2385 \\ 0 & 0 & 0 \\ 4.2385 & 0 & 0 \end{bmatrix} q_{ufy1}^F\\
&+ \begin{bmatrix} 0 & 0 & 3.2026 \\ 0 & 0 & 0 \\ -3.2026 & 0 & 0 \end{bmatrix} q_{ufy2}^F + \begin{bmatrix} 0 & 4.2385 & 0 \\ 0 & 0 & 0 \\ -4.2385 & 0 & 0 \end{bmatrix} q_{ufz1}^F + \dots\\
&+ \begin{bmatrix} 0 & 0.1095 & 0.0173 \\ -0.1095 & 0 & 0 \\ -0.0173 & 0 & 0 \end{bmatrix} q_{ue2}^L + \begin{bmatrix} 0 & 0 & -0.1252 \\ 0 & 0 & 0 \\ 0.1252 & 0 & 0 \end{bmatrix} q_{ue1}^V\\
&+ \begin{bmatrix} 0 & 0 & 0.0219 \\ 0 & 0 & 0 \\ -0.0219 & 0 & 0 \end{bmatrix} q_{ue2}^V,\ M_{13}^F = \begin{bmatrix} 0 & 0 & 0 & 0 \\ 4.2385 & -3.2026 & 0 & 0 \\ 0 & 0 & 4.2385 & -3.2026 \end{bmatrix}, \dots,
\end{aligned}
$$

$$
\begin{aligned}
M_{22} = J = &\begin{bmatrix} 182795.8456 & -18.6695 & -37747.5473 \\ -18.6695 & 566091.8052 & 74.4042 \\ -37747.5473 & 74.4042 & 704068.0911 \end{bmatrix} + \begin{bmatrix} -0.0025 & -863.2814 & 0 \\ -863.2814 & 0 & -21.1022 \\ 0 & -21.1022 & -0.0025 \end{bmatrix} q_{ufy1}^F\\
&+ \begin{bmatrix} 0.0010 & 367.2116 & 0 \\ 367.2116 & 0 & 7.3208 \\ 0 & 7.3208 & 0.0010 \end{bmatrix} q_{ufy2}^F + \begin{bmatrix} 42.2044 & 0 & -863.2814 \\ 0 & 42.2044 & 0.0012 \\ -863.2814 & 0.0012 & 0 \end{bmatrix} q_{ufz1}^F + \dots\\
&+ \begin{bmatrix} 6.9557 & 3.2162 & -20.3065 \\ 3.2162 & 7.5394 & -1.2456 \\ -20.3065 & -1.2456 & -0.5837 \end{bmatrix} q_{ue2}^L + \begin{bmatrix} -0.0075 & 35.9911 & 0 \\ 35.9911 & 0 & 12.8965 \\ 0 & 12.8965 & -0.0075 \end{bmatrix} q_{ue1}^V\\
&+ \begin{bmatrix} 0.0022 & -4.0598 & 0 \\ -4.0598 & 0 & 4.0187 \\ 0 & 4.0187 & 0.0022 \end{bmatrix} q_{ue2}^V,\ \dots,
\end{aligned}
\tag{5.53}
$$

$$M_{23}^F = \begin{bmatrix} -21.1022 & 7.3208 & -0.0012 & 0.0005 \\ 0 & 0 & -863.2814 & 367.2116 \\ 863.2814 & -367.2116 & 0 & 0 \end{bmatrix} + \begin{bmatrix} 0 & 0 & 2.4362 & -0.7090 \\ 0 & 0 & 0 & 0 \\ 0 & 0 & 0 & 0 \end{bmatrix} q_{ufy1}^F + \dots$$
$$+ \begin{bmatrix} 0.7090 & -2.3655 & 0 & 0 \\ 0 & 0 & 0 & 0 \\ 0 & 0 & 0 & 0 \end{bmatrix} q_{ufz2}^F, \dots, \; M_{28}^V = \begin{bmatrix} 68.3900 & 72.7325 \\ 0 & 0 \\ -344.8056 & -402.1912 \end{bmatrix}, \; \dots,$$
$$M_{33}^A = \begin{bmatrix} 2.4862 & -0.7090 & 0 & 0 \\ -0.7090 & 2.3655 & 0 & 0 \\ 0 & 0 & 2.4862 & -0.7090 \\ 0 & 0 & -0.7090 & 2.3655 \end{bmatrix}, \; \dots,$$
$$M_{88}^L = \begin{bmatrix} 17.3669 & 10.8317 \\ 10.8317 & 32.5338 \end{bmatrix}, \; M_{88}^V = \begin{bmatrix} 34.1002 & 32.0129 \\ 32.0129 & 65.4667 \end{bmatrix}$$

Next, we consider the time-varying part of the first-order problem, Eqs. (3.9) with all quantities measured from the constant static solution. To this end, we use Eq. (4.4) in which the coefficient matrices are given by

$$A = \begin{bmatrix} 0 & 0 & 0 & 0 & 0 & 0 & \dots & 0.0004 & -0.0002 & 0 \\ 0 & 0 & 0 & -596.0114 & 0 & 0 & \dots & -0.0020 & 0.0086 & 0.0008 \\ 0 & 0 & 0 & 0 & -5000 & 0 & \dots & 0.0009 & -0.0003 & 0 \\ 0 & 0 & 0 & 0 & 0.0529 & 0 & \dots & 0 & 0.0001 & 0 \\ 0 & 0 & 0 & -0.0524 & 0 & 0 & \dots & 0 & 0.0001 & 0 \\ \dots & \dots & \dots & \dots & \dots & \dots & \dots & \dots & \dots & \dots \\ 0 & 0 & 0 & 174.9021 & 42.3914 & 0 & \dots & -76.1495 & 0.4819 & 0.0057 \\ 0 & 0 & 0 & 370.8378 & -25.9627 & 0 & \dots & 0.1808 & -31.9444 & -9.6829 \\ 0 & 0 & 0 & 438.1920 & -30.6787 & 0 & \dots & 0.2767 & 62.7271 & -137.0011 \end{bmatrix} \tag{5.54}$$

$$B = \begin{bmatrix} 0 & 0 & 0 & 0 \\ \dots & \dots & \dots & \dots \\ 0 & 0 & 0 & 0 \\ 2 & 1.0326 & 176.1982 & 104.3594 \\ 0 & 0 & 0 & -1901.4388 \\ 0 & -10.2357 & -2143.1016 & 0 \\ 0 & 800910.3941 & 1.8988 & -153505.0524 \\ -27.92 & -116.9527 & -561836.0209 & -8425.0411 \\ 0 & 4654.3829 & 11.7819 & 527985.1550 \\ \dots & \dots & \dots & \dots \\ 0 & 0 & 0 & -7461.0801 \\ 0 & 0 & 0 & -3090.6705 \end{bmatrix}$$

and in which the feedback control vector has the form $\mathbf{u}^{(1)} = [F_E^{(1)} \quad \delta_a^{(1)} \quad \delta_e^{(1)} \quad \delta_r^{(1)}]^T$. In the case in which $\mathbf{u}^{(1)} = \mathbf{0}$ and $\mathbf{F}_{\text{ext}} = \mathbf{0}$, the state equations admit an exponential solution yielding an eigenvalue problem. Solving the eigenvalue problem, we conclude that the system is unstable, with four eigenvalues being equal to zero and one being real and positive. Using

a linear quadratic regulator in conjunction with the weighting matrices

$$Q = \begin{bmatrix} 1 & 0 & 0 & 0 & 0 & 0 & \dots & 0 \\ 0 & 1 & 0 & 0 & 0 & 0 & \dots & 0 \\ 0 & 0 & 1 & 0 & 0 & 0 & \dots & 0 \\ 0 & 0 & 0 & 1 & 0 & 0 & \dots & 0 \\ 0 & 0 & 0 & 0 & 1 & 0 & \dots & 0 \\ 0 & 0 & 0 & 0 & 0 & 1 & \dots & 0 \\ \dots & \dots & \dots & \dots & \dots & \dots & \dots & \dots \\ 0 & 0 & 0 & 0 & 0 & 0 & \dots & 0 \end{bmatrix}, \; R = \begin{bmatrix} 10 & 0 & 0 & 0 \\ 0 & 5 \times 10^8 & 0 & 0 \\ 0 & 0 & 10^8 & 0 \\ 0 & 0 & 0 & 10^8 \end{bmatrix} \tag{5.55}$$

solving the corresponding steady-state Riccati equation, Eq. (4.14), and using Eq. (4.9), we obtain the gain matrix

$$G = \begin{bmatrix} 0.2975 & 0 & 0 & 0 \\ -0.0162 & 0 & -0.0001 & 0 \\ -0.1061 & 0 & 0.0001 & 0 \\ 24.4405 & 0.5494 & 0.0629 & 0.0880 \\ -1038.0256 & -1.0770 & -1.2859 & -0.2399 \\ -51.0425 & 1.4756 & -1.4031 & 0.3618 \\ \dots & \dots & \dots & \dots \\ -0.0006 & 0 & 0 & 0 \\ 0.0001 & 0 & 0 & 0 \\ 0 & 0 & 0 & 0 \\ 0 & 0 & 0 & 0 \end{bmatrix}^T \tag{5.56}$$

Then, solving the closed-loop eigenvalue problem, Eq. (4.16), we obtain the closed-loop eigenvalues

$$\begin{aligned} &\lambda_{1,2} = -0.1032 \pm 0.0869i, \; \lambda_3 = -0.2420, \; \lambda_{4,5} = -0.1231 \pm 0.2234i, \\ &\lambda_{6,7} = -0.2919 \pm 0.3064i, \; \lambda_{8,9} = -0.7837 \pm 1.6222i, \; \dots, \\ &\lambda_{69,70} = -40.5616 \pm 604.1438i, \; \lambda_{71,72} = -171.1169 \pm 587.8119i \\ &\lambda_{73,74} = -83.6775 \pm 802.6206i, \; \lambda_{75,76} = -229.1693 \pm 1076.8509i \end{aligned} \tag{5.57}$$

Clearly, all the closed-loop eigenvalues are either real and negative or complex with negative real part, so that the closed-loop first-order system is asymptotically stable. Hence, any disturbances from the steady level turn maneuver will be driven to zero.

Finally, we compute the response of the closed-loop system to the gust given by Eqs. (5.30). Figures 11-13 show a selected number of rigid body and elastic variables, and Fig. 14 shows the control inputs.

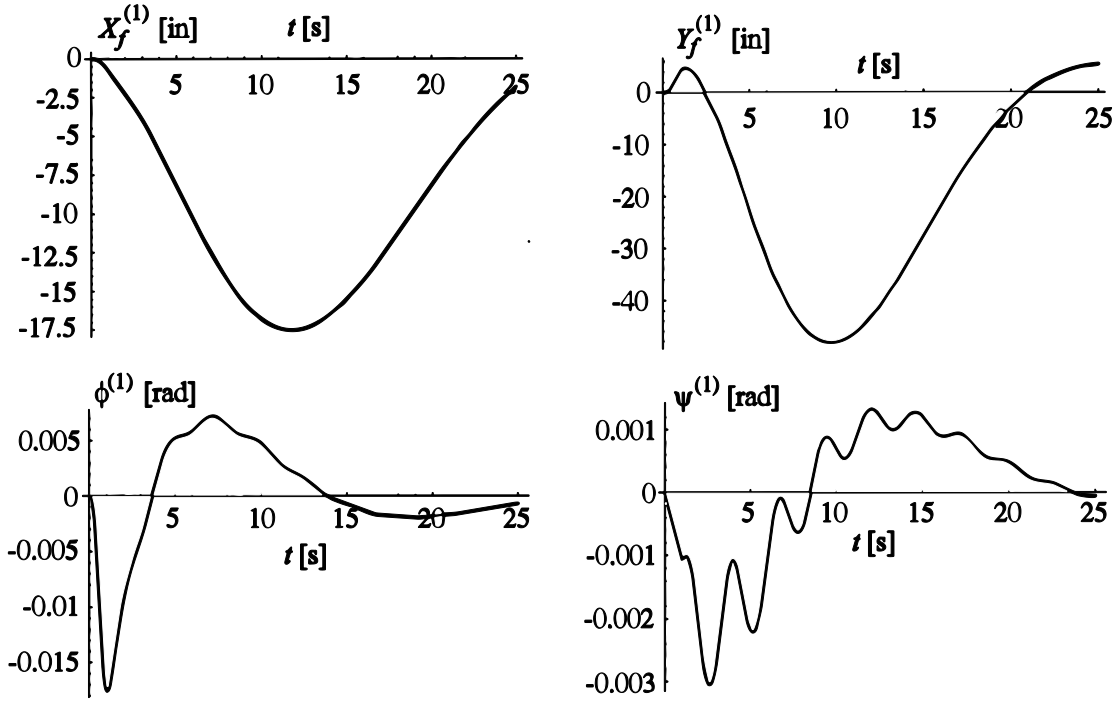

Figure 11. Rigid Body Displacements

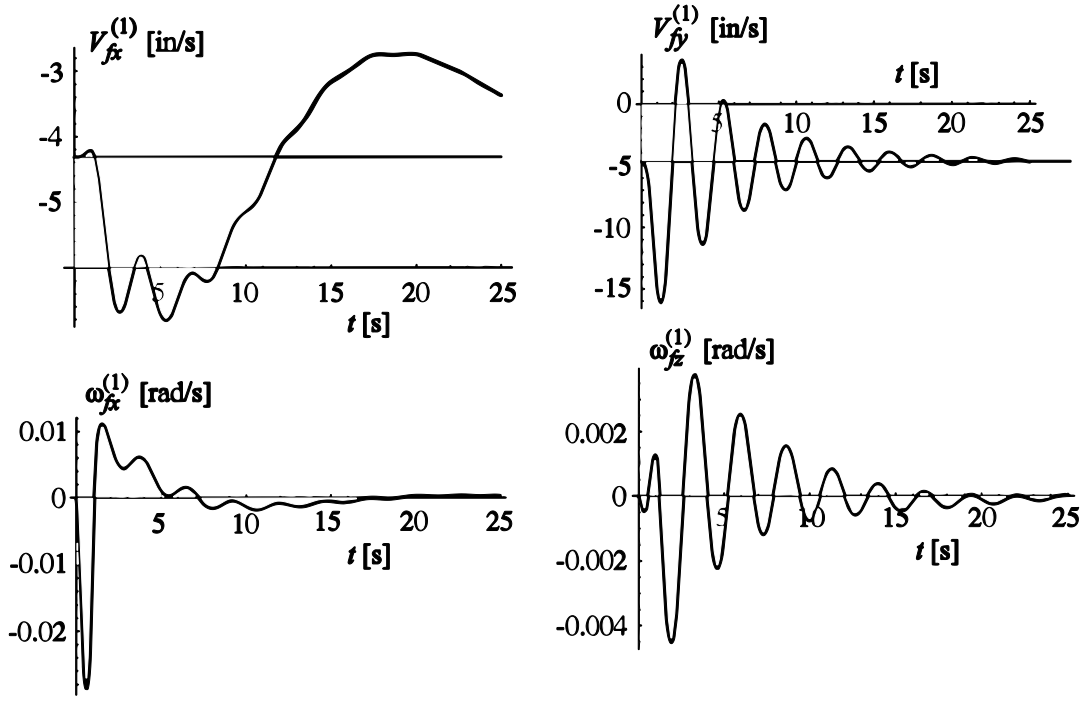

Figure 12. Rigid Body Velocities

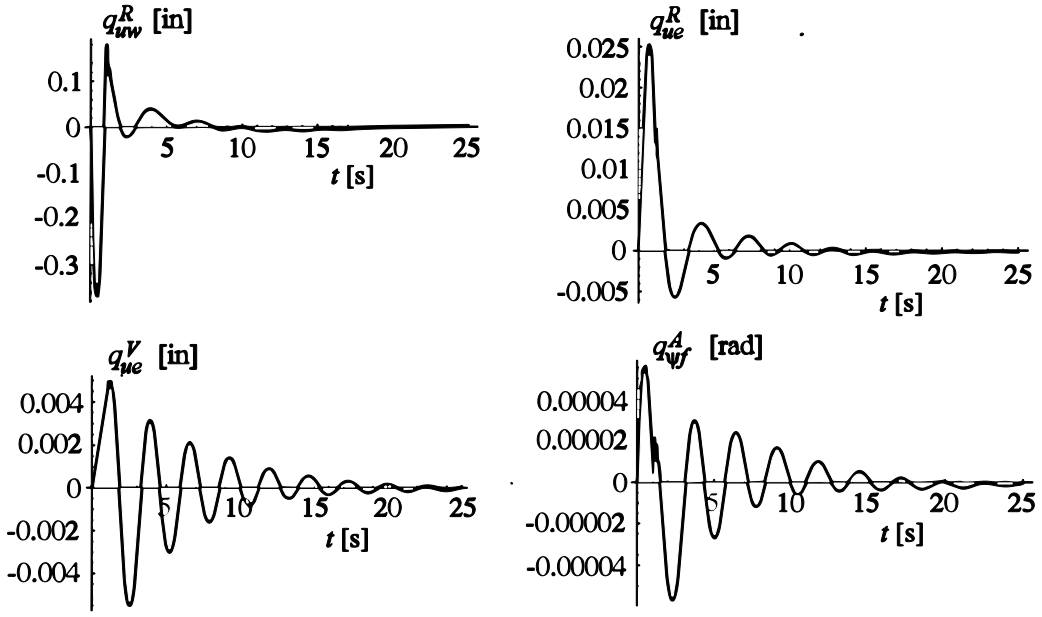

Figure 13. Generalized Elastic Displacements

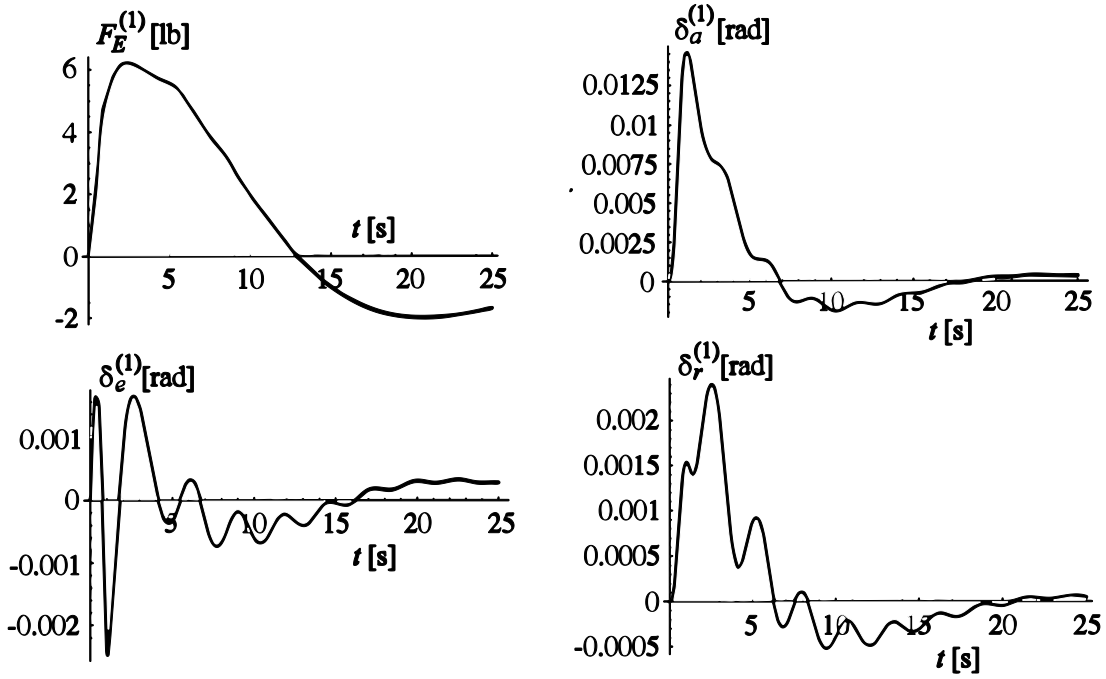

Figure 14. Control Inputs

Next, we turn our attention to the observer. To this end, we must compute the matrix C, Eq. (4.44), relating the output vector to the state vector. First, we use Eq. (4.41) and write

$$M_V = \begin{bmatrix} 0 & \dots & 0 & -0.1811 & 0.1369 & 0.1288 & \dots \\ 0 & \dots & 0 & 0 & 0 & 0.0219 & \dots \\ 0 & \dots & 0 & -0.0219 & 0.0166 & 0 & \dots \\ 0 & \dots & 0 & 1676.3711 & -1275.2629 & -1242.2537 & \dots \\ 0 & \dots & 0 & 3.5685 & -1.5887 & 21090.9413 & \dots \\ 0 & \dots & 0 & -21090.3030 & 15935.2420 & 0 & \dots \\ \dots & \dots & \dots & \dots & \dots & \dots & \dots \\ 0 & \dots & 0 & 0 & 0 & 0 & \dots \end{bmatrix}$$

$$\begin{bmatrix} -0.0030 & -0.0054 & 0.0009 & 0 & \dots & 0 \\ -0.0004 & 0 & 0 & 0 & \dots & 0 \\ -0.00007 & -0.0006 & 0.0001 & 0 & \dots & 0 \\ 27.2581 & 51.3897 & -8.9291 & 0 & \dots & 0 \\ -401.1684 & 0.3647 & 0.1928 & 0 & \dots & 0 \\ -63.5214 & -622.7178 & 109.2101 & 0 & \dots & 0 \\ \dots & \dots & \dots & \dots & \dots & \dots \\ 0 & 0 & 0 & 0 & \dots & 0 \end{bmatrix} \tag{5.58}$$

Then, inserting Eq. (5.58) into Eq. (4.44), we obtain

$$C = \begin{bmatrix} 1 & 0 & 0 & 0 & 0 & 0 & 0 & 0 & 0 & \dots & 0 & \dots & 0 & 0 \\ \dots & \dots & \dots & \dots & \dots & \dots & \dots & \dots & \dots & \dots & \dots & \dots & \dots & \dots \\ 0 & 0 & 0 & 0 & 0 & 1 & 0 & 0 & 0 & 0 & 0 & \dots & 0 & 0 \\ 0 & 0 & 0 & 0 & 0 & 0 & 0.6696 & -0.5045 & 0.0551 & -0.0396 & 0 & \dots & 0 & 0 \\ 0 & 0 & 0 & 0 & 0 & 0 & -1.0117 & 0.7754 & 4.8628 & -3.6584 & 0 & \dots & 0 & 0.0001 \\ 0 & 0 & 0 & 0 & 0 & 0 & 1.9066 & -1.4520 & 2.7844 & -2.1198 & 0 & \dots & 0 & 0.0011 \\ \dots & \dots & \dots & \dots & \dots & \dots & \dots & \dots & \dots & \dots & \dots & \dots & \dots & \dots \\ 0 & 0 & 0 & 0 & 0 & 0 & -10.6549 & 8.0593 & -5.6592 & 4.2880 & 0 & \dots & 0 & -0.0015 \\ 0 & 0 & 0 & 0 & 0 & 0 & -1.1592 & 0.8726 & 0.6274 & -0.4787 & 0 & \dots & 0 & 0.0002 \\ 0 & 0 & 0 & 0 & 0 & 0 & 9.1764 & -6.9361 & 3.6483 & -2.7602 & 0 & \dots & 0 & 0.0009 \end{bmatrix}$$

$$\begin{bmatrix} 0 & \dots & 0 & 0 \\ \dots & \dots & \dots & \dots \\ 0 & \dots & 0 & 0 \\ 0.0122 & \dots & 0.0005 & 0.0002 \\ 0.0320 & \dots & 0.0017 & 0.0003 \\ -0.0372 & \dots & -0.0031 & -0.0002 \\ \dots & \dots & \dots & \dots \\ 0.0871 & \dots & -0.4310 & -0.6603 \\ -0.0259 & \dots & 2.1744 & -1.4007 \\ -0.0384 & \dots & -1.4582 & 0.9927 \end{bmatrix} \tag{5.59}$$

We assume that the excitation noise $\mathbf{v}(t)$ and observation noise $\mathbf{w}(t)$ represent white noise processes with intensities V and W, respectively, and choose

$$\begin{aligned} V = \mathrm{diag}[&100000 \;\; 100000 \;\; 100000 \;\; 100000 \;\; 100000 \;\; 100000 \;\; 10^{-9} \;\; 10^{-9} \;\; 10^{-9} \;\; 10^{-9} \;\; 10^{-9} \;\; 10^{-9} \;\; 10^{-9} \\ &10^{-9} \;\; 10^{-9} \;\; 10^{-9} \;\; 10^{-9} \;\; 10^{-9} \;\; 10^{-9} \;\; 10^{-9} \;\; 10^{-9} \;\; 10^{-9} \;\; 10^{-9} \;\; 10^{-9} \;\; 10^{-9} \;\; 10^{-9} \;\; 10^{-9} \;\; 10^{-9} \;\; 10^{-9} \\ &10^{-9} \;\; 10^{-9} \;\; 10^{-9} \;\; 10^{-9} \;\; 10^{-9} \;\; 10^{-9} \;\; 10^{-9} \;\; 10^{-9} \;\; 10^{-9} \;\; 0 \;\dots\; 0] \end{aligned} \tag{5.60}$$

and

$$W = \mathrm{diag}[10^{-12} \;\; 10^{-12} \;\; 10^{-12} \;\; 10^{-6} \;\; 10^{-6} \;\; 10^{-6} \;\; 1 \;\dots\; 1] \tag{5.61}$$

so that, from Eq. (4.32), the steady-state Riccati equation

$$AQ + QA^T + V - QC^T W^{-1} CQ = 0 \tag{5.62}$$

yields

$$Q = \left[\begin{array}{cccccc|ccccccccc}
0.00032 & 0 & 0 & 0 & 0 & 0 & \dots & 0 & 0 & \dots & 0 & 0 & \dots & 0 \\
0 & 0.00032 & 0 & 0 & 0 & 0 & \dots & 0 & 0 & \dots & 0 & 0 & \dots & 0 \\
0 & 0 & 0.00032 & 0 & 0 & 0 & \dots & 0 & 0 & \dots & 0 & 0 & \dots & 0 \\
0 & 0 & 0 & 0.3162 & 0 & 0 & \dots & 0 & 0 & \dots & 0 & 0 & \dots & 0 \\
0 & 0 & 0 & 0 & 0.3162 & 0 & \dots & 0 & 0 & \dots & 0 & 0 & \dots & 0 \\
0 & 0 & 0 & 0 & 0 & 0.3162 & \dots & 0 & 0 & \dots & 0 & 0 & \dots & 0 \\
0 & 0 & 0 & 0 & 0 & 0 & \dots & 0 & 0 & \dots & 0 & 0 & \dots & 0 \\
0 & 0 & 0 & 0 & 0 & 0 & \dots & 0 & 0 & \dots & 0 & 0 & \dots & 0 \\
\hline
0 & 0 & 0 & 0 & 0 & 0 & \dots & 0 & 0 & \dots & 0 & 0 & \dots & 0 \\
0 & 0 & 0 & 0 & 0 & 0 & \dots & 0 & 0 & \dots & 0 & 0 & \dots & 0 \\
0 & 0 & 0 & 0 & 0 & 0 & \dots & 0 & 0 & \dots & 0 & 0 & \dots & 0 \\
\hline
0 & 0 & 0 & 0 & 0 & 0 & \dots & 0 & 0 & \dots & 0 & 0 & \dots & 0 \\
0 & 0 & 0 & 0 & 0 & 0 & \dots & 0 & 0 & \dots & 0 & 0 & \dots & 0
\end{array}\right]$$

$$\left[\begin{array}{cccccccc}
0 & 0 & \dots & 0 & 0 & \dots & 0 \\
0 & 0 & \dots & 0 & 0 & \dots & 0 \\
0 & 0 & \dots & 0 & 0 & \dots & 0 \\
0 & 0 & \dots & 0 & 0 & \dots & 0 \\
0 & 0 & \dots & 0 & 0 & \dots & 0 \\
0 & 0 & \dots & 0 & 0 & \dots & 0 \\
0.0001 & 0 & \dots & 0 & 0 & \dots & 0 \\
-0.0001 & -0.0001 & \dots & 0 & 0 & \dots & 0 \\
\hline
0 & 0 & \dots & 0 & 0 & \dots & 0 \\
0.0705 & 0.0288 & \dots & 0 & 0 & \dots & 0 \\
0.0288 & 0.0133 & \dots & 0 & 0 & \dots & 0 \\
\hline
0 & 0 & \dots & 0 & 0 & \dots & 0 \\
0 & 0 & \dots & 0 & 0 & \dots & 0
\end{array}\right] \tag{5.63}$$

Hence, from Eq. (4.31), the optimal observer gain matrix is

$$K_o = QC^T W^{-1} = \left[\begin{array}{ccccc}
3.1623 \times 10^8 & 0 & 0 & 0 & 0 \\
0 & 3.1623 \times 10^8 & 0 & -0.0006 & 0 \\
0 & 0 & 3.1623 \times 10^8 & 0 & -0.0050 \\
0 & -595.4161 & -3.3517 \times 10^{-6} & 316227.7660 & 0.0003 \\
-1.2214 \times 10^{-6} & 0.00003 & -4995.0050 & 0.0003 & 316227.7661 \\
0 & 4995.0050 & -2.1160 \times 10^{-6} & -7.6872 \times 10^{-6} & 0.0026 \\
0.2723 & -3.1077 & 1.7989 & -0.0339 & -0.0977 \\
-0.2055 & 2.3548 & -1.3560 & 0.0251 & 0.0740 \\
3.0983 & -9.7270 & 11.2778 & 0.0105 & -0.3083 \\
-2.3406 & 7.3588 & -8.5164 & -0.0072 & 0.2347 \\
\hline
0.0003 & -0.00001 & 0.0009 & 3.4367 \times 10^{-6} & -0.00002 \\
0.0004 & -0.0020 & 0.0009 & -0.00001 & -0.00003 \\
-0.0002 & 0.0086 & -0.0003 & 0.00006 & 0.00006 \\
-0.00001 & 0.0008 & 0.00002 & 5.6532 \times 10^{-6} & 4.6189 \times 10^{-6}
\end{array}\right]$$

$$\begin{bmatrix}
0 & \dots & 0 & 0 & 0 \\
0.0050 & \dots & 0 & 0 & 0 \\
0 & \dots & 0 & 0 & 0 \\
-7.6873 \times 10^{-6} & \dots & 1.4188 \times 10^{-6} & 0 & -1.4392 \times 10^{-6} \\
0.0026 & \dots & 0.00001 & 0 & -9.6036 \times 10^{-6} \\
316227.7661 & \dots & 0 & -1.1419 \times 10^{-6} & 1.0423 \times 10^{-6} \\
0.1056 & \dots & -1.8395 \times 10^{-6} & 0 & 1.6095 \times 10^{-6} \\
-0.0801 & \dots & 2.8997 \times 10^{-6} & 0 & -2.5602 \times 10^{-6} \\
-0.1962 & \dots & 0 & 0 & 0 \\
0.1492 & \dots & 0 & 0 & 0 \\
\cdots & \cdots & \cdots & \cdots & \cdots \\
-0.00002 & \dots & 0 & 0 & 0 \\
-0.00001 & \dots & 0 & 0 & 0 \\
-0.00003 & \dots & 0 & 0 & 0 \\
-2.0034 \times 10^{-6} & \dots & 0 & 0 & 0
\end{bmatrix} \tag{5.64}$$

Finally, solving the eigenvalue problem for $A - K_o C$, we obtain the observer eigenvalues

$$\begin{aligned}
&\lambda_1 = -0.0124,\ \lambda_{2,3} = -0.7826 \pm 1.6128i,\ \lambda_{4,5} = -0.4327 \pm 3.1155i, \\
&\lambda_6 = -5.7308,\ \lambda_{7,8} = -5.7282 \pm 36.9762i,\ \lambda_{9,10} = -3.5870 \pm 44.8308i, \\
&\lambda_{11,12} = -4.6556 \pm 60.7083i, \dots \lambda_{62,63} = -40.4104 \pm 603.8450i, \\
&\lambda_{64,65} = -177.1889 \pm 583.4363i,\ \lambda_{66,67} = -83.0638 \pm 802.2393i, \\
&\lambda_{68,69} = -229.1260 \pm 1077.0233i,\ \lambda_{70,71} = -316227.8058 \pm 0.0346i, \\
&\lambda_{72,73} = -316227.8459,\ \lambda_{74,75,76} = -3.1623 \times 10^8
\end{aligned} \tag{5.65}$$

To check the performance of the observer just designed, we simulate the response of the combined system, Eq. (4.25), to the initial conditions

$$\begin{aligned}
\mathbf{x}^{(1)}(0) = [&5\ \ 5\ \ 5\ \ 0.02\ \ 0.005\ \ 0.001\ \ 0.2\ \ 0.1\ \ 0.2\ \ 0.1\ \ 0.2\ \ 0.1\ \ -0.2\ \ -0.1 \\
&-0.2\ \ -0.1\ \ -0.2\ \ -0.1\ \ -0.2\ \ -0.1\ \ -0.2\ \ -0.1\ \ -0.2 \\
&-0.1\ \ 0.05\ \ 0.01\ \ -0.05\ \ -0.01\ \ 0.05\ \ 0.01\ \ -0.05\ \ -0.01 \\
&0.05\ \ 0.01\ \ -0.05\ \ -0.01\ \ 0.05\ \ 0.01\ \ 0\ \dots\ 0] \\
\mathbf{e}(0) = 0.15&\mathbf{x}^{(1)}(0)
\end{aligned} \tag{5.66}$$

Figures 15-17 show a selected number of rigid body and elastic variables and Fig. 18 shows the control inputs as given by Eq. (4.23).

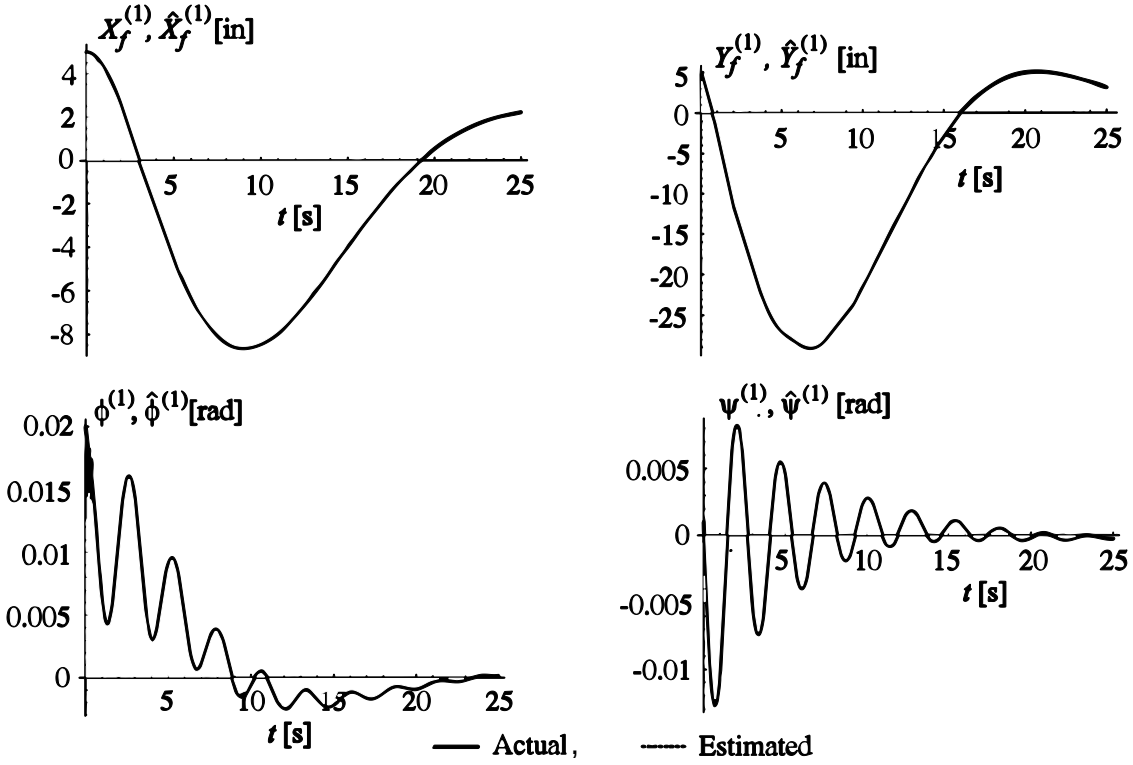

Figure 15. Rigid Body Displacements

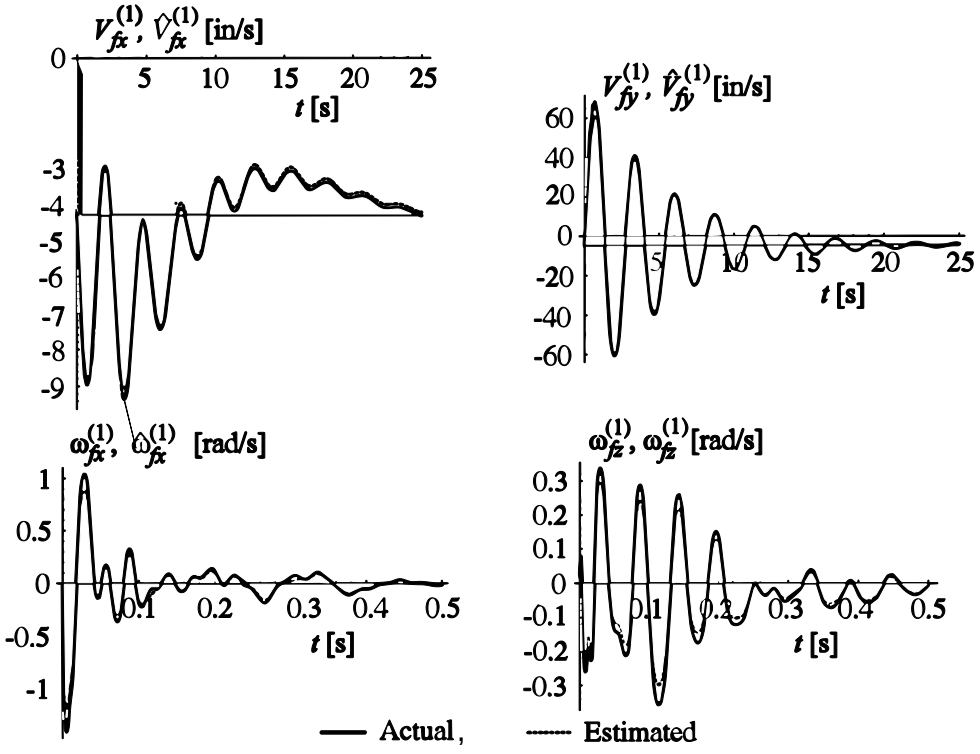

Figure 16. Rigid Body Velocities

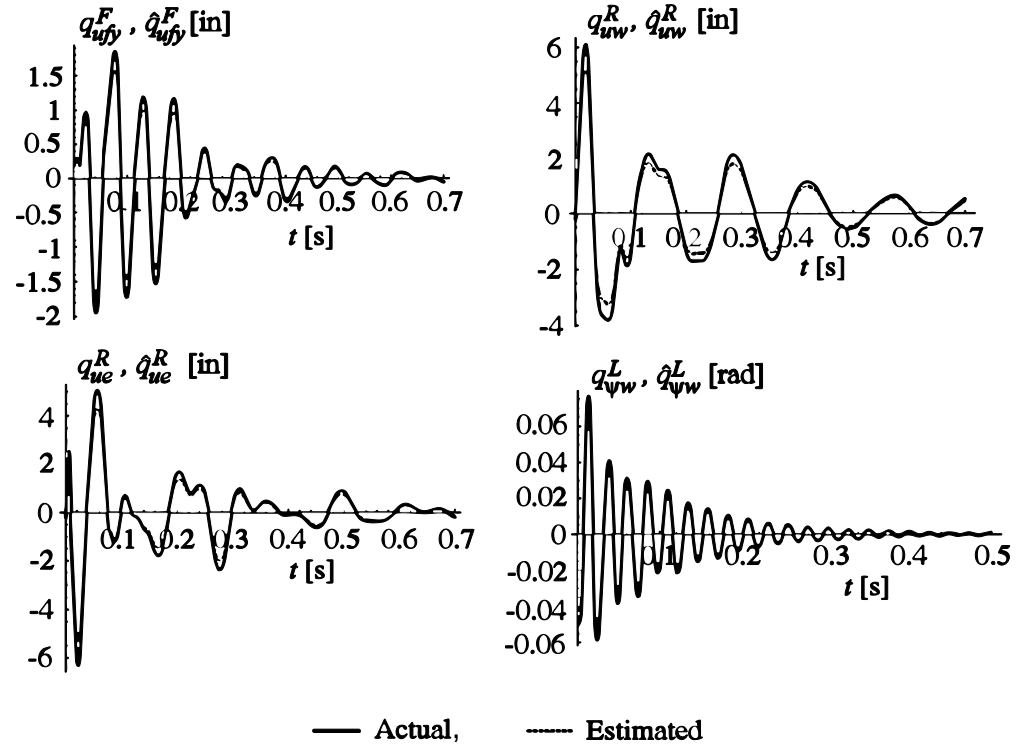

Figure 17. Generalized Elastic Displacements

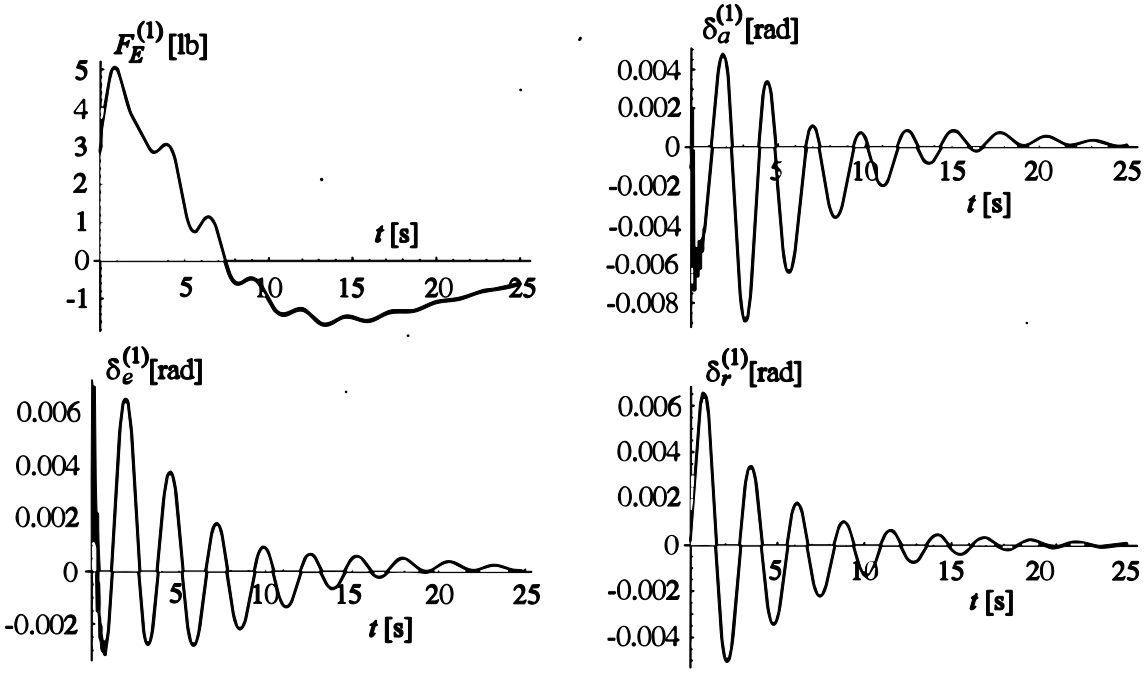

Figure 18. Control Inputs

Chapter 6

Summary and Conclusions

This dissertation presents a new theory for the dynamics and control of whole flexible aircraft. It integrates in a single mathematical formulation the disciplines pertinent to the flight of flexible aircraft, namely, analytical dynamics, structural dynamics, aerodynamics and controls. Essentially, the objective of this research is to unify the areas of flight dynamics and aeroelasticity for flexible aircraft, capturing coupling effects eluding when each of the two disciplines is considered separately. Flight dynamics and aeroelasticity merely view the same aircraft from different perspectives, prompted by different objectives, flight stability in the first and vibration and flutter in the second. Hence, the question arises as to whether, in so doing, certain deleterious effects due to the coupling between rigid body motions and the elastic deformations are not missed. This question can only be answered by a formulation integrating all disciplines impinging on the dynamic behavior of flexible aircraft.

The unified formulation is based on fundamental principles and incorporates in a natural manner both rigid body motions of the aircraft as a whole and elastic deformations of the flexible components (fuselage, wing and empennage), as well as the aerodynamic, propulsion, gravity and control forces. To describe the motion of the aircraft, we attach a reference frame to each of the flexible components and treat the one attached to the fuselage as the aircraft reference frame, where the reference frames represent respective body axes. Then, the motion is described by means of three translations (forward motion, sideslip and plunge) and three rotations (roll, pitch and yaw) of the fuselage body axes and elastic displacements of each of the flexible components relative to corresponding body axes. The mathematical formulation is based on the generic equations of motion in terms of quasi-coordinates derived earlier in Ref. 32. The formulation is hybrid in nature, in the sense that

it consists of ordinary differential equations for the rigid body translations and rotations of the aircraft as a whole and boundary-value problems for the elastic deformations for the flexible components of the aircraft, namely, the fuselage, wing and empennage. Because it is not feasible to work with hybrid equations, the distributed variables describing the boundary-value problems for the flexible components are discretized in space. In the discretization process, the distributed variables are represented by finite series of known space-dependent shape functions multiplied by time-dependent generalized coordinates, yielding a relatively large set of second-order ordinary differential equations for the whole aircraft. The derivation of the equations of motion in conjunction with the extended Hamilton principle requires expressions for the kinetic energy, potential energy, energy dissipation function and virtual work, all scalar quantities. In turn, the kinetic energy requires the velocity of every point of the aircraft, which can be obtained by means of an orderly kinematical synthesis, going from the fuselage to the wing and to the empennage. The potential energy is merely equal to the strain energy and the energy dissipation function is assumed to be proportional to the strain energy. Rather than deriving first hybrid equations of motion and then discretizing them in space, we carry out the discretization directly in the kinetic energy, potential energy, energy dissipation function and virtual work, thus obtaining the desired set of ordinary differential equations for the whole flexible aircraft without the need to derive boundary-value problems. For integration of the differential equations and for control design, we transform the set of second-order differential equations into a set of first-order differential equations, namely, into a set of state equations. It turns out that, for the problem at hand, it is more convenient to work with momenta rather than with velocities. Although the resulting first-order equations actually represent phase equations, we refer to them as state equations.

The generalized forces appearing in the differential equations are obtained in terms of actual gravity, aerodynamic and control forces by means of the virtual work. To obtain the aerodynamic forces, we use the strip theory, which has two advantages, namely it uses the same variables as the inertial and structural terms and it lends itself to faster computer evaluation. We stress that the aerodynamics used in this research is merely for the purpose of demonstrating how it fits in the general scheme, and a suitable aerodynamic theory for a whole flexible aircraft must eventually be developed.

The state equations for a flexible aircraft are nonlinear and of high dimension, where the nonlinearity is due to the large rigid body variable and the high dimensionality is due to the small elastic variables. Hence, one can expect difficulties both with a stability analysis

and with the control design. A perturbation approach to the solution obviates many of these difficulties. More specifically, the solution is represented as the sum of a zero-order part for the large rigid body variables and a first-order part for the small elastic variables and perturbations in the rigid body variables, where the zero-order quantities are larger than the first-order quantities by at least one order of magnitude. Then, we separate the state equations into a zero-order problem for the rigid body motions, corresponding to flight dynamics, and a first-order problem for the elastic displacements and the perturbations in the rigid body variables, corresponding to extended aeroelasticity, where extended refers to the fact that they include not only the elastic displacements but also perturbations in the rigid body variables. The perturbation approach permits us to show that the general formulation derived here includes the flight dynamics and the extended aeroelasticity as special cases, the latter in a broader context than the common practice.

The flight dynamics equations are nonlinear and describe the zero-order translations and rotations of the aircraft. They are used to design controls for a given maneuver by solving an inverse problem, in the sense that the state representing a desired maneuver is given and the equations are solved for the control vector. The extended aeroelasticity equations, on the other hand, are linear, but they include the solution of the flight dynamics equations as an input. Hence, there is a set of extended aeroelasticity equations for every conceivable aircraft maneuver. If the solution of the flight dynamics equations is constant, as it is the case for steady level cruise and steady level turn maneuver, then the extended aeroelasticity equations are linear time-invariant. In this case, the stability of the first-order state equations can be checked based on the roots of the eigenvalue problem and control design can be achieved by commonly used techniques, such as the LQG method. If the solution of the flight dynamics equations is time-dependent, then the extended aeroelasticity equations are linear time-dependent, which does not permit a standard stability analysis. However, the control design can still be achieved.

Control design is carried out to steer the aircraft and suppress the undesirable disturbances tending to drive the aircraft from the intended maneuver and to cause vibration. The control inputs consist of the engine thrust and the control surface angles. Steering control involves the rigid-body motions and is obtained by solving the inverse problem mentioned above. On the other hand, control design for disturbances involves the elastic vibration and perturbations in the rigid body motions and is obtained by means of linear quadratic theory. This control requires the knowledge of the first-order state vector, which is obtained

through a Kalman-Bucy filter design permitting an estimate of the state vector from the output measurements.

A numerical solution of the flight dynamics equations and the extended aeroelasticity equations requires the aircraft geometry, the mass and stiffness distributions and the aerodynamic coefficients, which were made available by an aircraft manufacturer in lumped form; the numerical data is listed in the **Appendix**. The lumped parameters are treated as distributed by means of spatial Dirac delta functions. All flexible components are represented by beams undergoing bending and torsion. The fuselage is modeled as two separate parts, namely, a fore part and an aft part, both cantilevered at the origin of the aircraft body axes. Similarly, the wing and the horizontal stabilizer are modeled as a right part and a left part and the vertical stabilizer as a single part. In the context of Galerkin's method, each bending displacement is represented by two cantilever shape functions and each torsional displacement by two clamped-free shaft shape functions. Both the fore and aft parts of the fuselage undergo two bending and one torsional displacements each while each of the remaining components undergo only one bending and one torsional displacement. Displacements of each component are measured relative to the respective elastic axis, which is assumed to be a straight line. Having chosen the explicit structural model, the stiffness matrices are obtained from the potential energy. The structural damping matrices, on the other hand, are assumed to be proportional to the stiffness matrices for each flexible component with proportionality coefficients depending on the structural damping factor and the lowest natural frequencies of the respective components. The extended aeroelasticity equations are linear and for the model at hand they are of order 76.

Two example cases have been considered, namely, steady level flight and steady level turn maneuver. In the former, the solution of the flight dynamics equations is constant and, hence, the extended aeroelasticity equations are linear time-invariant. In the latter, we refer the rigid body motions to a set of cylindrical axes rotating with the same yaw angular velocity as the aircraft, so that the resulting flight dynamics equations yield constant solutions and, hence, the extended aeroelasticity equations are once again linear time-invariant. In both cases, the extended aeroelasticity equations admit constant solutions due to zero-order forces. We assume that the first-order state is measured from these constant solutions.

The weighting matrices Q and R required for the linear quadratic regulator design have been chosen so that the desired performance of the system is achieved and the control gains are sufficiently small that the resulting controls are reasonable. The eigenvalues of the

closed-loop system are real and negative or complex with negative real parts. This is in contrast with the open-loop eigenvalues, the first four of which are zero and the fifth is real and positive. An optimal observer design achieves an estimate of the first-order state from output measurements containing the $\mathbf{R}_f^{(1)}$ and $\boldsymbol{\theta}_f^{(1)}$ and 32 velocity measurements at various locations of the aircraft. The noise intensity matrices V and W required for the design of the Kalman-Bucy filter is chosen so that the estimates approach the actual variables reasonably fast.

For both the steady level flight and the steady turn maneuver, the response of the closed-loop system to a gust acting on the wing has been obtained and plotted in Figures 3-5 and Figures 11-13. As seen in the figures, the disturbance due to the gust is driven to zero. The control inputs are plotted in Figures 6 and 14; they are reasonably small and approach zero with time. To demonstrate the performance of the observer design, the response of the combined system to an initial state and initial observer error have been obtained and plotted in Figures 7-9 and Figures 15-17. The figures indicate that the estimates approach the actual variables. The control inputs are plotted in Figures 10 and 18.

Bibliography

1. Collar, A. R., "The Expanding Domain of Aeroelasticity," *Journal of the Royal Aeronautical Society*, Vol. 50, 1946, p. 428.

2. J. B. Rea Co., "Aeroelasticity in Stability and Control," *Wright Air Development Center, Technical Report 55-173*, 1957.

3. Taylor, A. S., "The Present Status of Aircraft Stability Problems in the Aeroelastic Domain," *Journal of the Royal Aeronautical Society*, Vol. 63, 1959, p. 580.

4. Bisphinghoff, R. L. and Ashley, H., *Principles of Aeroelasticity* (Ch. 9), John Wiley & Sons, Inc., New York, 1962. (Reprinted by Dover Publications, Inc., New York, 1975).

5. Milne, R. D., "Dynamics of the Deformable Aeroplane, Parts I and II," *Her Majesty's Stationery Office, Reports and Memoranda No. 3345*, London, 1962.

6. Taylor, A. S. and Woodcock, D. L., "Mathematical Approaches to the Dynamics of Deformable Aircraft, Parts I and II, "*Her Majesty's Stationery Office*, Reports and Memoranda No. 3776, London, 1971.

7. Dusto, A.R. et al., "A Method for Predicting the Stability Characteristics of an Elastic Airplane, Vol. 1-FLEXSTAB Theoretical Description," *NASA CR-114712*, October 1974.

8. Roger, K. L., "Airplane Math Modeling Methods for Active Control Design," *Structural Aspects of Active Control, AGARD-CP-228*, 1977, pp. 4-1 – 4-11.

9. Schwanz, R. C., "Consistency in Aircraft Structural and Flight Control Analysis," *Structural Aspects of Active Control, AGARD-CP-228*, 1977, pp. 5-1 – 5-16.

10. Miller, G. D., Wykes, J.H. and Brosnan, M. J., "Rigid-Body Structural Mode Coupling on a Forward Swept Wing Aircraft," *Journal of Aircraft*, Vol. 20, No. 8, 1983, pp. 696-702.

11. Weisshaer, T. A. and Zeiler, T. A., "Dynamic Stability of Flexible Forward Swept Wing Aircraft," *Journal of Aircraft*, Vol. 20, No. 12, 1983, pp. 1014-1020.

12. Rodden, W. P. and Love, J. R., "Equations of Motion of a Quasi-Steady Flight Vehicle Utilizing Restrained Static Aeroelastic Characteristics," *Journal of Aircraft*, Vol. 22, No. 9, 1985, pp. 802-809.

13. Cerra, J. J.II, Calico, R. A. and Noll, T. E., "Modeling of Rigid-Body and Elastic Aircraft Dynamics for Flight Control Development," *Proceedings of the Atmospheric Flight Mechanics Conference*, Williamsburg, VA, Aug. 18-20, 1986, pp. 386-395.

14. Arbuckle, P. D., Buttrill, C.S. and Zeiler, T. A., "A New Simulation Model Building Process for Use in Dynamic Systems Integration Research," *Paper 87-2498, AIAA Flight Simulation Technologies Conference*, Monterey, CA, August 17-19, 1987.

15. Buttrill, C. S., Zeiler, T. A. and Arbuckle, P.D., "Nonlinear Simulation of a Flexible Aircraft in Maneuvering Flight, *Paper 87-2501-CP, AIAA Flight Simulation Technologies Conference*, Monterey, CA, Aug. 17-19, 1987.

16. Zeiler, T. A. and Butrill, C. S., "Dynamic Analysis of an Unrestrained, Rotating Structure Through Nonlinear Simulation," *Proceedings of the AIAA/ASME/ASCE/AHS 29th Structures, Structural Dynamics and Materials Conference*, Williamsburg, VA, April 18-20, 1988, pp. 167-177.

17. Waszak, M. R. and Schmidt, D. K., "Flight Dynamics of Aeroelastic Vehicles," *Journal of Aircraft*, Vol. 25, No. 6, 1988, pp. 563-571.

18. Sipcic, S. R. and Morino, L., "Dynamic Behavior of Fluttering Two-Dimensional Panels on an Airplane in Pull-Up Maneuver," *AIAA Journal*, Vol. 29, No. 8, 1991, pp. 1304-1312.

19. Waszak, M. R., Buttrill, C. S. and Schmidt, D. K., "Modeling and Model Simplification of Aeroelastic Vehicles: An Overview," *NASA TM 107691*, September 1992.

20. Bilimoria, K. D. and Schmidt, D. K., "Integrated Development of the Equations of Motion for Elastic Hypersonic Flight Vehicles," *Journal of Guidance, Control, and Dynamics*, Vol. 18, No. 1, 1995, pp. 73-81.

21. Olsen, J. J., "Unified Flight Mechanics and Aeroelasticity for Accelerating, Maneuvering, Flexible Aircraft," *RTO AVT Specialists' Meeting on "Structural Aspects of Flexible Aircraft Control"*, Ottawa, Canada, Oct. 18-20, 1999, pp. 6-1 – 6-12.

22. Teufel, P., Hanel, M. and Well, K. H., "Integrated Flight Mechanics and Aeroelastic Modeling and Control of a Flexible Aircraft Considering Multidimensional Gust Input," *RTO AVT Specialists' Meeting on "Structural Aspects of Flexible Aircraft Control"*, Ottawa, Canada, Oct. 18-20, 1999, 21, pp. 18-1 – 18-9.

23. König, K. and Schuler, J., "Integral Control of Large Flexible Aircraft," *RTO AVT Specialists' Meeting on "Structural Aspects of Flexible Aircraft Control"*, Ottawa, Canada, Oct. 18-20, 1999, 21, pp. 19-1 – 19-12.

24. Samareh, J. A. and Bhatia, K. G., "A Unified Approach to Modeling Multidisciplinary Interactions," *Paper 2000-4704, 8th AIAA/NASA/USAF/ISSMO Multidisciplinary Analysis and Optimization Symposium*, Long Beach, CA, September 6-8, 2000.

25. Schmidt, D. K. and Raney, D. L., "Modeling and Simulation of Flexible Flight Vehicles," *Journal of Guidance, Control, and Dynamics*, Vol. 24, No. 3, 2001, pp. 539-546.

26. Meirovitch, L., *Methods of Analytical Dynamics*, McGraw-Hill Book Co., New York, 1970.

27. Meirovitch, L. and Nelson, H. D., "On the High-Spin Motion of a Satellite Containing Elastic Parts," *Journal of Spacecraft and Rockets*, Vol. 3, No. 11, 1966, pp. 1597-1602.

28. Meirovitch, L., "Hybrid State Equations of Motion for Flexible bodies in Terms of Quasi-Coordinates," *Journal of Guidance, Control, and Dynamics*, Vol. 14, No. 5, 1991, pp. 1008-1013.

29. Platus, D. H., "Aeroelastic Stability of Slender, Spinning Missiles," *Journal of Guidance, Control, and Dynamics*, Vol. 15, No. 1, 1992, pp. 144-151.

30. Meirovitch, L., "Derivation of Equations for Flexible Multibody Systems in Terms of Quasi-Coordinates from the Extended Hamilton's Principle," *Journal of Shock and Vibration*, Vol. 1, Issue 2, 1993/94, pp. 107-119.

31. Meirovitch, L. and Stemple, T. J., "Hybrid Equations of Motion for Flexible Multibody Systems Using Quasi-Coordinates," *Journal of Guidance, Control, and Dynamics*, Vol. 18, No. 4, 1995, pp. 678-688.

32. Meirovitch, L., "A Unified Theory for the Flight Dynamics and Aeroelasticity of Whole Aircraft," *Proceedings of the Eleventh Symposium on Structural Dynamics and Control*, Blacksburg, VA, May 12-14, 1997, pp. 461-468.

33. Nydick, I. and Friedmann, P. P., "Aeroelastic Analysis of a Trimmed Generic Hypersonic Vehicle," *Proceedings of the CEAS/AIAA/ICASE/NASA International Forum on Aeroelasticity, and Structural Dynamics*, Research Center, Hampton, VA, 1999, pp. 777-809.

34. Meirovitch, L. and Tuzcu, I., "Multidisciplinary Approach to the Modeling of Flexible Aircraft," International Forum on Aeroelasticity and Structural Dynamics," Madrid, Spain, June 5-7, 2001, pp. 435-448.

35. Etkin, B., *Dynamics of Flight* (2nd Ed.), John Wiley & Sons, New York, 1982.

36. Meirovitch, L., *Principles and Techniques of Vibrations*, Prentice-Hall, Inc., Upper Saddle River, NJ, 1997.

37. Dowell, E. H. (Editor), *A Modern Course in Aeroelasticity* (3rd Ed.), Kluwer Academic Publishers, Dordrecht/Boston/London, 1995.

38. Meirovitch, L. and Seitz, T. J., "Structural Modeling for Optimization of Low-Aspect-Ratio Wings, " *Journal of Aircraft*, Vol. 32, No. 5, 1995, pp. 1114-1123.

39. Meirovitch, L., *Dynamics and Control of Structures*, John Wiley & Sons, New York, 1990.

40. Biezad, D. J., *Integrated Navigation and Guidance Systems*, AIAA Education Series, Reston, VA, 1999.

Appendix

Numerical Values of the Aircraft Parameters

The values of the pertinent aircraft parameters were provided by an aircraft manufacturer in lumped form, and the current formulation assumes distributed parameters. This presents no problem, however, as lumped parameters can always be treated as distributed by means of spatial Dirac delta functions.[38]

In the first place, we consider the aircraft geometry. To this end, we regard the fuselage as consisting of two cantilever beams, a fore part and an aft part, with the origin of both sets of body axes at point O_f and with axes x_f^F and x_f^A collinear (Fig. 2), where the second subscript denotes the fore part and aft part. The wing is also divided into two parts, the right half-wing and the left half-wing, both with the origin of the respective body axes at O_w and with the longitudinal axes coinciding with the respective elastic axes. Moreover, the empennage consists of the horizontal stabilizer, divided into a right half and a left half, both with the origin at the of the respective body axes at O_e^R and O_e^L, and a vertical stabilizer with the origin of the body axes at O_{eV}. The radius vectors from O_f to the corresponding origins are

$$\begin{aligned} &\mathbf{r}_{fw}^R = \mathbf{r}_{fw}^L = [-5.04 \;\; 0 \;\; 38.33]^T \text{ in} \\ &\mathbf{r}_{fe}^R = \mathbf{r}_{fe}^L = [-244.75 \;\; 0 \;\; -43.13]^T \text{ in}, \;\; \mathbf{r}_{fe}^V = [-238.97 \;\; 0 \;\; -24.01]^T \text{ in} \end{aligned} \tag{A1}$$

The formulation calls for matrices of direction cosines between the various component body axes and the fuselage body axes, and in particular the body axes of the fore part of the fuselage denoted by $x_f y_f z_f$. The component body axes can be obtained from $x_f y_f z_f$ through a sequence of rotations. For example, axes $x_w^R y_w^R z_w^R$ for the right half-wing can be obtained through a rotation γ_1 about $x_f y_f z_f$ to an intermediate set of axes $x'_w y'_w z'_w$ and a rotation γ_2 about y'_w to $x_w^R y_w^R z_w^R$, where in the case of the wing γ_2 is known as the dihedral angle. Table 2 gives the rotation angles for the individual components.

Table 2 - Rotation Angles for Component Body Axes

Component Body Axes	Rotations		
	γ_1	γ_2	γ_3
$x_f^A y_f^A z_f^A$ Aft fuselage	180°	0	0
$x_w^R y_w^R z_w^R$ Right half-wing	90°	4°	0
$x_w^L y_w^L z_w^L$ Left half-wing	−90°	4°	0
$x_e^R y_e^R z_e^R$ Right horizontal stabilizer	94.30°	9°	0
$x_e^L y_e^L z_e^L$ Left horizontal stabilizer	−94.30°	9°	0
$x_e^V y_e^V z_e^V$ Vertical Stabilizer	0	118.74°	−90°

Using analogies with the first of Eqs. (2.2), the various matrices of direction cosines are as follows:

$$
\begin{aligned}
C_f^A &= \begin{bmatrix} -1 & 0 & 0 \\ 0 & -1 & 0 \\ 0 & 0 & 1 \end{bmatrix}, \; C_w^R = \begin{bmatrix} 0 & 0.9976 & -0.0698 \\ -1 & 0 & 0 \\ 0 & 0.0698 & 0.9976 \end{bmatrix} \\
C_w^L &= \begin{bmatrix} 0 & -0.9976 & -0.0698 \\ 1 & 0 & 0 \\ 0 & -0.0698 & 0.9976 \end{bmatrix}, \; C_e^R = \begin{bmatrix} -0.0750 & 0.9849 & -0.1560 \\ -0.9972 & -0.0741 & 0.0117 \\ 0 & 0.1564 & 0.9877 \end{bmatrix} \\
C_e^L &= \begin{bmatrix} -0.0750 & -0.9849 & -0.1560 \\ 0.9972 & -0.0741 & -0.0117 \\ 0 & -0.1564 & 0.9877 \end{bmatrix}, \; C_e^V = \begin{bmatrix} -0.4808 & 0 & -0.8768 \\ -0.8768 & 0 & 0.4808 \\ 0 & 1 & 0 \end{bmatrix}
\end{aligned}
\tag{A2}
$$

The inertia properties of the aircraft model are given in lumped form. To this end, the flexible components are divided into certain numbers of bays and the mass corresponding to each bay is lumped at the mass center of the bay. Moreover, the manner in which the mass is distributed over the associated cross-sectional area is represented by mass moments and mass products of inertia about axes with the origin at the mass center and parallel to the body axes of the respective component. Table 3 lists the coordinates of the mass centers, the mass values and the mass moments and mass products of inertia, in which the symmetry of the inertia matrices is implied. The masses have units $\text{lb}\cdot\text{s}^2/\text{in}$ and the mass moments and mass products of inertia have units $\text{lb}\cdot\text{s}^2\cdot\text{in}$. The cantilever beams lengths are $L_f^F = 295.86$ in, $L_f^A = 279.79$ in, $L_w^R = L_w^L = 328.83$ in, $L_e^R = L_e^L = 127.46$ in, $L_e^V = 113.48$ in.

Table 3 - Inertia Properties

Fore Part of the Fuselage										
No.	x_f^F	y_f^F	z_f^F	m_f^F	J_{xxf}^F	J_{yyf}^F	J_{zzf}^F	J_{xyf}^F	J_{xzf}^F	J_{yzf}^F
1	7.41	0	5.20	0.7237	514.6542	230.8500	313.3728	−0.1010	−7.9229	0
2	24.74	0	1.98	0.2095	206.4986	115.1881	97.2035	−0.3495	1.4603	0
3	38.95	0	-1.54	0.3014	333.7084	182.4735	160.9599	0.1424	−1.9160	0
4	48.49	0	3.25	0.7558	354.9372	129.9051	251.8536	1.2350	−0.6913	0
5	55.08	0	8.60	0.3555	351.5220	181.4974	177.6291	1.3775	3.0682	0
6	69.88	0	7.88	0.5562	559.9651	274.9544	306.9516	−2.2111	2.9413	0
7	84.47	0	7.32	0.3167	298.6947	182.3156	124.5506	−0.3573	−2.2086	0
8	101.30	0	5.29	0.7053	501.1153	418.5278	480.2490	0.1657	5.3648	0
9	111.10	0	5.40	0.1546	137.1911	84.7780	54.2436	−0.1605	0.3754	0
10	129.67	0	1.62	1.0289	934.8339	556.8193	535.0830	−10.4733	1.2842	0
11	160.23	0	6.60	1.2664	919.9719	477.2896	595.6675	3.1044	17.3295	0
12	189.38	0	−0.30	1.0170	673.8353	340.9581	437.3046	2.3821	−20.5815	0
13	204.35	0	1.98	1.0789	623.3512	354.2640	386.3648	−0.4686	−1.1859	0
14	223.81	0	1.16	1.0497	394.7331	245.3210	192.5843	−0.8907	9.7354	0
15	237.71	0	6.55	0.2496	86.3807	41.6213	48.6587	−0.5308	0.0829	0
16	251.30	0	6.57	0.7234	135.0187	96.6805	69.4034	0.9425	−9.6525	0
17	266.50	0	14.02	0.4702	65.4238	49.4018	57.8918	1.1289	7.6562	0
18	281.47	0	17.71	0.0979	14.8309	8.2310	10.2739	−0.0104	−0.0647	0
19	292.08	0	17.66	0.0640	3.0164	2.1283	2.1801	−0.0673	0.0104	0
Aft Part of the Fuselage										
No.	x_f^A	y_f^A	z_f^A	m_f^A	J_{xxf}^A	J_{yyf}^A	J_{zzf}^A	J_{xyf}^A	J_{xzf}^A	J_{yzf}^A
1	1.67	0	0.81	0.1434	160.7476	76.2673	84.8272	−0.0052	0.1320	0
2	10.66	0	17.72	0.6147	2114.0956	253.7152	1887.3572	0.7172	8.8913	0
3	22.18	0	19.00	1.4282	3571.1313	848.8131	2879.2026	7.9514	−102.4285	0
4	40.41	0	2.00	0.1183	133.0820	72.5725	60.7063	0.0233	0.0777	0
5	46.82	0	8.04	0.5808	354.6912	221.2985	163.5387	-0.1709	-4.8263	0
6	66.11	0	9.51	0.2506	259.3829	186.0932	84.9230	0.4246	−0.7664	0
7	83.74	0	8.39	0.7843	900.7860	470.6690	478.1052	8.3087	−14.4348	0
8	98.21	0	3.87	0.5821	317.6683	222.4144	138.4934	−3.6275	2.4908	0
9	117.50	0	−8.33	0.5870	634.8913	217.1299	530.1143	−0.3728	11.5375	0
10	142.62	0	−6.45	0.6048	317.3757	146.8824	212.2078	0.5593	−4.3913	0
11	156.28	0	−10.77	0.4945	168.9475	127.7664	71.1511	3.7414	−6.0380	0
12	173.22	0	−11.04	0.1165	62.1588	48.9953	21.8166	0.4609	1.1496	0
13	189.26	0	−12.24	0.2131	49.4821	37.8178	19.5795	0.5644	1.3852	0
14	203.41	0	−6.82	0.1220	36.0701	28.0876	15.0225	−0.1605	−3.7207	0
15	218.31	0	−19.66	0.0880	40.5364	37.9395	11.4727	−0.0129	3.5368	0
16	238.30	0	−10.17	0.0585	14.7040	11.5064	5.9785	0.0078	−0.8596	0
17	253.16	0	−14.94	0.0580	6.6491	6.2555	3.7440	0.1036	−0.4220	0
18	278.12	0	−17.35	0.0098	0.4143	0.9580	0.8415	−0.0052	−0.1087	0

Table 3 - Continued

Wing										
No.	x_w^R	y_w^R	z_w^R	m_w^R	J_{xxw}^R	J_{yyw}^R	J_{zzw}^R	J_{xyw}^R	J_{xzw}^R	J_{yzw}^R
1	17.34	−5.67	−0.41	0.7932	592.7715	135.2155	675.5300	−11.4074	−20.6970	23.8870
2	41.44	−0.36	0.64	0.3380	259.1733	13.6761	253.5778	2.9790	0.1402	14.4486
3	55.80	7.21	0.72	0.5481	203.2508	22.5351	202.0929	−2.4412	−0.1781	16.5185
4	68.45	0.92	−1.55	0.2900	145.9962	10.7568	144.9995	1.1106	0.4620	4.8288
5	80.75	4.29	−0.63	0.3517	109.3290	19.5652	117.3550	0.4698	−1.1316	4.4349
6	95.11	2.34	−0.89	0.1960	87.6687	7.3973	86.7071	−3.5075	−0.1369	3.3911
7	109.21	5.70	−0.49	0.1405	68.3377	5.1512	67.9640	0.3682	−0.0707	3.2896
8	123.58	10.93	−0.20	0.2014	98.0351	8.6246	100.8629	−5.1787	−0.2981	4.7601
9	141.58	6.17	−0.36	0.1441	62.7718	6.3306	64.6489	−0.3631	−0.0224	2.5948
10	159.69	5.62	−0.59	0.1550	58.9409	7.3054	62.3486	−2.4040	−0.0168	1.5852
11	180.67	2.46	−0.60	0.1481	57.8061	6.8510	61.6321	−1.7038	0.0205	1.7613
12	199.99	5.62	−0.49	0.1504	44.7968	8.9780	51.3853	−4.0862	−0.1240	1.2184
13	223.12	3.28	−0.46	0.1146	26.2412	4.9868	29.6906	0.2463	0.0071	0.5415
14	242.88	1.87	−0.49	0.0825	16.9014	4.1168	19.9998	−0.2915	−0.0464	0.3456
15	260.53	−0.02	−0.71	0.0700	11.9896	2.0960	13.3314	0.1592	0.0681	0.3213
16	278.05	1.04	−0.46	0.0628	9.2044	1.9160	10.6262	0.1316	0.0019	0.0663
17	295.21	−0.06	−0.38	0.0471	6.9537	1.6338	8.2733	0.2092	−0.0066	−0.0035
18	311.97	−3.95	−0.38	0.0334	4.6844	0.6266	5.1908	0.1694	−0.0063	−0.0284
19	328.86	0.04	−0.40	0.0287	2.3874	0.7263	3.0305	−0.0109	−0.0045	−0.0293
Horizontal Stabilizer										
No.	x_e^R	y_e^R	z_e^R	m_e^R	J_{xxe}^R	J_{yye}^R	J_{zze}^R	J_{xye}^R	J_{xze}^R	J_{yze}^R
1	3.4154	−2.0199	4.8360	0.1298	152.7019	24.5226	24.9826	9.4614	−20.3966	0.6193
2	14.6498	4.1648	−0.0644	0.0618	13.3528	2.0288	14.9172	1.0676	−0.0060	0.0244
3	32.5615	6.2772	−0.0954	0.0625	12.1552	1.9324	13.7307	0.2775	0.0112	0.0409
4	50.7350	3.5463	−0.1694	0.0574	8.3296	2.7220	10.7676	0.5878	0.0612	−0.0078
5	66.0100	3.8814	−0.0389	0.0273	3.6287	0.3475	3.8652	0.2049	−0.0006	0.0143
6	76.5595	2.0048	0.0296	0.0173	2.3491	0.2014	2.4673	0.1894	0.0006	0.0055
7	88.2275	2.7918	−0.1213	0.0348	3.6527	0.9998	4.5598	0.3189	0.0164	0.0305
8	105.1312	2.4328	−0.0898	0.0259	2.2711	0.6068	2.8183	−0.0003	−0.0048	0.0187
9	121.3090	3.3819	−0.0468	0.0199	1.6192	0.4246	2.0069	0.1574	−0.0007	0.0040
10	128.5213	−2.0644	−0.0276	0.0135	0.3576	0.0114	0.3586	0.0197	−0.0001	−0.0010
Vertical Stabilizer										
No.	x_e^V	y_e^V	z_e^V	m_e^V	J_{xxe}^V	J_{yye}^V	J_{zze}^V	J_{xye}^V	J_{xze}^V	J_{yze}^V
1	−3.0130	−4.0388	0	0.0867	26.0215	26.8758	50.3184	18.1691	0.1131	0.1417
2	17.3464	−5.0753	0	0.0419	8.2448	2.9690	10.2273	3.9298	0.0052	0.0149
3	32.7117	−3.0312	0	0.0347	6.6885	2.6766	8.6842	3.2180	0.0097	0.0124
4	48.0499	−0.6415	0	0.0298	7.0021	2.2154	8.7929	3.2766	0.0395	0.0935
5	49.3577	25.8074	0	0.0741	5.0234	42.2968	46.9395	−2.2970	−0.0025	−0.0045
6	90.2614	−3.2365	0	0.0176	1.7168	1.1158	2.6177	1.0828	−0.1246	−0.1088
7	101.9491	19.9499	0	0.0062	0.2111	0.1462	0.3470	0.0991	0	0
8	103.6312	−3.8959	0	0.0150	1.3610	0.8632	2.1464	0.8286	−0.0010	0.0035
9	114.7248	−10.6405	0	0.0065	0.3567	0.2077	0.5619	0.2227	0	0
10	116.1657	2.4489	0	0.0523	4.5419	1.0689	5.5228	1.0377	0	0
Engine Pylon (Attached to the Aft Part of the Fuselage)										
No.	x_f^A	y_f^A	z_f^A	m_f^A	J_{xxf}^A	J_{yyf}^A	J_{zzf}^A	J_{xyf}^A	J_{xzf}^A	J_{yzf}^A
1	102.44	−64.05	−19.15	3.0115	347.7133	1947.0343	1872.5444	−18.0506	34.9386	4.6139
2	108.62	−37.00	−13.96	0.2647	35.2545	137.1807	162.3658	7.4957	11.3756	5.7131

The stiffness properties consist of the flexural rigidity and torsional rigidity of the cross-sectional area at certain locations of the elastic components. Both have units $\text{lb} \cdot \text{in}^2$. Table 4 gives the locations of the cross-sectional areas and the values of the corresponding rigidities.

Table 4 - Stiffness Properties

Fuselage									
Fore Part					**Aft Part**				
No.	x_f^F	EI_{fy}^F	EI_{fz}^F	GJ_f^F	No.	x_f^A	EI_{fy}^A	EI_{fz}^A	GJ_f^A
1	0.00	1.10×10^{11}	7.40×10^{10}	4.07×10^{10}	1	1.29	1.1×10^{11}	7.44×10^{10}	4.1×10^{10}
2	10.21	1.10×10^{11}	7.44×10^{10}	4.10×10^{10}	2	5.04	1.09×10^{11}	7.40×10^{10}	4.07×10^{10}
3	25.21	1.10×10^{11}	7.47×10^{10}	4.12×10^{10}	3	8.79	1.04×10^{11}	7.37×10^{10}	4.04×10^{10}
4	38.21	1.10×10^{11}	7.47×10^{10}	4.12×10^{10}	4	26.29	9.44×10^{10}	6.87×10^{10}	3.67×10^{10}
5	47.21	1.10×10^{11}	7.47×10^{10}	4.12×10^{10}	5	40.29	7.98×10^{10}	6.17×10^{10}	3.23×10^{10}
6	55.21	1.10×10^{11}	7.47×10^{10}	4.12×10^{10}	6	49.79	6.72×10^{10}	5.32×10^{10}	2.87×10^{10}
7	70.21	1.10×10^{11}	7.45×10^{10}	4.12×10^{10}	7	65.79	6.72×10^{10}	4.15×10^{10}	2.27×10^{10}
8	84.71	1.10×10^{11}	7.36×10^{10}	4.12×10^{10}	8	82.79	6.45×10^{10}	3.21×10^{10}	1.72×10^{10}
9	99.71	1.10×10^{11}	7.20×10^{10}	4.12×10^{10}	9	101.29	5.15×10^{10}	2.43×10^{10}	1.37×10^{10}
10	111.21	1.10×10^{11}	7.03×10^{10}	4.12×10^{10}	10	120.29	4.07×10^{10}	1.94×10^{10}	1.12×10^{10}
11	129.21	1.08×10^{11}	6.80×10^{10}	4.11×10^{10}	11	138.79	2.30×10^{10}	1.37×10^{10}	8.39×10^{9}
12	144.21	1.02×10^{11}	6.54×10^{10}	3.87×10^{10}	12	156.29	1.09×10^{10}	9.68×10^{9}	5.79×10^{9}
13	160.21	9.06×10^{10}	6.14×10^{10}	3.14×10^{10}	13	172.79	1.63×10^{10}	6.62×10^{9}	3.92×10^{9}
14	185.71	6.5×10^{10}	5.25×10^{10}	1.71×10^{10}	14	188.79	2.10×10^{10}	4.39×10^{9}	2.58×10^{9}
15	205.71	4.37×10^{10}	4.23×10^{10}	8.67×10^{9}	15	204.79	1.38×10^{10}	2.80×10^{9}	1.63×10^{9}
16	224.71	2.68×10^{10}	3.97×10^{10}	2.98×10^{9}	16	220.79	7.48×10^{9}	1.70×10^{9}	9.67×10^{8}
17	238.11	1.76×10^{10}	2.04×10^{10}	2.19×10^{9}	17	237.29	4.67×10^{9}	9.22×10^{8}	5.46×10^{8}
18	251.11	1.11×10^{10}	1.28×10^{10}	1.27×10^{9}	18	256.29	3.02×10^{9}	4.88×10^{8}	3.08×10^{8}
19	267.06	6.01×10^{9}	6.42×10^{9}	6.43×10^{8}	19	279.79	1.30×10^{9}	2.40×10^{8}	1.17×10^{8}
20	282.06	3.13×10^{9}	2.87×10^{9}	3.05×10^{8}					
21	295.86	1.16×10^{9}	6.15×10^{8}	7.72×10^{7}					
Wing					**Horizontal Stabilizer**				
No.	x_w^R	EI_w^R		GJ_w^R	No.	x_e^R	EI_e^R		GJ_e^R
1	0.00	1.09×10^{10}		1.07×10^{10}	1	0.00	3.92×10^{8}		2.43×10^{8}
2	17.10	9.70×10^{9}		1.07×10^{10}	2	2.41	3.78×10^{8}		2.36×10^{8}
3	34.19	8.65×10^{9}		1.04×10^{10}	3	13.84	3.16×10^{8}		2.09×10^{8}
4	40.95	8.10×10^{9}		9.95×10^{9}	4	31.89	2.32×10^{8}		1.73×10^{8}
5	54.45	6.95×10^{9}		8.80×10^{9}	5	49.94	1.66×10^{8}		1.35×10^{8}
6	67.85	5.70×10^{9}		7.60×10^{9}	6	64.33	1.23×10^{8}		1.03×10^{8}
7	81.11	4.84×10^{9}		6.40×10^{9}	7	75.11	9.70×10^{7}		8.05×10^{7}
8	94.45	4.28×10^{9}		5.30×10^{9}	8	88.35	7.10×10^{7}		5.85×10^{7}
9	107.95	3.49×10^{9}		4.50×10^{9}	9	103.98	4.82×10^{7}		4.14×10^{7}
10	122.95	2.81×10^{9}		3.92×10^{9}	10	119.63	3.27×10^{7}		2.98×10^{7}
11	140.45	2.18×10^{9}		3.19×10^{9}	11	127.46	2.74×10^{7}		2.19×10^{7}
12	159.45	1.68×10^{9}		2.43×10^{9}	**Vertical Stabilizer**				
13	179.45	1.35×10^{9}		1.86×10^{9}	No.	x_e^V	EI_e^V		GJ_e^V
14	200.70	1.02×10^{9}		1.37×10^{9}	1	0.00	1.56×10^{9}		7.30×10^{8}
15	221.95	7.35×10^{8}		8.80×10^{8}	2	7.40	1.33×10^{9}		6.70×10^{8}
16	241.70	5.65×10^{8}		5.55×10^{8}	3	21.15	9.66×10^{8}		5.57×10^{8}
17	259.95	4.28×10^{8}		3.56×10^{8}	4	34.90	6.86×10^{8}		4.45×10^{8}
18	276.70	3.54×10^{8}		2.53×10^{8}	5	49.73	4.61×10^{8}		3.55×10^{8}
19	293.95	2.82×10^{8}		1.71×10^{8}	6	63.98	3.06×10^{8}		2.41×10^{8}
20	311.10	2.02×10^{8}		8.55×10^{7}	7	77.63	2.01×10^{8}		1.38×10^{8}
21	327.01	1.27×10^{8}		6.50×10^{6}	8	91.31	1.26×10^{8}		8.69×10^{7}
					9	105.82	6.88×10^{7}		3.56×10^{7}
					10	113.48	4.25×10^{7}		8.51×10^{6}

The aerodynamic forces involve the slope $C_{L\alpha i}$ of the lift curve, the drag coefficient C_{Di0}, the slope $C_{s\beta i}$ of the lateral force curve and the control effectiveness coefficients $C_{L\delta a},\ C_{s\delta e}$ and

$C_{s\delta r}$. To determine the aerodynamic forces, the aircraft components are divided into a given number of sections and the coefficients are given for each of the sections. A typical section has a trapezoidal shape defined by two points $x_{ia}y_{ia}z_{ia}$ and $x_{ib}y_{ib}z_{ib}$ and by respective chords c_{ia} and c_{ib}, where the chords are parallel to the longitudinal axis x_f of the fuselage (Fig. A). For all sections, $C_{Df0} = C_{Dw0} = 0.016$ and $k_f = k_w = 0.04$. The lines of the aerodynamic centers are also shown in Fig. A; they are located at one quarter of the chord of the wing and horizontal and vertical stabilizers. The line of aerodynamic centers are located at one half of the chord, as shown in Fig. A. The aerodynamic forces for the fore and aft parts of the fuselage are acting at the line of the aerodynamic centers. The control forces, on the other hand, are acting at 0.55 of the chord. The aerodynamic coefficients corresponding to the sections just mentioned are listed in Table 5. The slope of the lift coefficients and the control effectiveness for the aileron and the elevator listed in Table 5 are given for a single Mach number of 0.75. They must be corrected for different Mach numbers by the compressibility factor given in Fig. A. Note that there are only seven sections for the wing with control effectiveness coefficients; they correspond to the aileron.

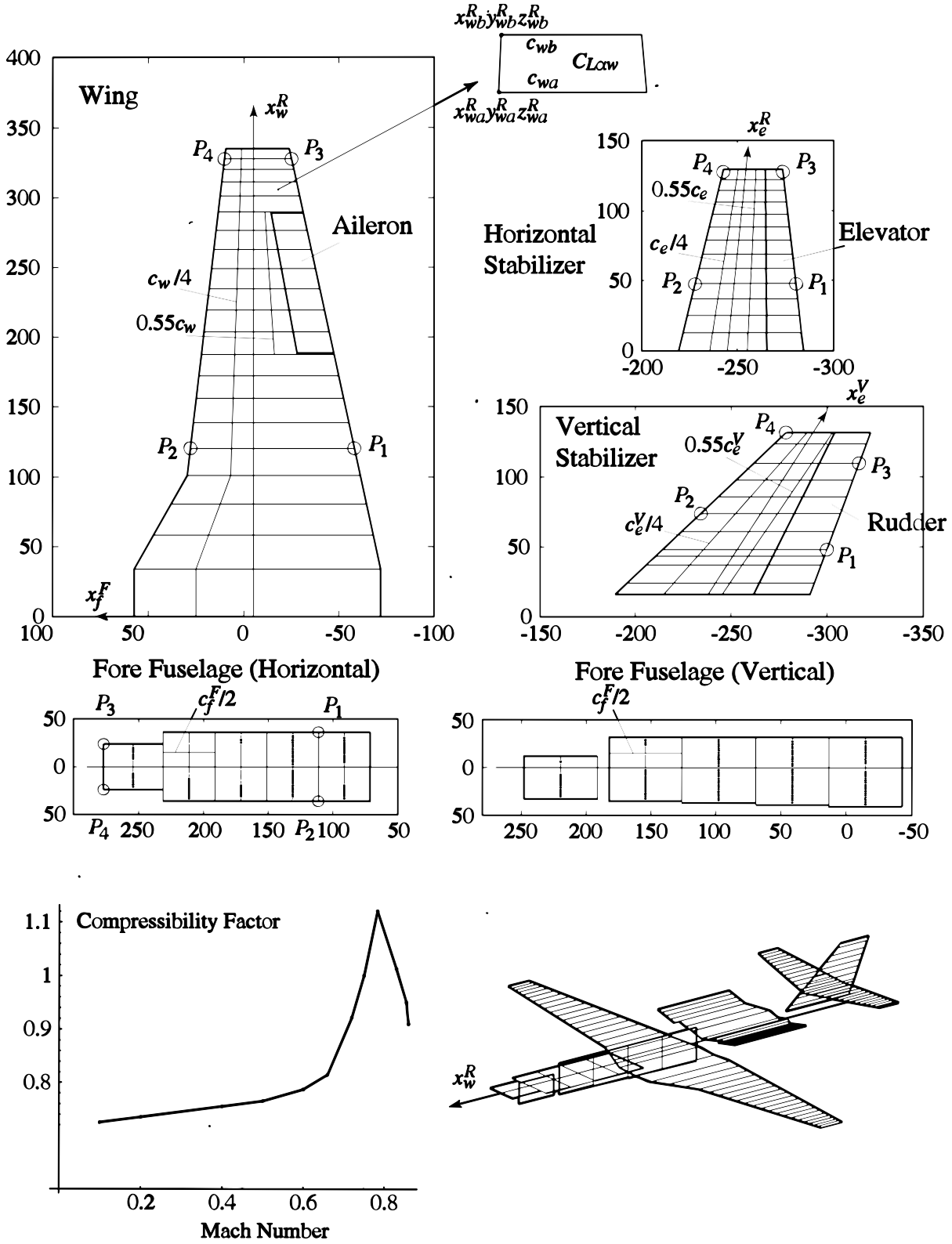

Figure A. Aerodynamic Sections for the Model

Table 5 - Aerodynamic Coefficients

Fore Part of the Fuselage - Horizontal Lifting Surface									
x^F_{fa}	y^F_{fa}	z^F_{fa}	c^F_{fa}	x^F_{fb}	y^F_{fb}	z^F_{fb}	c^F_{fb}	$C^F_{l_{\alpha f}}$	
111.21	−24.00	0.17	40.00	111.21	24.00	0.17	40.00	0.065	
151.21	−36.25	0.17	40.00	151.21	36.25	0.17	40.00	0.065	
191.21	−36.25	0.17	40.00	191.21	36.25	0.17	40.00	0.20	
231.21	−36.25	0.17	40.00	231.21	36.25	0.17	40.00	0.50	
277.21	−36.25	0.17	46.00	277.21	36.25	0.17	46.00	0.50	
Fore Part of the Fuselage - Vertical Lifting Surface									
x^F_{fa}	y^F_{fa}	z^F_{fa}	c^F_{fa}	x^F_{fb}	y^F_{fb}	z^F_{fb}	c^F_{fb}	$C^F_{l_{\beta f}}$	
13.21	0	41.17	56.00	13.21	0	41.17	56.00	0.142	
69.21	0	39.17	56.00	69.21	0	39.17	56.00	0.142	
126.23	0	37.17	56.80	126.23	0	37.17	56.80	0.142	
182.21	0	35.17	55.98	182.21	0	35.17	55.98	0.242	
248.21	0	33.17	57.00	248.21	0	33.17	57.00	0.305	
				Wing					
x^R_{wa}	y^R_{wa}	z^R_{wa}	c^R_{wa}	x^R_{wb}	y^R_{wb}	z^R_{wb}	c_{wb}	$C_{L\alpha w}$	$C_{L\delta a}$
0	−62.49	0	129.49	34.00	−62.49	0	129.49	4.9675	
34.00	−62.49	0	129.49	58.36	−52.40	0	115.51	6.1879	
58.36	−52.40	0	115.51	80.71	−43.15	0	102.68	6.5604	
80.71	−43.15	0	102.68	101.07	−34.72	0	90.99	6.7609	
101.07	−34.72	0	90.99	120.35	−33.06	0	86.25	6.9328	
120.35	−33.06	0	86.25	138.62	−31.49	0	81.75	7.1620	
138.62	−31.49	0	81.75	155.90	−30.00	0	77.50	7.4485	
155.90	−30.00	0	77.50	172.17	−28.60	0	73.50	7.7349	
172.17	−28.60	0	73.50	187.43	−27.29	0	69.75	7.9641	
187.43	−27.29	0	69.75	203.59	−25.89	0	65.77	8.1647	2.4494
203.59	−25.89	0	65.77	219.20	−24.55	0	61.93	8.2792	2.4838
219.20	−24.55	0	61.93	234.30	−23.25	0	58.21	8.3365	2.5010
234.30	−23.25	0	58.21	248.91	−21.99	0	54.62	8.3365	2.5010
248.91	−21.99	0	54.62	263.01	−20.78	0	51.15	8.2506	2.4752
263.01	−20.78	0	51.15	276.62	−19.61	0	47.80	8.0214	2.4064
276.62	−19.61	0	47.80	289.72	−18.48	0	44.58	7.7063	2.3119
289.72	−18.48	0	44.58	301.25	−17.49	0	41.74	7.2766	
301.25	−17.49	0	41.74	311.27	−16.62	0	39.28	6.6463	
311.27	−16.62	0	39.28	320.29	−15.85	0	37.06	5.7869	
320.29	−15.85	0	37.06	327.66	−15.21	0	35.25	4.5837	
327.66	−15.21	0	35.25	335.02	−14.58	0	33.43	2.5783	
Horizontal Stabilizer									
x^R_{ea}	y^R_{ea}	z^R_{ea}	c^R_{ea}	x^R_{eb}	y^R_{eb}	z^R_{eb}	c_{eb}	$C_{L\alpha e}$	$C_{L\delta e}$
0	−25.40	0	65.31	10.98	−24.06	0	61.62	1.5783	0.7891
10.98	−24.06	0	61.92	23.37	−22.77	0	58.67	1.6844	0.8422
23.37	−22.77	0	58.67	35.24	−21.54	0	55.55	1.8104	0.9052
35.24	−21.54	0	55.55	46.60	−20.36	0	52.57	1.9828	0.9414
46.60	−20.36	0	52.57	57.44	−19.23	0	49.72	2.2282	1.1141
57.44	−19.23	0	49.72	67.88	−18.14	0	46.98	2.5398	1.2699
67.88	−18.14	0	46.98	77.91	−17.10	0	44.34	2.8913	1.4457
77.91	−17.10	0	44.34	87.53	−16.10	0	41.82	3.1632	1.5816
87.53	−16.10	0	41.82	96.74	−15.15	0	39.40	3.3025	1.6512
96.74	−15.15	0	39.40	105.54	−14.23	0	37.09	3.2958	1.6479
105.54	−14.23	0	37.09	113.93	−13.36	0	34.88	3.1300	1.5650
113.93	−13.36	0	34.88	121.91	−12.53	0	32.79	2.7454	1.3727
121.91	−12.53	0	32.79	129.08	−11.79	0	30.90	1.9828	0.9914

Table 5 (Continued)

Vertical Stabilizer									
x_{ea}^V	y_{ea}^V	z_{ea}^V	c_{ea}^V	x_{eb}^V	y_{eb}^V	z_{eb}^V	c_{eb}^V	$C_{s\beta e}^V$	$C_{s\delta r}^V$
−31.15	−39.58	0	102.00	−20.81	−37.96	0	97.85	0.9482	0.4267
−20.81	−37.96	0	97.85	−4.81	−35.44	0	91.43	1.4740	0.6633
−4.81	−35.44	0	91.43	3.05	−34.20	0	88.28	1.7290	0.7781
3.05	−34.20	0	88.28	8.92	−33.28	0	85.92	2.6550	1.1948
8.92	−33.28	0	85.92	25.14	−30.73	0	79.42	2.8540	1.2843
25.14	−30.73	0	79.42	41.37	−28.18	0	72.91	3.1030	1.3964
41.37	−28.18	0	72.91	56.34	−25.82	0	66.90	3.3020	1.4859
56.34	−25.82	0	66.90	71.32	−23.47	0	60.89	3.4280	1.5426
71.32	−23.47	0	60.89	86.30	−21.11	0	54.88	3.4350	1.5458
86.30	−21.11	0	54.88	103.37	−18.43	0	48.03	3.2020	1.4409
103.37	−18.43	0	48.03	113.44	−16.84	0	43.99	2.3430	1.0544
Engine Pylon									
x_{fa}^A	y_{fa}^A	z_{fa}^A	c_{fa}^A	x_{fb}^A	y_{fb}^A	z_{fb}^A	c_{fb}^A	$C_{D\alpha f}^A$	
50.79	0.00	−5.13	126.00	50.79	20.00	−11.83	126.00	1.2376	
50.79	20.00	−11.83	126.00	50.79	33.00	−16.16	117.33	1.2892	
50.79	33.00	−16.16	117.33	50.79	47.00	−20.83	108.00	1.2900	
42.79	47.00	−20.83	116.00	42.79	56.00	−23.84	116.00	1.1250	
42.79	56.00	−23.84	116.00	42.79	65.00	−26.85	116.00	1.0500	
42.79	65.00	−26.85	116.00	42.79	74.00	−29.86	116.00	0.8500	
42.79	74.00	−29.86	116.00	42.79	82.00	−32.53	116.00	0.5500	

Vita

İlhan Tuzcu was born on April 27, 1968 in Muş, Turkey. He received a Bachelor of Science degree in Mechanical Engineering from Dokuz Eylul University in Izmir, Turkey in September 1990. In January 1994, he was awarded a scholarship by the Turkish Council of Higher Education to pursue graduate studies in the United States. After receiving a Master of Science degree in Mechanical Engineering from the University of Connecticut in August 1996, he enrolled in the Mechanical Engineering Department at Virginia Tech as a doctoral student in January 1997 and has been working towards the Doctor of Philosophy degree in Mechanical Engineering.